

Reductive Coupling and Related Reactions with Mo and Ti *tris*-Anilides

by

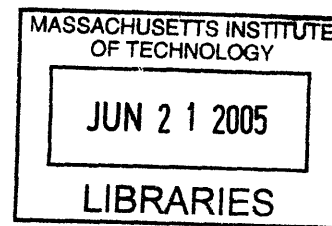
Arjun Mendiratta

B.S. Chemistry
California Institute of Technology
Pasadena, CA
2000

Submitted to the Department of Chemistry
in Partial Fulfillment of the Requirements
for the Degree of

DOCTOR OF PHILOSOPHY
in Chemistry
at the
MASSACHUSETTS INSTITUTE OF TECHNOLOGY

JUNE 2005



© 2005 Massachusetts Institute of Technology. All rights reserved.

Signature of Author _____
Department of Chemistry
May 4, 2005

Certified by _____
Christopher C. Cummins
Professor of Chemistry
Thesis Supervisor

Accepted by _____
Robert W. Field
Professor of Chemistry
Chairman, Department Committee on Graduate Students

ARCHIVES

This doctoral thesis has been examined by a Committee of the Department of Chemistry as follows:

Professor Stephen J. Lippard _____
Arthur Amos Noyes Professor of Chemistry
Chairman

Professor Christopher C. Cummins _____
Professor of Chemistry
Thesis Supervisor

Professor Alan Davison _____
Professor of Chemistry

For my parents.

Biographical Note

Arjun Mendiratta was born in Skokie, Illinois, on June 5, 1978, interrupting his mother's attempts to write her doctoral dissertation. Having neither siblings nor pets, he spent much of his childhood reading and playing the violin. At the age of 13, he left the suburbs of Chicago to attend Phillips Exeter Academy in Exeter, New Hampshire, where he became adept at tying a necktie and helped found the juggling club. Upon graduation in 1996, he moved west to Caltech, having been rather quickly seduced by the San Gabriel mountains. At Caltech, Arjun was introduced to the joys of synthetic chemistry by Dr. Seth Marder, who agreed to hire him despite his lack of laboratory experience and his professed desire to study mathematics. A year in the laboratory remedied these flaws and Arjun moved on to study computational chemistry with Prof. Bill Goddard followed by a brief encounter with metallocene chemistry under the supervision of Prof. John Bercaw. Arjun also ran on the Caltech cross-country team for four seasons, resulting in an intimate knowledge of the area running trails as well as several lasting friendships. In the fall of 2000, Arjun headed to MIT to pursue his doctoral research with Prof. Kit Cummins. When not in the laboratory, Arjun can often be spotted attending live music performances and agitating for various left-wing causes.

Table of Contents

Abstract	6
Abbreviations used in the text	7
Introduction	9
Chapter 1 <i>Radical reactions at a Mo-coordinated nitrile</i>	12
Chapter 2 <i>Beta-elimination from Mo(IV) ketiminates: a new strategy for Mo–N cleavage</i>	42
Chapter 3 <i>Synthesis of an oxotitanium(IV) anion</i>	59
Chapter 4 <i>Four-component couplings with Mo and Ti: the one-electron activation of CO₂</i>	69
Appendix <i>Synthesis of a Ti(III) paddlewheel</i>	88
Acknowledgements	93
Curriculum Vitae	95

Reductive Coupling and Related Reactions with Mo and Ti *tris*-Anilides

by

Arjun Mendiratta

Submitted to the Department of Chemistry
May, 2005 in Partial Fulfillment of the
Requirements for the Degree of Doctor of Philosophy in
Chemistry

ABSTRACT

Chapter 1: The capability of $\text{Mo}(\text{N}[t\text{-Bu}]\text{Ar})_3$ to act as a powerful one, two, and three electron reductant have been previously demonstrated. In this work, we show that $\text{Mo}(\text{N}[t\text{-Bu}]\text{Ar})_3$ forms a metastable adduct with the moderate π acid PhCN; coordination of PhCN activates the nitrile carbon towards reaction with a variety of one-electron reagents such as dichalcogenides, nitric oxide, hydrogen atom donors, cobaltocene, and elemental phosphorus. Evidence is presented for the existence of an inner-sphere electron transfer mechanism for these reactions.

Chapter 2: With the facile cleavage of N_2 by $\text{Mo}(\text{N}[t\text{-Bu}]\text{Ar})_3$ already established, a $\text{Mo}(\text{N}[t\text{-Bu}]\text{Ar})_3$ -mediated process for the incorporation of N_2 into organic molecules is an exciting prospect; its realization depends critically on the development of methods for cleavage of the Mo-N bond formed in the early stages of the process. In this chapter, we demonstrate that appropriately-substituted Mo(IV) ketiminates (synthesized using the methods of Chapter 1) undergo β -elimination to cleave the Mo-N bond and liberate PhCN. We present the kinetics of the reaction, substituent effects, and—in three cases—activation parameters.

Chapter 3: Deprotonation of the titanium formate complex $(\text{Ar}[t\text{-Bu}]\text{N})_3\text{TiOC}(\text{O})\text{H}$ with $\text{LiN}(i\text{-Pr})_2$ resulted in the release of free CO and the formation of a titanium(IV) oxoanion complex, isolated as its lithium salt.

Chapter 4: Previous work from these labs has shown that the unique combination of well-defined composition, steric bulk, and strong reducing ability embodied in $\text{Ti}(\text{N}[t\text{-Bu}]\text{Ar})_3$ lends itself particularly well to mechanistic studies of the classical Pinacol coupling. As shown in Chapter 1, a similar relationship can be drawn between $\text{Mo}(\text{N}[t\text{-Bu}]\text{Ar})_3$ and reductive nitrile coupling. In this chapter we draw on this mechanistic understanding to develop three new classes of reductive cross-couplings: nitrile is coupled with pyridine to form dihydropyridines, with benzophenone to form substituted 1,4-cyclohexadienes, and with carbon dioxide to form α -iminocarboxylates.

Abbreviations Used in the Text

Anal Calcd.	Calculated elemental analysis values
Å	angstrom (10^{-10} m)
Ar	3,5-dimethylphenyl
br	broad
CCD	charge coupled device
Cp	cyclopentadienyl
Cp*	pentamethylcyclopentadienyl
d	doublet
Et ₂ O	diethyl ether
Fc	ferrocene
fc	ferrocenium
h	hours
ΔH^\ddagger	enthalpy of activation
Hz	hertz (s^{-1})
IR	infrared
<i>i</i> -Pr	isopropyl
M	molarity, mol•L ⁻¹
Me	methyl
min	minute
NMR	nuclear magnetic resonance
OTf	trifluoromethanesulfonate
Ph	phenyl

ppm	parts per million
ΔS^\ddagger	entropy of activation
THF	tetrahydrofuran

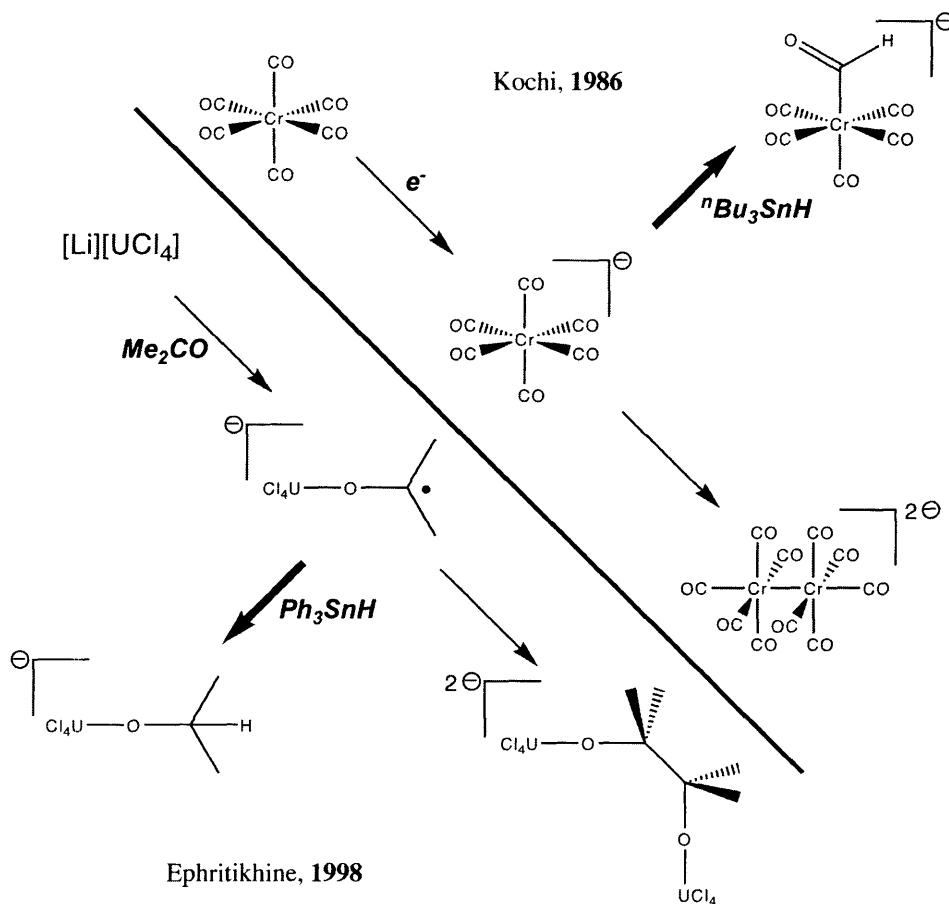
Introduction

In 1859, Fittig observed that treatment of acetone with sodium metal resulted in its reductive, C–C coupling to pinacol.¹ This reaction became known as the Pinacol coupling, and was observed to be general with respect to both the reducing metal and the carbonyl-containing substrate.² The reaction has since been embraced by the synthetic organic community, and several stereoselective variants have been developed.^{3,4}

Over one hundred years later, pioneering work by McCarley⁵ and Cotton⁶ demonstrated that this reaction could be generalized further: the use of reduced group V metals allowed for the reductive, C–C coupling of organic nitriles. Subsequent work demonstrated that a variety of other low-valent transition metals were capable of mediating this transformation.⁷

Reductive coupling methodology has since been extended to include imines,⁸ CS₂,⁹ and—in one case—CO₂.¹⁰ All of these reactions are presumed to proceed by a similar mechanism. In the first step, the reducing metal attacks the substrate at the heteroatom, resulting in formation of an adduct postulated to have considerable radical character at carbon. The radical coupling of two such molecules, followed by hydrolysis, generates the observed product. There has been considerable mechanistic investigation carried out on the Pinacol reaction,¹¹ whereas—for reductive coupling of non-carbonyl substrates—the mechanism is generally assumed by analogy. Of particular note is the elegant work of Ephritikhine.¹² As shown in Scheme 1, use of the UCl₄/Li/Me₂CO system allows not only for isolation of the metallopinacolate **1**, but also for trapping of the putative ketyl radical with excess Ph₃SnH to form the uranium alkoxide **2**.

Such a trapping reaction is naturally related to the ligand-centered reactivity often encountered in the study of 19-electron metal complexes.¹³ In 1986, Kochi and Naryanan showed that electrochemically generated [Cr(CO)₆]^{•-}, normally subject to rapid ligand loss followed by metal-metal bond formation, could be trapped as the formyl complex, [(OC)₅CrC(O)H]^{•-}, when generated in the presence of excess ⁿBu₃SnH.¹⁴ Further parallels are found in the reduction of [Cp₂Rh]⁺ to yield CpRh(μ:η⁴,η⁴-C₁₀H₁₀)RhCp, in which two Cp rings have been “reductively coupled.”¹⁵



Scheme 1

In this work, we explore the twin themes of reductive coupling and ligand-centered radical reactivity through the use of the well-defined metal complexes $(\text{Ar}[t\text{-Bu}]\text{N})_3\text{M}$ ($\text{M} = \text{Ti},^{16} \text{Mo}^{17}$). These odd-electron compounds are both strongly reducing and sterically encumbered, which allows access to relatively well-defined species displaying a strong propensity for ligand-centered radical reactivity. In the following chapters, we will exploit this preference in order to elucidate the mechanism of reductive nitrile coupling, carry out unusual small-molecule activations, synthesize model compounds for nitrogen fixation, and synthesize an anionic oxo of Ti(IV).

¹ Fittig, R. *Liebigs Ann. Chem.* **1859**, 110, 23.

² (a) Gomberg, M.; Bachmann, W. E. *J. Am. Chem. Soc.* **1927**, 49, 236. (b) Schreibmann, A. P. *Tetrahedron Lett.* **1970**, 4271. (c) Corey, E. J.; Danheiser, R. L.; Chandrasekaran, S. *J. Org. Chem.* **1976**, 41, 260.

-
- ³ (a) McMurry, J. E. *Chem. Rev.* **1989**, *89*, 1513. (b) Kahn, B. E.; Rieke, R. D. *Chem. Rev.* **1988**, *88*, 733.
- ⁴ (a) Handa, Y.; Inanaga, J. *Tetrahedron Lett.* **28**, 5717 (1987). (b) Barden, M. C.; Schwartz, J. J. *J. Am. Chem. Soc.* **118**, 5484 (1996).
- ⁵ Finn, P. A.; King, M. S.; Kilty, P. A.; McCarley, R. E. *J. Am. Chem. Soc.* **1975**, *97*, 220.
- ⁶ (a) Cotton, F. A.; Hall, W. T. *Inorg. Chem.* **1978**, *17*, 3525. (b) Cotton, F. A.; Hall, W. T. *J. Am. Chem. Soc.* **1979**, *101*, 5094.
- ⁷ (a) De Boer, E. J. M.; Teuben, J. H. J. *J. Organomet. Chem.* **1978**, *153*, 53. (b) Young, C. G.; Philipp, C. C.; White, P. S.; Templeton, J. L. *Inorg. Chem.* **1995**, *34*, 6412.
- ⁸ Roskamp, E. J.; Pedersen, S. F. *J. Am. Chem. Soc.* **1987**, *109*, 3152.
- ⁹ Harris, H. A.; Rae, D. A.; Dahl, L. F. *J. Am. Chem. Soc.* **1987**, *109*, 4739.
- ¹⁰ Evans, W. J.; Seibel, C. A.; Ziller, J. W. *Inorg. Chem.* **1998**, *37*, 770.
- ¹¹ See for example: Mundy, B. P.; Srinivasa, R.; Kim, Y.; Dolph, T.; Warnet, R. J. *J. Org. Chem.* **47**, 1652 (1982).
- ¹² Ephritikhine, M.; Maury, O.; Villers, C.; Lance, M.; Nierlich, M. *J. Chem. Soc., Dalton Trans.* **1998**, 3021.
- ¹³ Torraca, K. E.; McElwee-White, L. *Coord. Chem. Rev.* **2000**, *206-207*, 469.
- ¹⁴ (a) Narayanan, B. A.; Amatore, C.; Kochi, J. K. *Organometallics* **1986**, *5*, 926. (b) Narayanan, B. A.; Kochi, J. K. *J. Organomet. Chem.* **1984**, *272*, C49.
- ¹⁵ Elmurr, N.; Sheats, J. E.; Geiger, W. E.; Holloway, J. D. L. *Inorg. Chem.* **1979**, *18*, 1443.
- ¹⁶ (a) Peters, J. C.; Johnson, A. R.; Odom, A. L.; Wanandi, P. W.; Davis, W. M.; Cummins, C. C. *J. Am. Chem. Soc.* **1996**, *118*, 10175. (b) Wanandi, P. W.; Davis, W. M.; Cummins, C. C.; Russell, M. A.; Wilcox, D. E. *J. Am. Chem. Soc.* **1995**, *117*, 2110.
- ¹⁷ (a) Laplaza, C. E.; Johnson, M. J. A.; Peters, J. C.; Odom, A. L.; Kim, E.; Cummins, C. C.; George, G. N.; Pickering, I. J. *J. Am. Chem. Soc.* **1996**, *118*, 8623. (b) Laplaza, C. E.; Cummins, C. C. *Science* **1995**, *268*, 861. (c) Laplaza, C. E.; Odom, A. L.; Davis, W. M.; Cummins, C. C.; Protasiewicz, J. D. *J. Am. Chem. Soc.* **1995**, *117*, 4999.

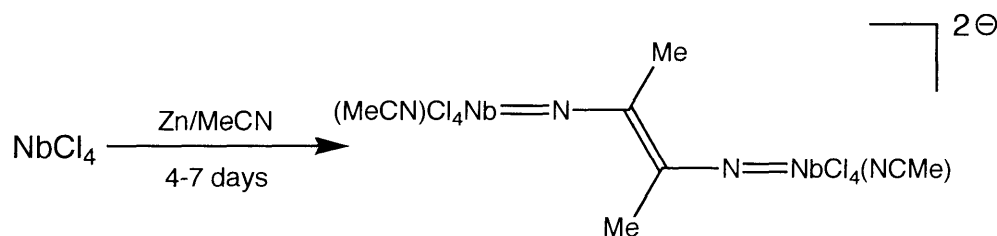
1

Radical reactions at a Mo-coordinated nitrile

Portions of the following have appeared in *Inorganic Chemistry* **42**, 8621
(2003). Reproduced with permission

1.1 Introduction

In 1975, McCarley and co-workers observed that treatment of MeCN solutions of Nb and Ta halides with Zn resulted in activation of the MeCN solvent and resultant formation of dinuclear complexes in which the bridging ligand had been formed by C-C coupling of two MeCN molecules.¹ As shown in Equation 1, the use of NbCl₄ resulted in the isolation of $\{[\mu^2\text{-NC(Me)C(Me)N}][\text{NbCl}_4(\text{MeCN})]_2\}^{2-}$. Since that time, it has been demonstrated that the reductive coupling of nitriles is a general feature of the reactivity of low-valent, early transition metals, having been observed for Ti(II)² and Ti(III)³, Ta(III),⁴ and W(IV).⁵ In this regard, it is rather reminiscent of the Pinacol coupling of carbonyl compounds, which is also mediated by a wide variety of reducing metal centers. The reductive coupling of nitriles, however, differs in that it can be carried out in either one-electron or two-electron (per metal) fashion. Thus while the Nb compound discussed above is best described as containing an ene-diimido bridging ligand (in which each nitrile has been reduced by two electrons), examples are also known in which the bridging ligand is better described as a diiminato ligand.



Equation 1

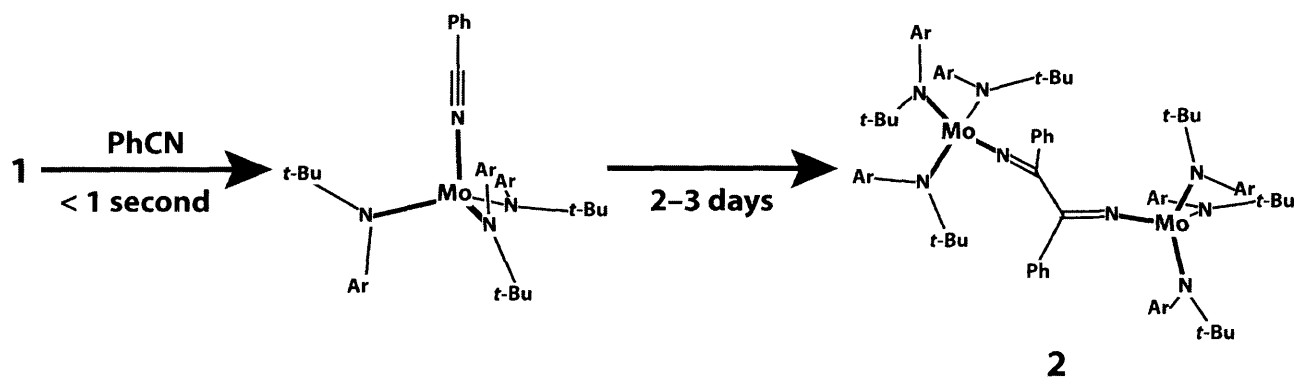
To date, mechanistic information on nitrile reductive coupling remains rather scarce. While the reaction is postulated to occur through reactive, mononuclear, nitrile adducts, the rapidity of the reaction has, in general, precluded the observation of such compounds. In 2003, we reported that three-coordinate $\text{Mo}(\text{N}|t\text{-Bu|Ar})_3$ (**1**) reacted with PhCN to form an observable 1:1 adduct (**1**•PhCN) which dimerized sluggishly.⁶ In the first section of this chapter we present detailed characterization data on **1**•PhCN, including a reassignment of its structure, along with crystallographic characterization of its C–C coupled dimer **2**.

Subsequent sections focus on the extension of the reactivity of **1**•PhCN beyond simple dimerization. We show that **1**•PhCN engages in atom abstraction, E–E bond

cleavage ($E = S, Se, Te, P$), radical combination, and cross-coupling with other organometallic radicals; in all cases, reaction occurs at the nitrile carbon of coordinated PhCN. Ligand-centered reactivity in organometallic radicals is an active area of research.⁷ Such reactivity is typically observed in cases in which delocalization of the unpaired electron into a ligand orbital allows the metal center to maintain an 18-electron configuration. The reactions presented here constitute unique examples of reaction at coordinated nitrile,⁸ which occur despite the presence of an electronically *unsaturated* metal center. In addition, they constitute a new synthesis of metal ketimide compounds, which have recently come under increasing scrutiny.⁹

1.2 Complexation of PhCN by **1**

As first reported by Tsai, treatment of **1** with PhCN results in a rapid color change to deep purple and formation of a new, paramagnetic product.⁶ While this product persists for several hours at concentrations of *ca.* 0.1M, concentration leads to irreversible formation of a C-C bonded dimer (see Equation 2). The dimer is also formed when solutions are allowed to stand for 2-3 days.



The solid-state structure of the dimer (**2**), shown in Figure 2, illustrates clearly that **2** is the product of symmetrical coupling of two **1**•PhCN units through the nitrile carbon. The central C–C distance of 1.503(3) Å is flanked by C–N distances of 1.313(2) Å and 1.314(3) Å, wholly consistent with a di-iminato formulation featuring two Mo(IV) centers. The angle at the ketimide nitrogens is approximately 167°. As shown in Table 1, these structural parameters are relatively similar to those observed in the analogous acetonitrile dimer.

Previous work has established that an analogous synthetic route allows preparation of the variant of **2** in which the *t*-butyl groups have been replaced by isopropyl groups.⁶ Compound **2**^{*i*-Pr} was shown to be readily oxidized using excess I₂, thereby generating the triiodide salt [**2**^{*i*-Pr}][I₃]. The solid-state structure of this compound contains a crystallographic inversion center relating one Mo center to the other, indicating a Class III mixed valent compound.¹⁰ Relative to **2**, [**2**^{*i*-Pr}][I₃] features a contracted Mo–N bond, an elongated N–C bond, a contracted C–C bond and a more linear Mo–N–C angle. These structural changes can be rationalized by viewing the monocation as occupying an intermediate position between the neutral compound and the dication depicted in Table 1. Supporting this supposition is the existence, in the cyclic voltammogram of **2**^{*i*-Pr}, of *two* oxidation waves, suggesting that the dication is a viable species.

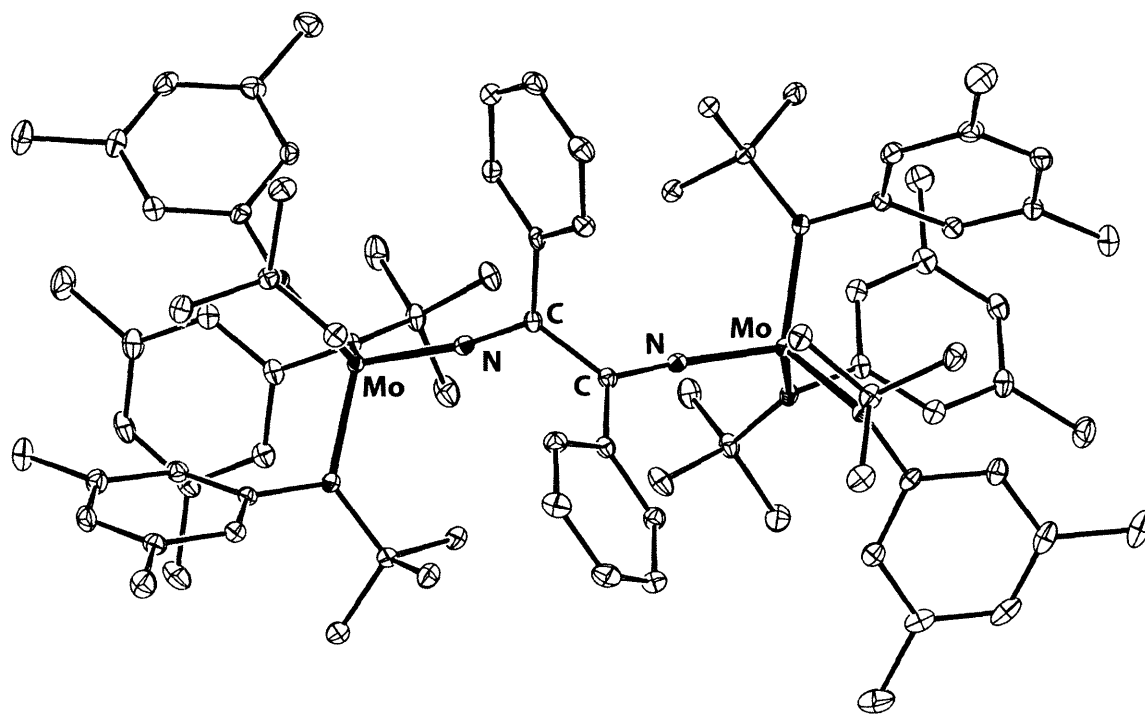
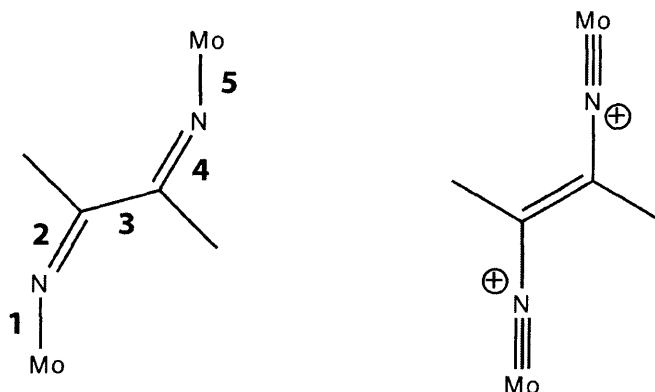


Figure 1 Solid-state structure of **2** (30% ellipsoids).



Parameter	2	(1•MeCN) ₂	[2 ^{2-Pr}][I ₃]
1	1.811(2)	1.814(8)	1.740(5)
2	1.313(3)	1.325(12)	1.393(8)
3	1.503(3)	1.43(2)	1.368(12)
4	1.314(3)	1.325(12)	1.393(8)
5	1.820(2)	1.814(8)	1.740(5)
Mo-N-C	166.74 (avg.)	161.7(8)	175.6(5)

Table 1 Comparison of structural parameters for nitrile dimers (Å/deg)

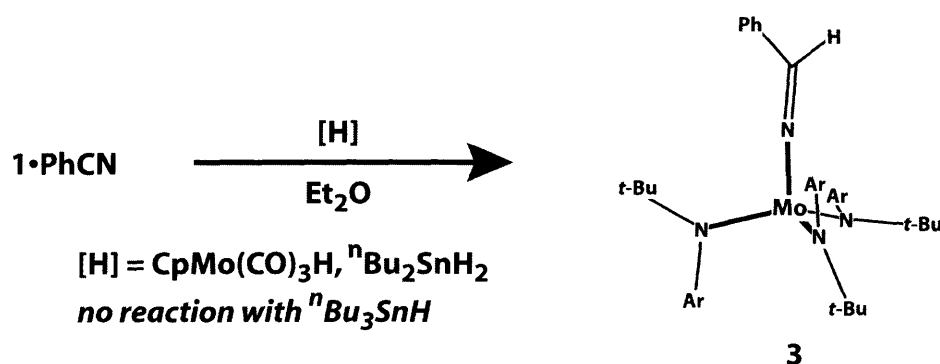
Whereas 1•PhCN was originally postulated to contain an η^2 coordinated nitrile,⁶ subsequent physical characterization suggests that the nitrile is likely η^1 coordinated. Complexation of PhCN to **1**, a ground-state quartet, along its three-fold axis should destabilize the $d(z^2)$ orbital, resulting in electron-pairing to give a doublet ground state. This supposition is borne out by the observed solution magnetic moment of 2.00(5) B.M. (293 K, Evans' method). Diagnostic evidence as to the coordination mode of PhCN is found from IR spectroscopy. While η^1 nitrile adducts typically exhibit C-N stretches in 2000-2400 cm^{-1} range, η^2 coordination results in a large shift to lower energy.¹¹ In collaboration with Prof. Carl Hoff, we have observed a band at 2030 cm^{-1} , which we assign to the C-N stretch of η^1 coordinated PhCN.

The binding of PhCN to **1** is readily followed by UV-vis spectroscopy in combination with stopped-flow techniques. In collaboration with Prof. Rybak-Akimova and her group at Tufts University, it has been found that although PhCN binding appears to be stoichiometric when probed by ¹H NMR, the interaction between **1** and PhCN is actually one of equilibrium binding. At room temperature, K_{eq} is approximately 45 M^{-1} and it

increases steadily with decreasing temperature; at $-40\text{ }^{\circ}\text{C}$, $K_{\text{eq}} = 3120\text{ M}^{-1}$. As will be shown below, the presence, in solutions of $1\bullet\text{PhCN}$, of small but non-negligible concentrations of **1** can have significant effects on reaction outcomes.

1.3 Reaction of $1\bullet\text{PhCN}$ with hydrogen atom donors

The observation that $1\bullet\text{PhCN}$ undergoes facile dimerization suggested that it may exhibit radical reactivity at the nitrile carbon. As hydrogen atom abstraction is a typical reaction of carbon-based radicals, it was decided to examine the reactivity of $1\bullet\text{PhCN}$ with a variety of H-dot donors.



Equation 3

When a freshly-prepared, purple, pentane solution of $1\bullet\text{PhCN}$ is treated with one equivalent of crystalline $\text{CpMo}(\text{CO})_3\text{H}$,^{12,13} a color change to deep blue along with precipitation of a red solid is observed over 5 minutes. Removal of the red solid (presumed to be $[\text{CpMo}(\text{CO})_3]_2$) followed by crystallization from Et_2O resulted in the isolation of $(\text{Ar}[t\text{-Bu}]\text{N})_3\text{Mo}-\text{N}=\text{C}(\text{Ph})\text{H}$ (**3**) as large blue blocks in 53% yield. Compound **3** is diamagnetic and exhibits a resonance at 7.41 ppm attributed to the aldimine proton.

The solid-state structure of **3** is shown in Figure 2. Of note is the short Mo-N(4) distance of 1.7896(12) Å as compared to the average Mo-amide distance of 1.9725 Å. This contraction is likely a consequence of the hybridization change upon going from an amide to a ketimide nitrogen, as well as the π -acceptor character of the ketimide ligand. The ability of the N-C π^* orbital to act as a π -acceptor is facilitated by the nearly linear ($166.84(11)^\circ$) Mo-N-C angle. A relevant structural comparison is to the parent ketimide complex $(\text{Ar}[t\text{-Bu}]\text{N})_3\text{Mo}-\text{N}=\text{CH}_2$ (**4**) prepared by deprotonation of the cationic

methylimido complex.¹⁴ Compared to **3**, **4** features similar Mo–N and N–C distances (1.777(4) and 1.300(7) respectively) although the Mo–N–C unit is considerably closer to linearity ($\angle\text{Mo–N–C} = 178.04(4)^\circ$). As will be seen, this feature appears to be unique to parent ketimide **4**.

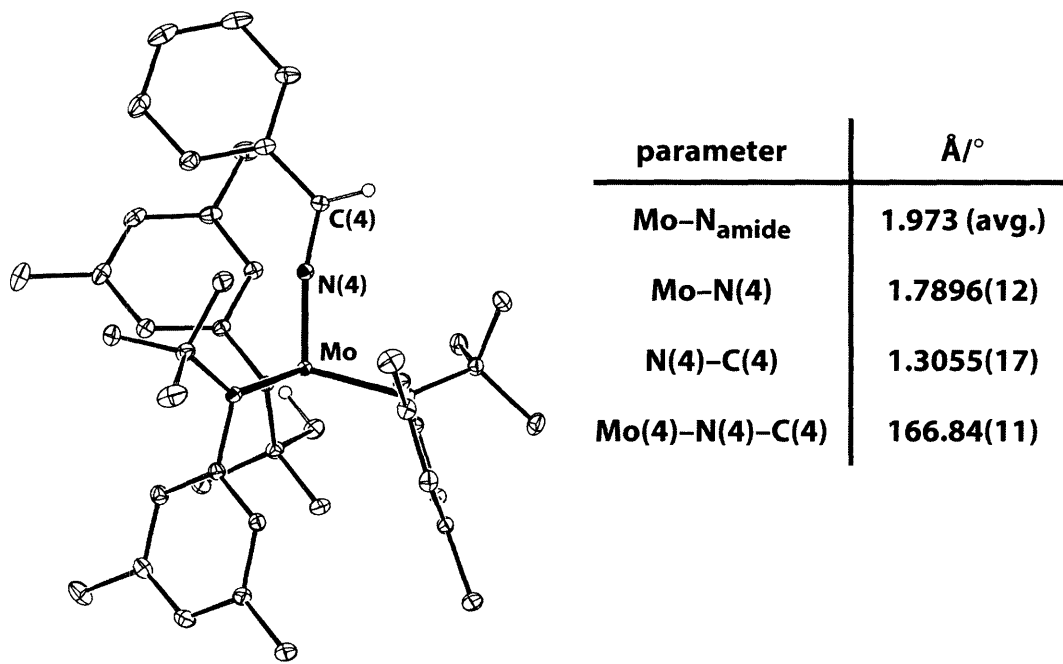
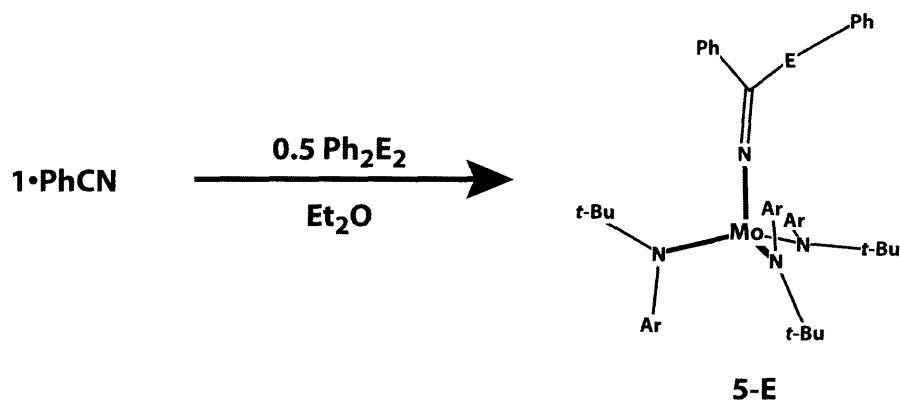


Figure 2 Solid-state structure of **3** (30% ellipsoids).

Compound **3** can also be prepared by reaction of **1**•PhCN with 0.5 eq. ⁿBu₂SnH₂. While the reaction appears to be quantitative by ¹H NMR, the presence of the Sn byproduct hinders isolation, rendering the former method more attractive for synthetic purposes. Interestingly, **1**•PhCN shows no reaction with ⁿBu₃SnH. ⁿBu₃SnH is known to be a less active H dot donor than ⁿBu₂SnH₂, for both steric and electronic reasons.¹⁵

1.4 Reaction with diphenyldichalcogenides

Sequential room-temperature treatment of **1** (0.05 M in Et₂O solvent) with 1.0 equiv of PhCN and 0.5 equiv of PhEPh (E = S or Se) furnishes cleanly the



Equation 4

corresponding chalcogenobenzimidates $\text{Ph}[\text{PhE}]\text{C}=\text{N})\text{Mo}(\text{N}[\text{t-Bu}]\text{Ar})_3$ (see Equation 4). These dark blue compounds, **5-S** and **5-Se**, were isolated in yields of 64% and 70%, respectively, and were characterized structurally by single-crystal X-ray diffraction methods. The molecular structure of **5-S** is shown in Figure 3; **5-Se** is isomorphous. As in **3**, the Mo-ketimide distance in **5-S** is short, at 1.794(5) Å, and the angle at the ketimide nitrogen is 164.3(4)°. The possibility that **5-E** (E = S, Se) formation is a consequence of the direct reaction of **1** with PhEPh to produce thiolate or selenolate complexes **6-E** followed by PhCN insertion is ruled out by control experiments in which **6-S** and **6-Se** (synthesized independently from **1** and Ph_2S_2 or Ph_2Se_2) were treated

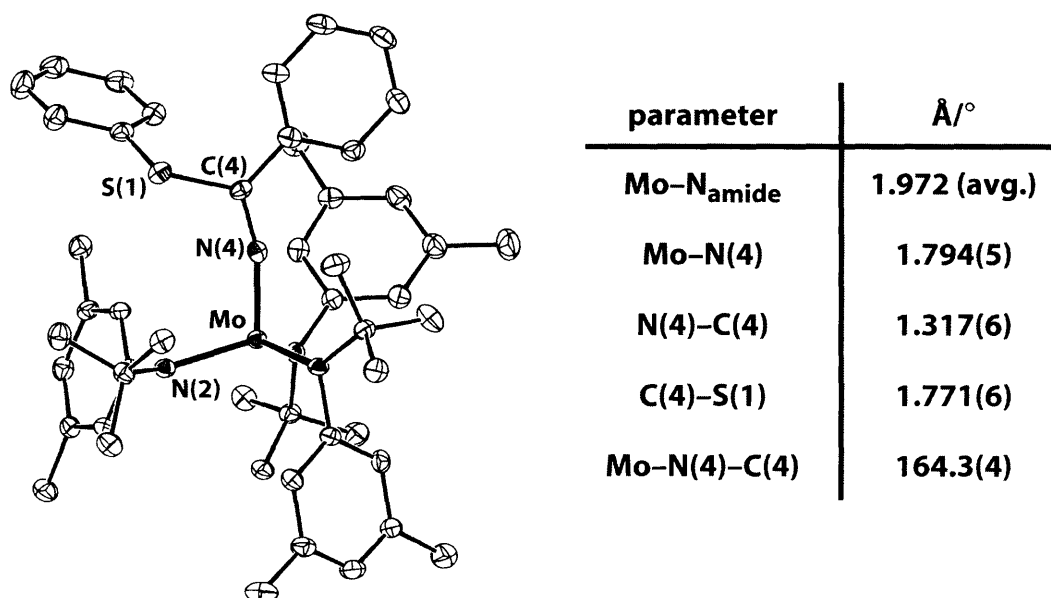


Figure 3 Solid-state structure of **5-S** (50% ellipsoids, one out of two molecules in the asymmetric unit).

with 10 equiv of PhCN under the synthesis reaction conditions and found to undergo no reaction.

Interestingly, use of PhTeTePh in the above synthesis did *not* result in tellurobenzimidate **5-Te** formation. Specifically, sequential room-temperature treatment of **1** (0.05 M in Et₂O) with 1.0 equiv of PhCN and 0.5 equiv of PhTeTePh led exclusively to phenyltellurolate PhTe–Mo(N[*t*-Bu]Ar)₃ (**6-Te**) formation. Nitrile was not incorporated. The solid-state structure of **6-Te** is shown in Figure 4.

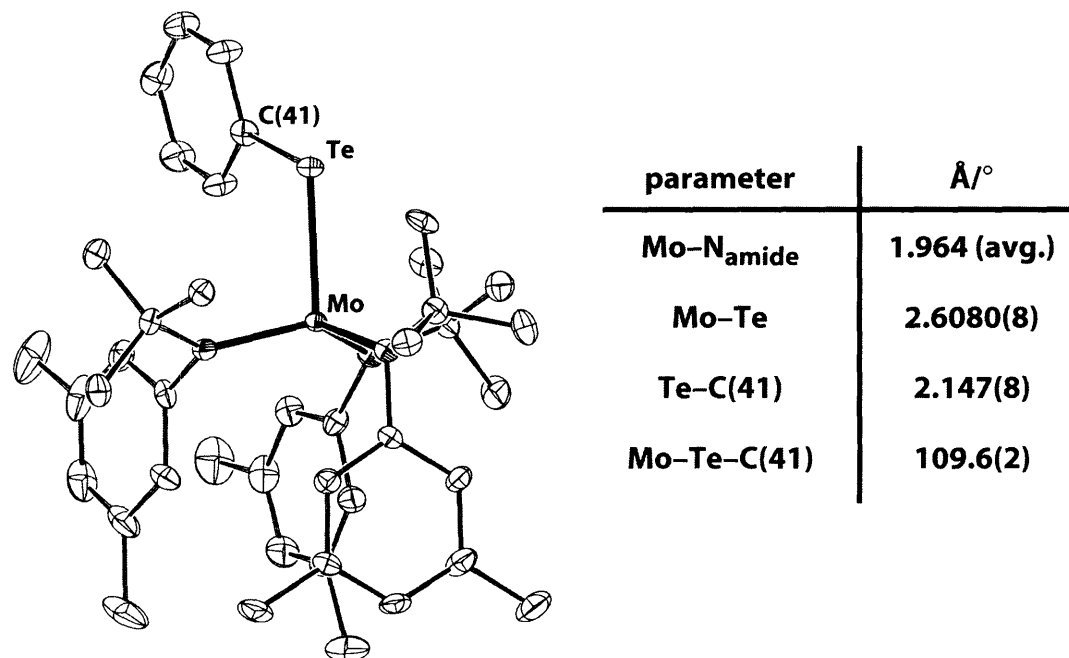


Figure 4 Solid-state structure of **6-Te** (50% ellipsoids).

Two possible mechanisms can be envisioned for the formation of **6-Te** in the above reaction. As illustrated in Scheme 1, one pathway involves prior dissociation of PhCN from **1**•PhCN (*vide supra*) followed by direct reaction of **1** with PhTeTePh. Consistent with this proposal is the observation that **6-Te** is readily synthesized from the direct reaction of **1** with PhTeTePh. An alternate pathway begins with formation of **5-Te**, in analogy to the results for S and Se. Postulated to occur next is a facile β-TePh elimination to generate the observed **5-Te** along with release of PhCN.

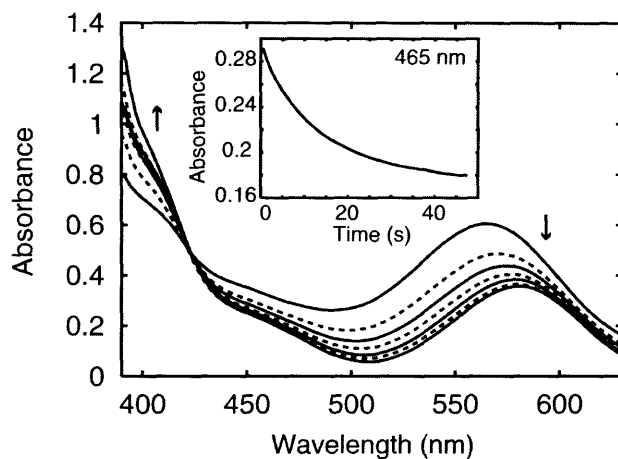
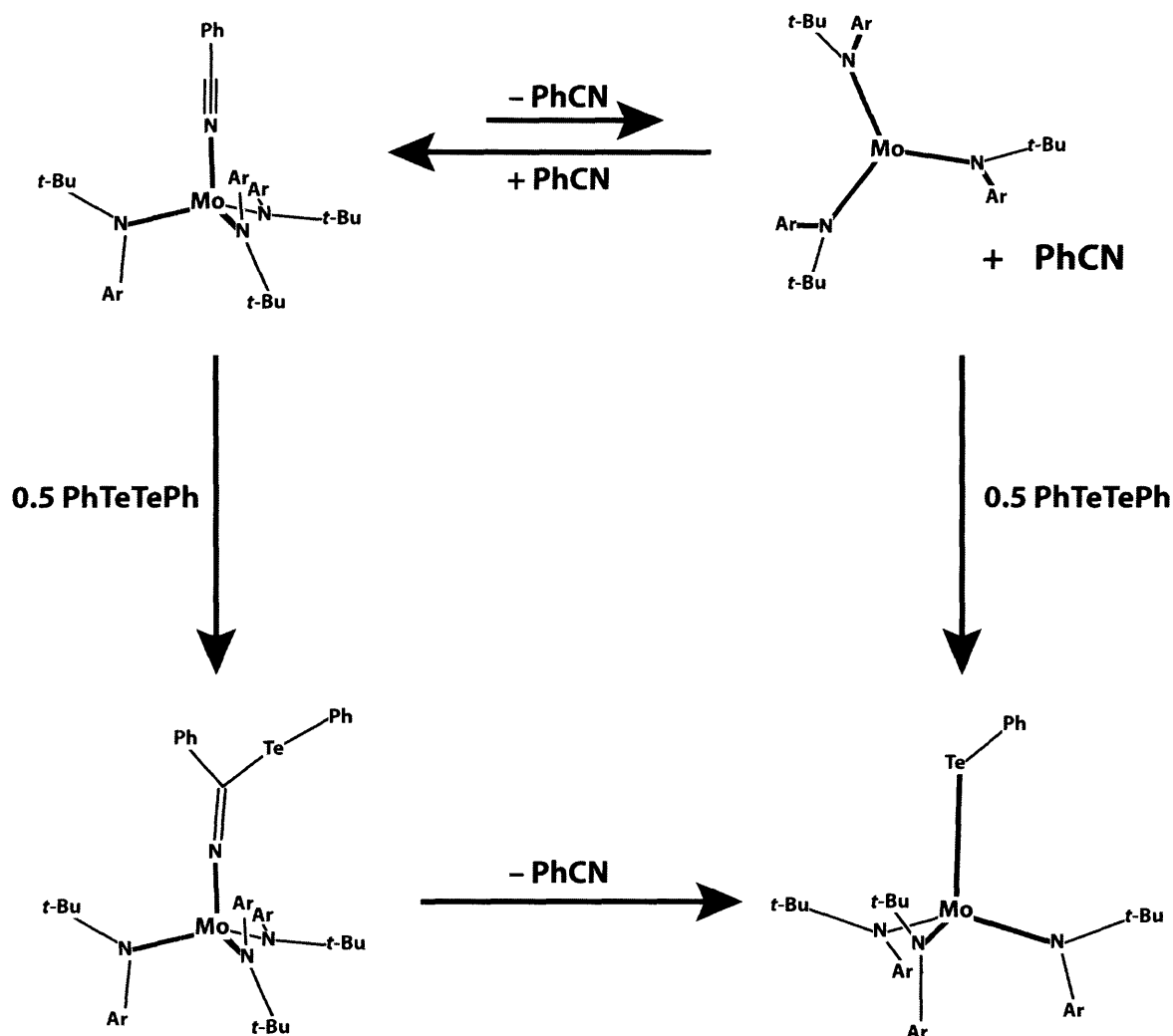


Figure 5 Spectral changes accompanying the reaction of **1**•PhCN and Ph₂Te₂ at -40 °C.

To probe this issue, we once again turned to stopped-flow spectroscopy. First, the binary reaction between **1** and PhTeTePh was probed, in the absence of added PhCN. Kinetic measurements (carried out by the group of Prof. Rybak-Akimova at Tufts University) indicated this reaction to be first order in each reactant with the following activation parameters: $\Delta H^\ddagger = 11.6 \text{ kJ mol}^{-1}$, $\Delta S^\ddagger = -141 \text{ J K}^{-1} \text{ mol}^{-1}$. Shown in Figure 5 are kinetic data for this reaction obtained at -40 °C. When the reaction was conducted in the presence of 1 equivalent of PhCN, a very similar kinetic profile was observed, with no evidence for an intermediate corresponding to **5**-Te. Thus, under these conditions, the reaction proceeds via initial dissociation of PhCN. However, as the concentration of PhCN was increased, small amounts of a new compound were observed. This compound had a UV-vis spectrum very similar to that of **5**-S and **5**-Se, and its formation was promoted both by high PhCN concentrations and by low temperature. When the reaction was carried out in the presence of a 40-fold excess of PhCN, clean formation of the new product was observed in the temperature range -50 °C to +5 °C. This new reaction was first-order in **1** and PhTeTePh, with activation parameters ($\Delta H^\ddagger = 15.8 \text{ kJ mol}^{-1}$, $\Delta S^\ddagger = -121 \text{ J K}^{-1} \text{ mol}^{-1}$) that differed significantly from those for the formation of **6**-Te. The data suggest that the combination of high PhCN concentration and low temperature shifts the PhCN binding equilibrium to the right, thereby allowing for the formation of **5**-Te.

Further evidence for the formation of **5**-Te came from the adaptation of the above procedure to the glovebox. THF solutions of PhTeTePh and of **1** with *ca.* 40 equivalents of PhCN were prepared and pre-cooled to -35 °C. Upon mixing, the solution rapidly took



Scheme 2 Possible pathways for the formation of **6-Te** from **1•PhCN**.

on a characteristic blue color, as opposed to the green color of **5-Te**. UV-vis spectra of solutions prepared in this manner reproduced those obtained in the stopped-flow apparatus. In addition, interrogation of this solution by ^{125}Te NMR yielded a singlet at +699 ppm, which compares favorably to the value of +617 ppm obtained computationally for $(\text{H}[\text{PhTe}]\text{C}=\text{N})\text{Mo}(\text{NH}_2)_3$. Computations on $(\text{PhTe})\text{Mo}(\text{NH}_2)_3$ predict a shift of +1572 ppm, although our attempts to observe such a signal for **6-Te** have thus far been unsuccessful.

1.5 Reaction with P_4

Similar to what was observed in the case of PhTeTePh, treatment of **1•PhCN** with 0.5 equivalents of P_4 results in exclusive formation of the previously synthesized terminal

phosphide (Ar[*t*-Bu]N)₃MoP (**7**) when carried out in the presence of 1-5 equivalents of PhCN in rapidly thawing toluene.¹⁶ However, when the reaction mixture is held at -35 °C for 2 hours in the presence of *ca.* 40 equivalents of PhCN, a blue solution results. A work-up involving removal of excess PhCN by short-path distillation (40 °C, full vacuum), precipitation with MeCN, and subsequent crystallization from Et₂O results in the isolation of [(Ar[*t*-Bu]N)₃Mo-N=C(Ph)]₂(P₄) (**8**) in moderate yield. The structural assignment of **8** is based primarily on its ³¹P NMR spectrum (shown in Figure 6), which consists of a triplet at -147 ppm and a triplet at -339 ppm, with J_{P,P} = 175 Hz. Additionally, the ¹³C NMR exhibits a doublet at 151 ppm (J_{C,P} = 11 Hz), assigned to the former nitrile carbon of PhCN. These parameters are similar to those observed for other compounds featuring the bicyclic R₂P₄ unit.¹⁷⁻²⁰

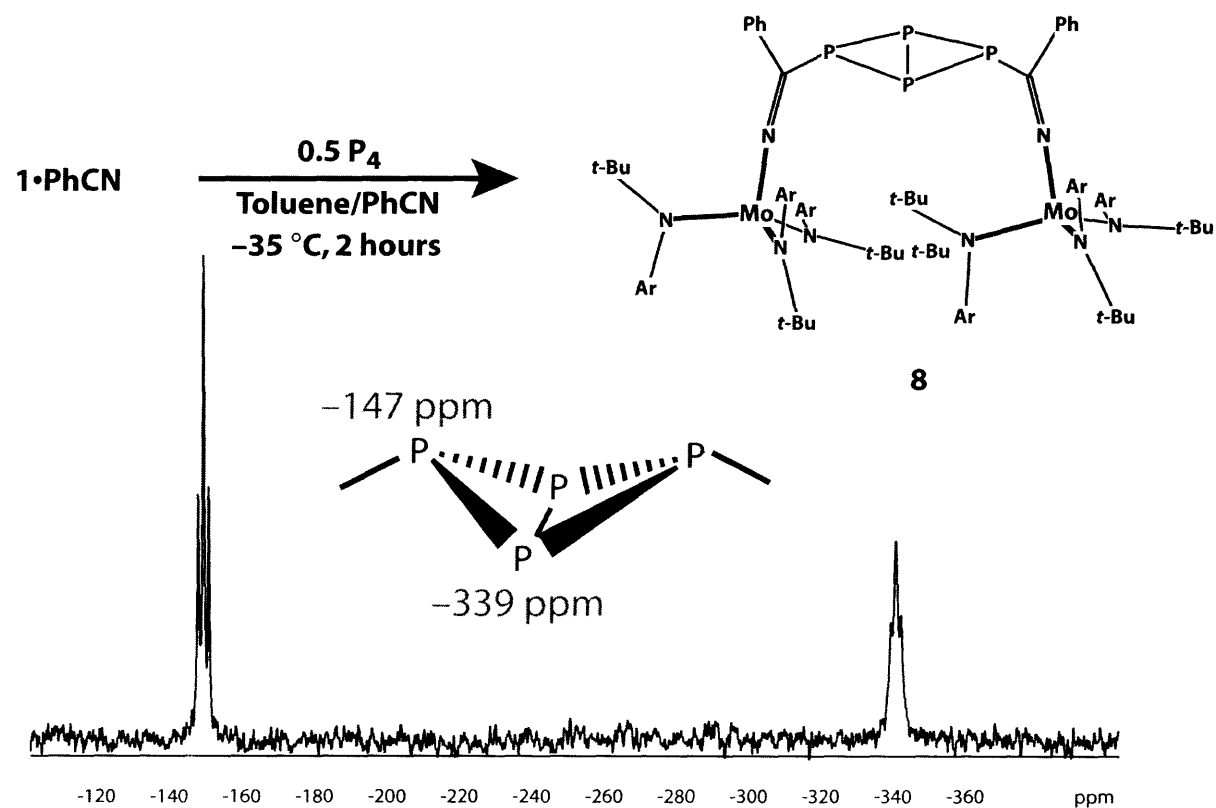


Figure 6 Synthesis and ³¹P NMR spectrum of **8**.

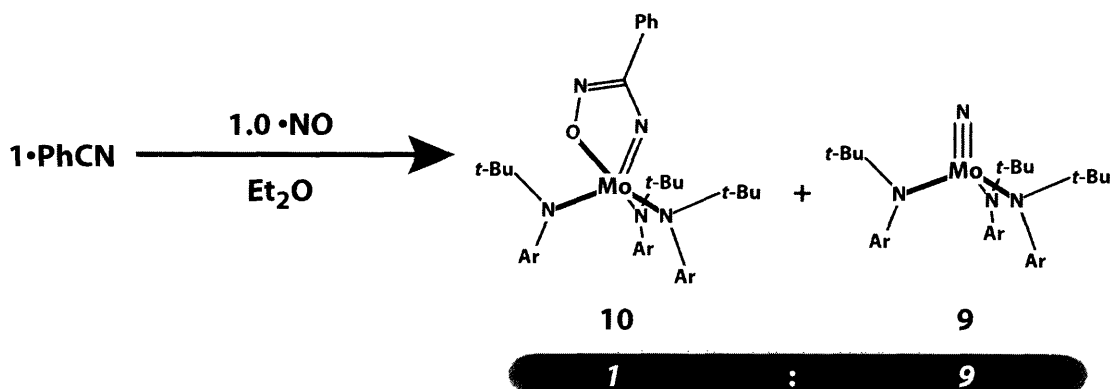
The formation of **8** illustrates the ability of PhCN to attenuate the reactivity of **1**. Thus, while **1** is capable of the complete destruction of the P₄ tetrahedron to generate terminal phosphide **7**, prior coordination of PhCN results in a gentle element activation, in which only one bond of the P₄ tetrahedron has been cleaved. In addition, the formation of a C-P bond is of interest with respect to organophosphorus chemistry. Compounds

similar to **8** have been previously synthesized (generally in low yield) by alkali metal reduction of RPX_2 compounds ($X = \text{Cl}, \text{Br}$),¹⁷ treatment of P_4 with aryllithium reagents,¹⁸ and irradiation¹⁹ or thermolysis²⁰ of compounds containing P–P bonds. A computational study on the parent tetraphosphabicyclobutane, H_2P_4 , has also been carried out.²¹

1.6 Reaction with NO

The small, gaseous molecule NO represents a unique example of an easily accessible, sterically unhindered free radical. As such, its reaction with **1**•PhCN was of considerable interest. If the reaction were to proceed as envisioned, the product would be a Mo(IV) ketimide bearing phenyl and nitroso substituents. Such a moiety would perhaps be most closely related to acylnitroso compounds of the form $\text{RC}(\text{O})\text{NO}$. Such compounds are commonly generated *in situ*, and undergo rapid cycloadditions with unsaturated substrates.²²

When an Et_2O solution of freshly prepared **1**•PhCN was treated with 1 equivalent of NO at $-78\text{ }^\circ\text{C}$ and allowed to warm to room temperature, it took on a pale brown color. Rather surprisingly, ^1H NMR analysis indicated that the major product was the molybdenum terminal nitride $(\text{Ar}[t\text{-Bu}]\text{N})_3\text{MoN}$ (**9**).²³ Also observed, as perhaps 10% of the total isolated material, was a new product **10** that exhibited, in addition to the usual anilide resonances, a set of resonances corresponding to a phenyl group.



Equation 5

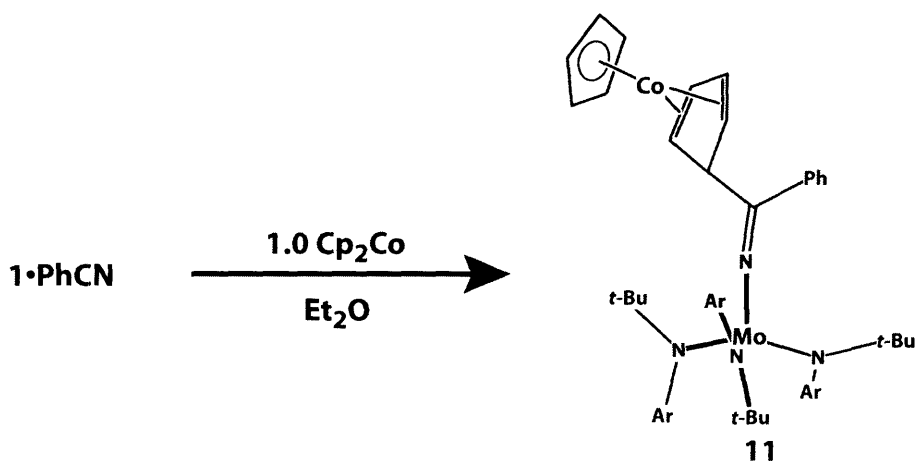
Fortunately, **10** was readily separated from **9** due to its low solubility in pentane. Crystals grown from a THF/ Et_2O mixture were subjected to an X-ray diffraction study. While the data were of low quality and the crystal was plagued by extensive disorder, it

was unambiguously determined that the connectivity was as drawn in equation 5. Compound **10** is the first structurally verified example of *bona fide* 5-coordination in the (Ar[t-Bu]N)₃Mo system. Previously characterized in this group is the η² nitrile complex (η²-Me₂NCN)Mo(N[t-Bu]Ar)₃.⁶ Taken together, these results suggest that pentacoordination can be achieved through the use of a relatively small, chelating ligand.

While the formation of **10** is readily rationalized, the formation of **9** is rather more difficult to understand, and we have yet to conceive of a compelling mechanism. The following observations rule out various mechanistic scenarios. Compound **10** is stable for at least 2 days at 80° C; thus **10** cannot be an intermediate in the formation of **9**. One might envision that the *equilibrium* nature of PhCN binding to **1** could be responsible for the observed complexity; moreover, free **1** is known to bind NO irreversibly. However, varying the reaction temperature and the initial nitrile concentration (both of which affect *K*_{eq} of binding) has no observable effect on the product distribution. More tellingly, isolated **1**•NO shows no reaction with PhCN, even when an excess is used.

1.7 Reaction with Cobaltocene

Cobaltocene has enjoyed wide use as an outer-sphere reductant since its synthesis in 1953.^{24,25} Cobaltocene differs from ferrocene, whose synthesis preceded it by only two years, by the presence of one additional electron, thus neatly explaining its competence as a reductant.^{26,27}



Equation 6

When freshly-prepared, ethereal **1**•PhCN is treated with one equivalent of solid cobaltocene, a rapid color change to deep blue is observed (see Equation 6). This new compound is freely soluble in pentane, an observation inconsistent with salt formation. ¹H NMR analysis indicates the quantitative formation of a new, diamagnetic product (**11**) with one intact Cp ring and one split into three resonances at 2.75, 3.68 and 4.81 ppm, characteristic of an *exo*-substituted cyclopentadiene ring.²⁸ On the basis of these data, the product is formulated as (Ar[*t*-Bu]N)₃Mo-N=C(Ph)(η⁴-C₅H₅)Co(η⁵-Cp) in which a new C-C bond has been formed at the nitrile carbon, and one Cp ring has been converted into an η⁴ diene ligand. This formulation is confirmed by an X-ray diffraction study, as shown in Figure 7. The pyramidal geometry at C56 is the most striking structural manifestation of the electronic rearrangement of the lower Cp ring. A comparison of C-C distances within the ring is also instructive. The unperturbed Cp ring has C-C distances ranging from 1.386–1.414 Å; in the lower ring, the C56–C510 and C56–C57 distances are both 1.515(4) Å, consistent with single bonds, whereas the other three bonds in the ring are between 1.410–1.411 Å, consistent with a conjugated diene moiety. The newly-formed C4–C56 bond has a length of 1.535(4) Å.

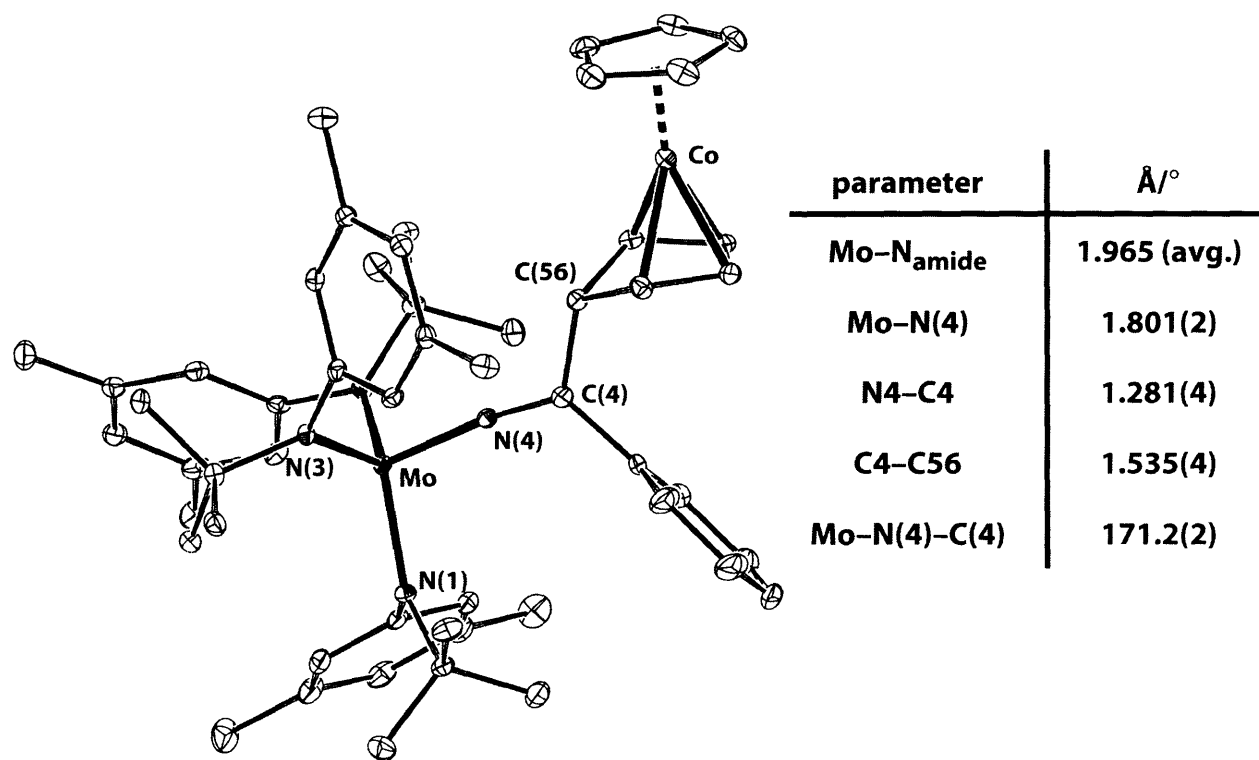


Figure 7 Solid state structure of **11** (35% ellipsoids).

While alkyl halides have been shown to undergo ring addition to cobaltocene,²⁸ more direct precedent for the above reaction comes from a 1992 report by Herberich and coworkers. As shown in Figure 8, reduction of $[\text{CpNi}(\text{C}_4\text{Ph}_4)]\text{Br}$ to the neutral species is smoothly accomplished with one equivalent of cobaltocene; however, when *two equivalents* of cobaltocene are employed, the bimetallic compound $\text{CpNi}[\mu, \eta^3: \eta^4-(\text{C}_4\text{Ph}_4-\text{C}_5\text{H}_5)]\text{CoCp}$ is isolated, along with $[\text{Cp}_2\text{Co}]\text{Br}$.²⁹ Intriguingly, this compound is reported to undergo reversible dissociation to $\text{CpNi}(\text{C}_4\text{Ph}_4)$ and cobaltocene at temperatures above -10°C . We have seen no evidence for such a process in the case of **11**.

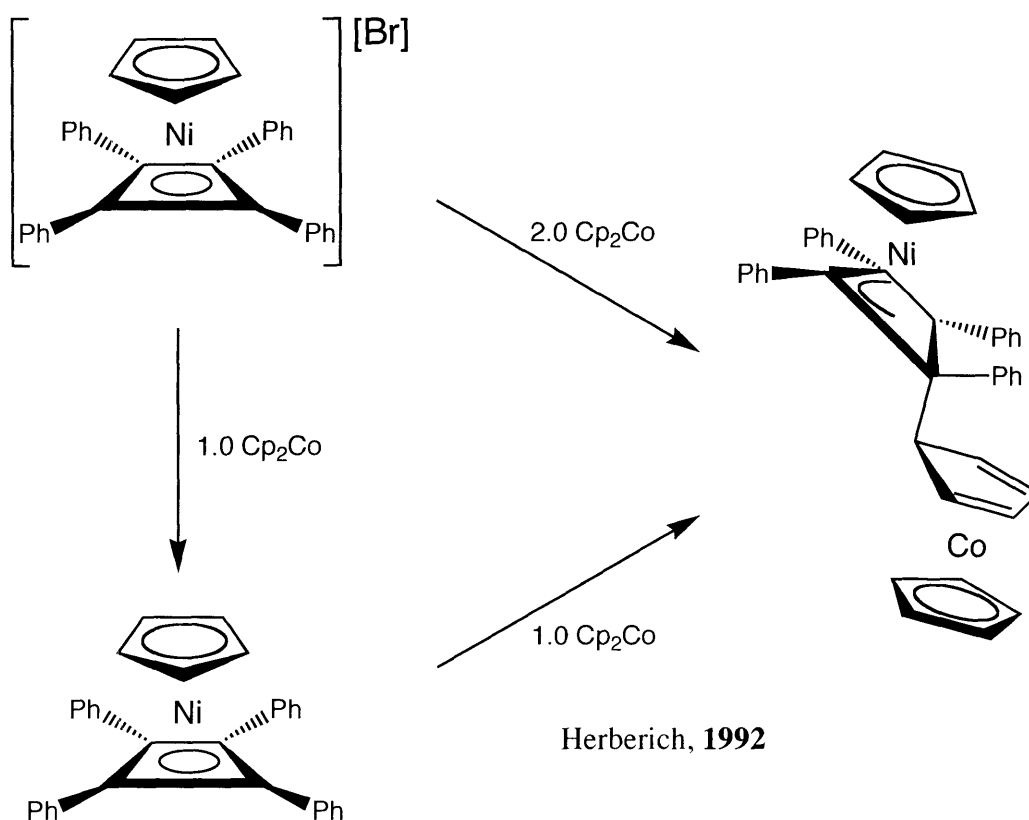
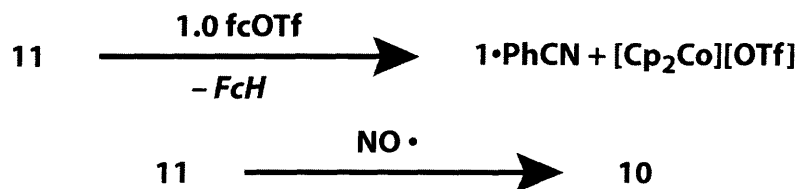


Figure 8

In an aesthetically appealing turn of events, the reductive coupling of PhCN and cobaltocene can be reversed by treatment with ferrocenium triflate. As shown in equation 7, purified **11** reacts with ferrocenium triflate over 90 minutes to regenerate $\mathbf{1}\cdot\text{PhCN}$ along with $[\text{Cp}_2\text{Co}][\text{OTf}]$. The formation of $\mathbf{1}\cdot\text{PhCN}$ was verified by color and by its reaction with PhSSPh to generate **2-S**.



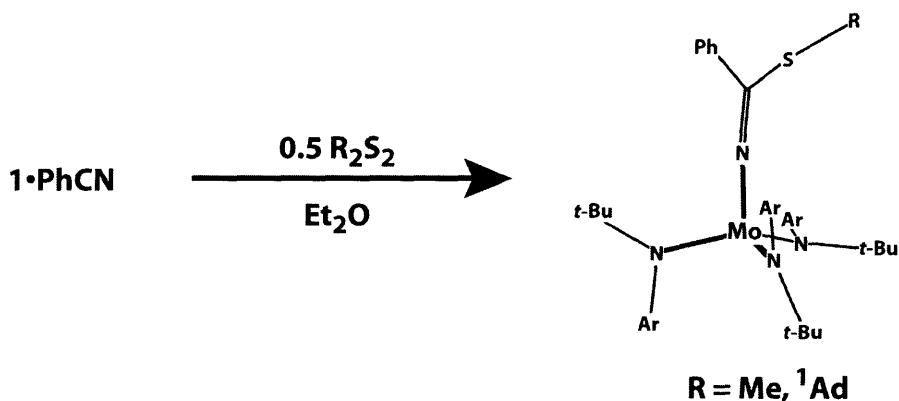
Equations 7 and 8

The reactivity profile of **11** is not limited to oxidative bond cleavage. Treatment of ethereal **11** with NO at 0 °C results in a color change to brown over 30 minutes. ¹H NMR analysis indicates that the major product is **10**, previously synthesized in low yield from **1•PhCN** and NO. The fact that nitride **9** is not observed in the reaction mixture suggests that **1•PhCN** is not an intermediate in this reaction. A plausible mechanistic scheme is as follows. In the first step, NO attacks at the ketimide carbon, resulting in a neutral imido of Mo(V). This intermediate can then undergo a radical fragmentation to lose cobaltocene and generate the observed product. Previous work in these labs has shown that compounds featuring the Mo(N[*t*-Bu]Ar)₃ fragment in the +5 oxidation state are often thermally unstable towards Mo(VI) products.³⁰

1.8 A brief mechanistic excursion

The preceding results provide clear demonstration of the ability of **1•PhCN** to serve as a source of carbon-based radical. An interesting question is whether these reactions proceed through direct attack of **1•PhCN** on the incoming reagent (an S_H2 process)³¹ or through a mechanism involving outer-sphere electron transfer. In the case of the reaction of **1•PhCN** with diphenyldichalcogenides, the latter mechanism would be followed by decomposition of the resulting dichalcogenide radical anion to chalcogenyl radical and chalcogenate.

The former should be quite sensitive to steric effects, whereas the latter should be relatively insensitive. Thus, we should be able to distinguish between the two mechanisms if we are able to find a pair of electronically similar but sterically dissimilar reaction partners for **1•PhCN**.



Equation 9

Accordingly, we chose to investigate the reaction of $1 \bullet \text{PhCN}$ with Me_2S_2 and ${}^1\text{Ad}_2\text{S}_2$ (see Equation 9). The former is commercially available, while the latter is readily obtained from the corresponding thiol.³² In the presence of only one equivalent of PhCN, the reaction of $1 \bullet \text{PhCN}$ with 0.5 equivalents of Me_2S_2 produces large amounts of $(\text{Ar}[t\text{-Bu}]\text{N})_3\text{Mo-SMe}$ (**12**). However, increasing the nitrile concentration and lowering the temperature allows for the synthesis of $(\text{Ar}[t\text{-Bu}]\text{N})_3\text{Mo-N}=\text{C}(\text{Ph})\text{SMe}$ (**13**) as the major product. The reaction is initiated at $-35\text{ }^\circ\text{C}$ and is allowed to warm to room temperature, whereupon it is observed to be complete. In contrasting fashion, ${}^1\text{Ad}_2\text{S}_2$ shows no reaction with $1 \bullet \text{PhCN}$; after 3 days, dimer **2** is the only observable product. This pair of observations suggests that, at least in the case of disulfides, $1 \bullet \text{PhCN}$ reacts via an $\text{S}_{\text{H}2}$ mechanism.³³

1.9 Reactions of **1** with other nitriles

As mentioned above, **1** forms an isolable, structurally characterized adduct with Me_2NCN .⁶ We have found that this adduct reacts with PhSSPh in an analogous fashion to $1 \bullet \text{PhCN}$, albeit at an attenuated rate. The solid-state structure of $(\text{Ar}[t\text{-Bu}]\text{N})_3\text{Mo-N}=\text{C}(\text{NMe}_2)\text{SPh}$ (**14**) is shown in Figure 9. It is intriguing to speculate that protonation or alkylation at the dimethylamino substituent may significantly perturb the electronic structure at the metal.

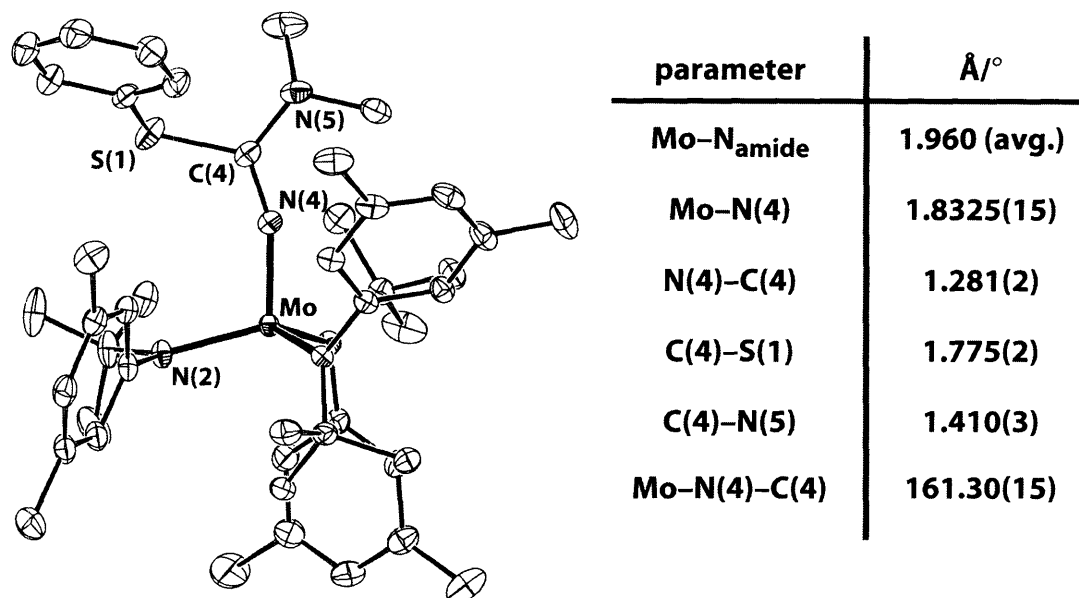


Figure 9 Solid-state structure of **14** (35% ellipsoids).

In contrast to Me₂NCN, the sterically similar reagents pivalonitrile, isovaleronitrile, and isobutyronitrile exhibit no detectable reaction with **1**. At present, we do not have a satisfactory explanation for this observation.

1.10 Conclusions

We have expanded the characterization of **1**•PhCN, a rare example of an intermediate in nitrile reductive coupling. PhCN interacts with **1** reversibly and in an η¹ fashion. Coordination of PhCN activates the nitrile carbon towards reaction with a variety of one-electron reagents such as tin hydrides, dichalcogenides, elemental phosphorus, NO, and cobaltocene. Comparison of reaction rates between Me₂S₂ and ¹Ad₂S₂ suggests an S_H2 mechanism for these reactions.

1.11 Experimental

General Considerations: Unless stated otherwise, all operations were performed in a Vacuum Atmospheres drybox under an atmosphere of purified nitrogen. Anhydrous diethyl ether was purchased from Mallinckrodt; pentane, n-hexane, and tetrahydrofuran (THF) were purchased from EM Science. Diethyl ether, toluene, benzene, pentane, and n-hexane were dried and deoxygenated by the method of Grubbs.³⁴

THF was distilled under nitrogen from purple sodium benzophenone ketyl. Distilled solvents were transferred under vacuum into vacuum-tight glass vessels before being pumped into a Vacuum Atmospheres drybox. C_6D_6 was purchased from Cambridge Isotopes and were degassed and dried over 4 Å sieves. THF- d_8 was passed through a column of activated alumina and stored over 4 Å sieves. The 4 Å sieves, alumina, and Celite were dried in vacuo overnight at a temperature just above 200 °C. Compounds **1**,³⁵ **6-*Se***,³⁰ $CpMo(CO)_3H$,³⁶ were prepared by literature methods. PhCN was distilled under vacuo before use and stored in a nitrogen-filled drybox. $CpMo(CO)_3H$ was sublimed before use. Elemental phosphorus was recrystallized from dry toluene and stored at -35 °C in the dark. All other compounds were used as received. 1H and ^{13}C NMR spectra were recorded on Unity 300, Mercury 300 or Varian INOVA-501 spectrometers at room temperature, unless indicated otherwise. ^{13}C NMR spectra are proton decoupled. Chemical shifts are reported with respect to internal solvent: 7.16 ppm and 128.38 (t) ppm (C_6D_6). ^{125}Te NMR spectra were recorded on a Varian INOVA-501 spectrometer and referenced to external Ph_2Te_2 in $CDCl_3$ (420 ppm with respect to Me_2Te). UV-vis absorption spectra were collected on a HP 8452A diode array spectrometer fitted with an HP 89090A Peltier temperature controller. CHN analyses were performed by H. Kolbe Mikroanalytisches Laboratorium (Mülheim, Germany). A summary of the compound numbering scheme is given in Table 2.

Evans' Method determination on **1•PhCN:** A solution of hexamethyldisiloxane (85 mg) and benzonitrile (47 mg, 0.46 mmol) in C_6D_6 (880 mg) was prepared. A small quantity of this solution was transferred to a small capillary which was then flame-sealed. **1** (28.9 mg, 0.046 mmol) was dissolved in 666 mg of the previously prepared solution and transferred to an NMR tube, into which was placed the previously mentioned capillary. Two peaks corresponding to hexamethyldisiloxane were observed in the 1H NMR, separated by 98 Hz ($\nu_o = 299.856$ MHz), corresponding to an effective magnetic moment of 2.00 B. M. This procedure was repeated two times, yielding values of 2.04 and 1.95 B. M.

Compound	
1	Mo(N[<i>t</i> -Bu]Ar) ₃
2	(Ar[<i>t</i> -Bu]N) ₃ Mo–N=C(Ph)C(Ph)=N–Mo(N[<i>t</i> -Bu]Ar) ₃
3	(Ar[<i>t</i> -Bu]N) ₃ Mo–N=C(Ph)H
4	(Ar[<i>t</i> -Bu]N) ₃ Mo–N=CH ₂
5-E	(Ar[<i>t</i> -Bu]N) ₃ Mo–N=C(Ph)EPh (E = S, Se, Te)
6-E	(Ar[<i>t</i> -Bu]N) ₃ Mo–EPh (E = S, Se, Te)
7	(Ar[<i>t</i> -Bu]N) ₃ MoP
8	[(Ar[<i>t</i> -Bu]N) ₃ Mo–N=C(Ph)] ₂ (P ₄)
9	(Ar[<i>t</i> -Bu]N) ₃ MoN
10	(Ar[<i>t</i> -Bu]N) ₃ Mo(<i>cyclo</i> -ONC(Ph)N)
11	(Ar[<i>t</i> -Bu]N) ₃ Mo–N=C(Ph)(η ⁴ -C ₅ H ₅)Co(η ⁵ -Cp)
12	(Ar[<i>t</i> -Bu]N) ₃ Mo–SMe
13	(Ar[<i>t</i> -Bu]N) ₃ Mo–N=C(Ph)SMe
14	(Ar[<i>t</i> -Bu]N) ₃ Mo–N=C(NMe ₂)SMe

Table 2

Synthesis of 3: A scintillation vial was charged with **1** (200 mg, 0.32 mmol) and 5 mL of pentane. PhCN (33 mg, 0.32 mmol) was added resulting in a rapid color change to purple. To this solution was added solid CpMo(CO)₃H (79 mg, 0.32 mmol) and the solution was allowed to stir for 40 minutes. After this time, the solution was dark blue and copious red precipitate had formed. The reaction mixture was filtered through Celite and the filtrate concentrated to dryness. Recrystallization from Et₂O (–35 °C) furnished **3** as large blue blocks (2 crops, 123 mg, 53%). ¹H NMR (500 MHz, C₆D₆): δ 1.30 (s, 27H, CMe₃); 2.18 (s, 18H, C₆H₃Me₂); 6.55 (d, 2H, Ph *ortho*); 6.67 (s, 6H, Ar *ortho*); 6.67 (t, 1H, Ph *para*); 6.69 (s, 3H, Ar *para*); 7.17 (t, 2H, Ph *meta*), 7.44 (s, 1H, N=CH) ppm. ¹³C NMR (75 Hz, C₆D₆): 21.31 (C₆H₃Me₂); 31.27 (CMe₃); 62.28 (N–CMe₃); 122.28; 124.42; 127.04; 127.30; 129.03; 135.77; 137.23; 150.27; 156.49 ppm. Anal. Calcd. for C₄₃H₆₀N₄Mo: C, 70.86; H, 8.30; N, 7.69. Found: C, 70.66; H, 8.23; N, 7.31.

Synthesis of 5-S: To an Et₂O solution of **1** (197 mg, 315 μmol) was added 32.5mg PhCN (315 μmol, 1 equiv). The solution took on an intense purple color. An Et₂O

solution (1 mL) of PhSSPh (34.4 mg, 158 μmol , 0.5 equiv) was then added dropwise over a few seconds. At the conclusion of the addition, the solution was blue. An aliquot taken at this time showed complete conversion to the desired product by ^1H NMR spectroscopy. Volatiles were removed in vacuo, and the resulting residue was dissolved in the minimal amount of ether, filtered through Celite, and stored at $-35\text{ }^\circ\text{C}$. Dark blue crystals grew over three days (169 mg, 64%). ^1H NMR (300 MHz, C_6D_6): $\delta = 7.336$ (d, 2H, S-Ph *ortho*); 7.066 (t, S-Ph and t, PhCN); 6.944 (br s, 6H, $\text{C}_6\text{H}_3\text{Me}_2$ *ortho*), 6.858 (t, 1H, S-Ph *para*); 6.831 (br, PhCN *ortho*); 6.688 (s, 3H $\text{C}_6\text{H}_3\text{Me}_2$ *para*); 2.193 (s, 18H, $\text{C}_6\text{H}_3\text{Me}_2$); 1.296 (br s, 27H, $\text{C}(\text{CH}_3)_3$) ppm. ^{13}C NMR (125 MHz, C_6D_6): $\delta = 160.87$ (Mo-N=C); 144.03; 138.02; 137.00; 129.486; 128.66; 127.95; 127.53; 126.44; 125.38; 124.81; 124.6; 63.87 (br, N- $\text{C}(\text{CH}_3)_3$); 31.64 (br, N- $\text{C}(\text{CH}_3)_3$); 21.75 ($\text{C}_6\text{H}_3\text{Me}_2$) ppm; 1 aryl peak missing. UV (25° , Et_2O): $\lambda_{\text{max}} = 251$ ($\epsilon = 41000$); 331 ($\epsilon = 19500$); 384 (sh, $\epsilon = 10000$); 576 ($\epsilon = 5900$) nm. Anal. Calcd. For $\text{C}_{49}\text{H}_{64}\text{N}_4\text{SMo}$: C, 70.31; H, 7.71; N, 6.69. Found: C, 70.95; H, 7.34; N, 6.70.

Synthesis of 5-Se: This compound was synthesized in an identical fashion to 5-S substituting PhSeSePh for PhSSPh. Yield: 497 mg, 70%, 2 crops. ^1H NMR (300 MHz, C_6D_6): $\delta = 7.437$ (d, 2H, *ortho* Se-Ph); 7.1-6.8 (multiple overlapping peaks, 14H); 6.950 (br s, 6H, $\text{C}_6\text{H}_3\text{Me}_2$ *ortho*); 6.693 (s, 3H $\text{C}_6\text{H}_3\text{Me}_2$ *para*); 2.187 (s, 18H, $\text{C}_6\text{H}_3\text{Me}_2$); 1.278 (s, 27H, CMe_3) ppm. ^{13}C NMR (125 MHz, benzene): $\delta = 163.81$ (Mo-N=C); 151.51 (br); 138.78; 138.08; 138.05; 129.70; 129.48; 128.25; 127.92; 127.59; 125.81; 125.61; 125.51; 64.01 (br, N- $\text{C}(\text{CH}_3)_3$); 31.54 (br, N- $\text{C}(\text{CH}_3)_3$); 21.77 ($\text{C}_6\text{H}_3\text{Me}_2$) ppm. ^{77}Se NMR (92 MHz, benzene): $\delta = 424$ ppm. UV (25° , THF): $\lambda_{\text{max}} = 344$ ($\epsilon = 14000$); 578 ($\epsilon = 5600$) nm. Anal. Calcd. For $\text{C}_{49}\text{H}_{64}\text{N}_4\text{SeMo}$: C, 66.56; H, 7.30; N, 6.34. Found: C, 66.68; H, 7.39; N, 6.26.

Attempted Synthesis of 5-Te: To a stirring solution of **1** (76 mg, 122 μmol) in Et_2O (2 mL) was added a solution of PhCN (12.5 mg, 1 equiv) in Et_2O (1 mL) *via* pipet. The resulting purple solution was chilled to $-100\text{ }^\circ\text{C}$ in a liquid nitrogen filled coldwell. To the thawing solution was added solid Ph_2Te_2 (24.8 mg, 0.5 equiv). After a few seconds, the solution turned green. The mixture was allowed to warm to room temperature and the

solvent removed *in vacuo*. ^1H NMR analysis of the resulting residue indicated the exclusive presence of **6-Te** and PhCN. Isolation of pure **6-Te** was accomplished by recrystallization from Et₂O (47 mg, 2 crops, 47%).

Glovebox Synthesis of 5-Te: In a typical preparation, a scintillation vial was charged with **1** (30 mg, 0.05 mmol), PhCN (300 mg, *ca.* 60 equiv.), and 1 mL of THF. In a separate vial, PhTeTePh (10 mg, *ca.* 0.5 equiv.) was dissolved in 1 mL THF. Both vials were cooled to $-35\text{ }^\circ\text{C}$ in the glovebox freezer. The vials were then removed from the freezer and immediately combined, resulting in a rapid color change to dark greenish-blue. A UV-vis spectrum taken at this point was identical to that obtained in the corresponding stopped-flow experiments. Removal of THF *in vacuo* yielded a mixture of PhCN and the desired compound. UV (25° , THF): $\lambda_{\text{max}} = 584\text{ nm}$. ^{125}Te NMR (158 MHz, benzene): $\delta = 699\text{ ppm}$.

Synthesis of 6-S: To a stirring solution of **1** (150mg, 240mmol) in Et₂O (2mL) was added Ph₂S₂ (26.4 mg, 0.5 equiv) as a solution in Et₂O (1 mL). The solution was allowed to stir for one hour, at which point it was a dark greenish-blue. Volatiles were removed *in vacuo*, and the resulting residue was extracted with pentane (5 mL) and filtered through Celite. Recrystallization from Et₂O ($-35\text{ }^\circ\text{C}$) furnished the desired compound (80 mg, 3 crops, 45%). ^1H NMR (300 MHz, benzene): $\delta = 8.72$ (d, 2H, *ortho* S-Ph); 7.388 (t, 2H, *meta* S-Ph); 7.15 (t, 1H, *para* S-Ph, partially obscured by C₆D₅H peak); 6.397 (br s, 3H, *para* C₆H₃Me₂); *ca.* 6.2 (br sh, 6H *ortho* C₆H₃Me₂); 2.098 (s, 18H, C₆H₃Me₂); 1.385 (s, 27H, C(CH₃)₃) ppm. ^{13}C NMR (125 MHz, benzene): $\delta = 155.51$; 152.70 (br s, S-C); 136.64; 131.86; 129.56; 128.74; 127.21; 125.76; 63.20 (br, N-C(CH₃)₃); 31.88 (N-C(CH₃)₃); 22.06 (C₆H₃Me₂) ppm. Anal. Calcd. for C₄₂H₅₉N₃S: C, 68.73; H, 8.10; N, 5.73. Found: C, 68.56; H, 8.04; N, 5.64.

Synthesis of 6-Te: To a stirring solution of **4** (100 mg, 160 mmol) in Et₂O (3 mL) was added a solution of PhTeTePh (33 mg, 1 equiv) in Et₂O (1mL) *via* pipet. The solution turned green. Volatiles were removed *in vacuo*, and the resulting residue was extracted with Et₂O. The extract was then filtered through Celite, concentrated, and cooled to -35

°C to afford **6-Te** as large green plates (88.3mg, 2 crops, 66%). UV (25°, Et₂O): λ_{\max} = 270 (ϵ =41000); 463 (ϵ =8000); 608 (ϵ =2000) nm. ¹H NMR (300 MHz, benzene): δ = 8.507 (d, 2H, *ortho* Te-Ph); 7.262 (t, 2H, *meta* Te-Ph); 7.204 (t, 1H, *para* Te-Ph); 6.402 (br s, 3H, *para* C₆H₃Me₂); 6.309 (v br, 6H *ortho* C₆H₃Me₂); 2.052 (s, 18H, C₆H₃Me₂); 1.429 (s, 27H, C(CH₃)₃) ppm. ¹³C NMR (125 MHz, benzene): δ = 152.84 (br s, Te-C); 139.72; 136.61; 129.98; 129.94; 128.66; 127.45; 126.64; 63.19 (br, N-C(CH₃)₃); 31.86 (N-C(CH₃)₃); 21.96 (C₆H₃Me₂) ppm. A ¹²⁵Te NMR signal could not be obtained. Anal. Calcd. for C₄₂H₅₉N₃Te: C, 60.82; H, 7.17; N, 5.10. Found: C, 61.54; H, 6.74; N, 5.03.

Synthesis of 8: A scintillation vial was charged with **1** (404 mg, 0.65 mmol) and toluene (2 mL). Benzonitrile (2.2 g, 21 mmol, *ca.* 33 equiv.) was added and the vial was cooled to -35 °C in the glovebox freezer. In a separate vial was dissolved P₄ (65 mg, 0.52 mmol, 0.8 equiv.) in 5 mL of toluene. This vial was also cooled to -35 °C. The chilled solutions were briefly removed from the freezer, rapidly combined, and then restored the freezer. After 2 h, the reaction mixture had turned blue. The toluene was removed *in vacuo*, and the remainder was transferred to a bulb-to-bulb distillation apparatus with the aid of a little THF. The excess PhCN was then distilled off over 4 hours at *ca.* 40 °C under full vacuum. The resulting residue was slurried in 5 mL MeCN, filtered, washed with additional MeCN (5 mL), and dried *in vacuo* to yield a dark blue solid. ¹H NMR analysis indicated that **8** was the major component of this solid, along with small amounts of **2**, **7**, and HN(*t*-Bu)Ar. Purification was accomplished through recrystallization from Et₂O over several weeks. Yield: 256 mg, 50%. ¹H NMR (500 MHz, C₆D₆): δ 1.27 (s, 27H, CMe₃); 2.33 (s, 18H, C₆H₃Me₂); 6.71 (s, 6H, Ar *ortho*); 6.82 (s, 3H, Ar *para*); 7.05-7.10 (multiple overlapping peaks, 5H, Ph) ppm. ¹³C NMR (125 Hz, C₆D₆): 22.04 (C₆H₃Me₂); 31.65 (CMe₃); 63.32 (N-CMe₃); 126.65; 127.66; 127.89; 128.66; 129.05; 131.21; 137.70; 137.90; 150.55 (d, J_{CP} = 11 Hz) ppm. ³¹P NMR (C₆D₆, 121.5 MHz): -339 (t, J_{PP} = 75 Hz); -147 (t, J_{PP} = 75 Hz). Anal. Calcd. for C₈₆H₁₁₈N₈MoP₄: C, 69.62; H, 8.02; N, 7.55. Found: C, 69.59; H, 7.82; N, 7.43.

Reaction of 1•PhCN with NO: A 100 mL round-bottom flask with sidearm was charged with **1** (200 mg, 0.32 mmol) and 10 mL Et₂O. To the red-orange solution was added

benzonitrile (33 mg, 0.32 mmol) in 2 mL Et₂O. The flask was briefly evacuated, sealed, and transferred to a dry ice/acetone bath. To the cold solution was added NO (7.2 mL, 0.32 mmol) *via* syringe. The dry ice/acetone bath was removed and the reaction mixture was allowed to warm to room temperature. Volatiles were removed *in vacuo*. ¹H NMR analysis revealed a 9:1 mixture of **9** and **10**. Isolation of **10** could be accomplished through washing with copious Et₂O. Yield: 18 mg (7.4 %). ¹H NMR (300 MHz, C₆D₆): δ 1.38 (s, 27H, CMe₃); 2.13 (s, 18H, C₆H₃Me₂); 4.9 (v br, 6H, Ar *ortho*); 6.65 (s, 3H, Ar *para*); 7.16 (t, 1H, Ph *para*); 7.39 (t, 2H, Ph *meta*); 8.56 (d, 2H, Ph *ortho*) ppm. ¹³C NMR (75 MHz, C₆D₆): d 23.08 (C₆H₃Me₂); 35.67 (CMe₃) ppm. IR (C₆D₆): 1600 cm⁻¹ (C=N).

Synthesis of 11: A solution of **1** (150 mg, 0.24 mmol) and PhCN (25 mg, 0.24 mmol) in Et₂O (5 mL) was frozen in the glovebox coldwell. To the thawing solution was added cobaltocene (45 mg, 0.24 mmol) in Et₂O (1 mL). The solution was allowed to warm to room temperature, at which point it was deep bluish-green in color. The reaction mixture was filtered through Celite, and the filtrate concentrated to dryness. ¹H NMR analysis indicates that **11** is the exclusive product. The product is readily purified through recrystallization from pentane (-35 °C). Yield: 154 mg, 70% (3 crops). ¹H NMR (300 MHz, C₆D₆): δ 1.212 (br s, 27H, CMe₃); 2.32 (s, 18H, C₆H₃Me₂); 2.75 (s, 2H); 3.68 (s, 1H); 4.69 (s, 5H, Cp); 4.81 (s, 2H); 6.77 (s, 3H, Ar *para*); 6.79 (s, 6H, Ar *ortho*); 7.01 (t, 1H, Ph *para*); 7.08 (d, 2H, Ph *ortho*); 7.24 (t, 2H, Ph *meta*) ppm. ¹³C NMR (125 Hz, C₆D₆): 22.06 (C₆H₃Me₂); 31.79 (CMe₃); 48.03; 52.12; 63.35 (N-CMe₃); 76.01; 79.47 (Cp); 116.30; 120.98; 126.48; 126.92; 127.64; 132.69; 137.24; 151.5 (br); 174.26 (N=C) ppm. Anal Calcd. for C₅₃H₆₉N₄MoCo: C, 69.42; H, 7.58; N, 6.11. Found: C, 69.28; H, 7.65; N, 5.98.

Reaction of 11 with ferrocenium triflate: Compound **11** (50 mg, 0.054 mmol) was dissolved in ether and cooled to near freezing. Solid ferrocenium triflate was added and the mixture was allowed to warm to room temperature. After stirring for 90 minutes, the reaction mixture had turned purple, indicating the formation of **1**•PhCN, and a precipitate had formed, presumably [Cp₂Co][OTf]. The mixture was then treated with excess Ph₂S₂, causing a rapid color change to the distinctive blue color of **5-S**. The reaction mixture

was filtered through Celite and the filtrate concentrated to dryness. ^1H NMR analysis indicated **5-Se**, PhCN, and ferrocene as the major products. A small amount of HN(*t*-Bu)Ar was present.

Reaction of 11 with NO: A 100 mL round-bottom flask with sidearm was charged with **11** (50 mg, 0.054 mmol) and 10 mL ether. The flask was removed from the glovebox, cooled to 0 °C, and treated with NO (2.5 mL, 0.11 mmol). After stirring for 45 minutes at 0 °C, the reaction mixture had taken on a brown color and some orange brown precipitate was visible. The flask was warmed to room temperature and volatiles were removed *in vacuo*. Analysis of the resulting residue by ^1H NMR indicated **10** as the major (> 70%) anilide-containing product.

Independent synthesis of 12: A vial containing **1** (100 mg, 0.16 mmol) dissolved in 3 mL Et₂O was frozen in the glovebox coldwell. To the thawing solution was added Me₂S₂ (*ca.* 10 mg, 1.3 equivalents) as a solution in Et₂O. The reaction turned blue upon mixing. The mixture was filtered through Celite and the filtrate concentrated to dryness. Recrystallization from Et₂O (-35 °C) furnished the product as large blue needles (82 mg, 76%). ^1H NMR (300 MHz, C₆D₆): δ 1.37 (s, 27H, CMe₃); 2.06 (s, 18H, C₆H₃Me₂); 3.34 (s, S-CH₃); 6.23 (br s, 6H, Ar *ortho*); 6.38 (s, 3H, Ar *para*) ppm. ^{13}C NMR (75 Hz, C₆D₆): 21.58 (C₆H₃Me₂); 31.15 (CMe₃); 34.38 (S-Me); 62.25 (N-CMe₃); 126.43; 136.10; 152.65 ppm (one aryl peak missing).

Attempted synthesis of 13: In a scintillation vial was prepared a solution of **1** (200 mg, 0.32 mmol) in 5 mL Et₂O to which was added PhCN (40 mg, 0.39 mmol). The resulting purple solution was cooled to near freezing in the glovebox coldwell. To the thawing solution was added a solution of Me₂S₂ (15 mg, 0.16 mmol) and the mixture was allowed to warm to room temperature, whereupon it became bright blue in color. Volatiles were removed *in vacuo*. ^1H NMR analysis indicated the presence of **12** and a new product, formulated as **13**, in a 1:1 ratio.

Synthesis of 13: Vial A was charged with **1** (100 mg, 0.16 mmol), PhCN (150 mg, 1.45 mmol), and 3 mL Et₂O. Vial B was charged with a solution of Me₂S₂ (10 mg, 0.10 mmol) in 2 mL Et₂O. Both vials were cooled to -35 °C, at which point the contents of vial B were added to vial A, and the reaction mixture returned to the glovebox freezer. Over the course of 1 h, the reaction mixture turned deep blue. Volatiles were removed *in vacuo*. ¹H NMR analysis showed that **13** was the dominant product, with a small amount of **12** present. ¹H NMR (300 MHz, C₆D₆): 1.30 (br s, 27H, CMe₃); 2.21 (s, 18H, C₆H₃Me₂); 2.24 (s, 3H, S-Me); 6.69 (s, 3H, Ar *para*); 6.75 (t, 1H, phenyl *para*); 6.90 (br s, Ar *ortho*); 7.16 (t, 2H, phenyl *meta*) ppm (phenyl ortho resonance obscured by excess PhCN).

Synthesis of 14: To a scintillation vial containing **1** (100 mg, 0.16 mmol) in 5 mL Et₂O was added Me₂NCN (12 mg, 0.21 mmol). Upon observation of the expected color change to green, PhSSPh (17.5 mg, 0.08 mmol) was added. The solution turned blue over 15 minutes. The solution was filtered through Celite, the filtrate concentrated to dryness, and the residue recrystallized from Et₂O (-35 °C). Yield: 53 mg, 42%. ¹H NMR (300 MHz, C₆D₆): δ 1.33 (s, 27H, CMe₃); 2.21 (s, 6H, NMe₂); 2.24 (s, 18H, C₆H₃Me₂); 6.66 (s, 3H, Ar *para*); 6.94 (tr, 1H, phenyl *para*); 6.96 (s, 6H, Ar *ortho*); 7.17 (tr, 2H, phenyl *meta*); 7.52 (d, 2H, phenyl *ortho*) ppm.

Crystallographic structure determinations: The X-ray crystallographic data collections were carried out on a Siemens Platform three circle diffractometer mounted with a CCD or APEX-CCD detector and outfitted with a low temperature, nitrogen-stream aperture. The structures were solved using direct methods, in conjunction with standard difference Fourier techniques and refined by full-matrix least-squares procedures. Compound **10** was plagued by extensive disorder and was not fully refined. Only the connectivity was determined. A summary of the crystallographic data for complexes **2**, **3**, **5-S**, **5-Se**, **6-Te**, **10**, **11**, and **14** is given in Tables 3 and 4. An empirical absorption correction (either psi-scans or SADABS) was applied to the diffraction data for all structures. All non-hydrogen atoms were refined anisotropically. Unless otherwise specified, all hydrogen atoms were treated as idealized contributions and refined isotropically. All software used for diffraction data processing and crystal-structure solution and refinement are contained

in the SAINT+ (v6.45) and SHELXTL (v6.14) program suites, respectively (G. Sheldrick, Bruker AXS, Madison, WI).

	2	3	5-S	5-Se
formula	C _{92.5} H ₁₁₈ Mo ₂ N ₈ O	C ₄₃ H ₆₀ MoN ₄	C ₁₀₆ H ₁₄₈ Mo ₂ N ₈ O ₂ S ₂	C ₁₀₆ H ₁₄₈ Mo ₂ N ₈ O ₂ Se ₂
fw	1549.83	728.89	1822.32	1912.1
space group	<i>P</i> $\bar{1}$	<i>C</i> 2/ <i>c</i>	<i>P</i> 2 ₁ / <i>n</i>	<i>P</i> 2 ₁ / <i>n</i>
<i>a</i> , Å	11.3936(6)	37.8513(15)	20.534(2)	20.534(2)
<i>b</i> , Å	19.3306(13)	11.7506(5)	24.450(2)	24.450(2)
<i>c</i> , Å	21.5731(13)	20.8316(9)	21.635(2)	21.635(2)
α , deg	102.913(2)			
β , deg	102.449(2)	119.5570(10)	111.261(2)	111.261(2)
γ , deg	102.387(2)			
<i>V</i> , Å ³	4346.7(5)	8059.6(6)	10122.5(18)	10122.5(18)
<i>Z</i>	2	8	4	4
<i>D</i> , g/cm ³	1.184	1.201	1.196	1.255
μ (Mo K α), mm ⁻¹	0.337	0.358	0.340	1.018
temp, K	100	100	193	193
F(000)	1642	3104	3888	4016
GoF(<i>F</i> ²)	1.057	1.065	1.078	1.100
R(<i>F</i>), %	0.0378	0.0312	0.0621	0.0799
wR(<i>F</i>), %	0.1012	0.0786	0.1505	0.1592

Table 3 Crystallographic parameters for **2**, **3**, **5-S**, and **5-Se**.

	6-Te	10	11	14
formula	C ₈₃ H ₁₁₈ Mo ₂ N ₆ Te ₂	C ₄₃ H ₅₉ N ₆ Mo	C ₅₃ H ₆₉ CoMoN ₄	C ₄₅ H ₆₅ MoN ₅ S
fw	1658.92	755.91	916.99	804.02
space group	$P\bar{1}$	$P2_1/n$	$Pca2_1$	$P2_1/c$
a, Å	11.1740(12)	12.3206(12)	16.2038(12)	13.8313(7)
b, Å	18.1215(19)	19.9849(18)	19.2460(19)	14.4109(7)
c, Å	20.134(2)	16.4804(16)	15.3320(15)	22.1159(10)
α, deg	91.445(2)			
β, deg	90.692(2)	90.049(2)	90.00	91.6090(10)
γ, deg	90.663(2)			
V, Å ³	4075.0(7)	4057.90	4781.4(8)	4406.4(4)
Z	2	4	4	4
D, g/cm ³	1.352	1.226	1.274	1.212
μ (Mo K _α), mm ⁻¹	1.054	0.36	0.648	0.380
temp, K	193	193	193	100
F(000)	1704	1600	1936	1712
GoF(F ²)	1.185	n/a	1.091	1.044
R(F), %	0.0566	n/a	0.0390	0.0356
wR(F), %	0.1521	n/a	0.0821	0.0878

Table 4 Crystallographic parameters for **6-Te**, **10**, **11**, and **14**.

¹ Finn, P. A.; King, M. S.; Kilty, P. A.; McCarley, R. E. *J. Am. Chem. Soc.* **97**, 220 (1975).

² Duchateau, R.; Williams, A. J.; Gambarotta, S.; Chiang, M. Y. *Inorg. Chem.* **30**, 4863 (1991).

³ De Boer, E. J. N.; Teuben, J. H. *J. Organomet. Chem.* **153**, 53 (1978).

⁴ (a) Cotton, F. A.; Hall, W. T. *Inorg. Chem.* **17**, 3525 (1978). (b) Cotton, F. A.; Hall, W. T. *J. Am. Chem. Soc.* **101**, 5094 (1979).

⁵ Cross, J. L.; Garrett, A. D.; Crane, T. W.; White, P. S.; Templeton, J. L. *Polyhedron* **23**, 2831 (2004).

⁶ Tsai, Y.-C.; Stephens, F. H.; Meyer, K.; Mendiratta, A.; Gheorghiu, M. D.; Cummins, C. C. *Organometallics* **22**, 2902 (2003).

⁷ Tyler, D.R. *Prog. Inorg. Chem.* **36**, 125.

⁸ Two-electron processes at coordinated nitriles: Kukushkin, V. Y.; Pombeiro, A. J. L. *Chem. Rev.* **102**, 1771 (2002).

⁹ Jantunen, K. C.; Burns, C. J.; Castro-Rodriguez, I.; Da Re, R. E.; Golden, J. T.; Morris, D. E.; Scott, B. L.; Taw, F. L.; Kiplinger, J. L. *Organometallics* **23**, 4682 (2004) and references therein.

-
- ¹⁰ Robin, M. B.; Day, P. *Adv. Inorg. Chem. Radiochem.* **10**, 247 (1967).
- ¹¹ (a) Malarek, M. S.; Logan, B. A.; White, J. M.; Young, C. G. *Organometallics* **23**, 4328 (2004). (b) Michelin, R. A.; Mozzon, M.; Bertani, R.; *Coord. Chem. Rev.* **147**, 299 (1996). (c) Storhoff, B. N.; Lewis, H. C.; *Coord. Chem. Rev.* **23**, 1 (1977).
- ¹² (a) Landrum, J. T.; Hoff, C. D. *J. Organomet. Chem.* **282**, 215 (1985). (b) Amer, S.; Kramer, G.; Poë, A. *J. Organomet. Chem.* **220**, 75 (1981).
- ¹³ H atom abstraction from CpMo(CO)₃H by carbon-centered radicals: Franz, J. A.; Linehan, J. C.; Birnbaum, J. C.; Hicks, K. W.; Alnajjar, M. S. *J. Am. Chem. Soc.* **121**, 9824 (1999).
- ¹⁴ Sceats, E. L.; Figueroa, J. S.; Cummins, C. C.; Loening, N. M.; Van der Wel, P.; Griffin, R. G. *Polyhedron* **23**, 2751 (2004).
- ¹⁵ Kuivila, H. G.; *Synthesis*, 499 (1970).
- ¹⁶ Laplaza, C. E.; Davis, W. M.; Cummins, C. C. *Angew. Chem., Int. Ed. Engl.* **34**, 2042 (1995).
- ¹⁷ Jutzi, P.; Wippermann, T. *J. Organomet. Chem.* **287**, C5 (1985).
- ¹⁸ Riedel, R.; Hausen, H. D.; Fluck, E. *Angew. Chem.* **97**, 1050 (1985).
- ¹⁹ Jutzi, P.; Meyer, U. *J. Organomet. Chem.* **333**, C18 (1987).
- ²⁰ (a) Cowley, A. H.; Knueppel, P. C.; Nunn, C. M. *Organometallics* **8**, 2490 (1989). (b) Jutzi, P.; Brusdeilins, N. *Z. Anorg. Allg. Chem.* **620**, 1375 (1994).
- ²¹ Schoeller, W. W.; Staemmler, V.; Rademacher, P.; Niecke, E. *Inorg. Chem.* **25**, 4382 (1986).
- ²² Recent reviews: (a) Adam, W.; Krebs, O. *Chem. Rev.* **103**, 4131 (2003). (b) Iwasa, S.; Fakhruddin, A.; Nishiyama, H. *Mini-Rev. Org. Chem.* **2**, 157 (2005).
- ²³ Laplaza, C. E.; Odom, A. L.; Davis, W. M.; Cummins, C. C.; Protasiewicz, J. D. *J. Am. Chem. Soc.* **117**, 4999 (1995).
- ²⁴ Connelly, N. G.; Geiger, W. E. *Chem. Rev.* **96**, 877 (1996).
- ²⁵ King, R. B. *Organometallic Synth.*; Academic Press: New York, 1965; Vol. 1, p. 70.
- ²⁶ Kealy, T. J.; Pauson, P. L. *Nature* **168**, 1039 (1951).
- ²⁷ Fischer, E. O.; Jira, R. *Z. Naturforsch., Teil B* **13**, 327 (1953).
- ²⁸ Herberich, G. E.; Bauer, E.; Schwarzer, J. *J. Organomet. Chem.* **17**, 445 (1969).
- ²⁹ Herberich, G. E.; Klein, W.; Kölle, U.; Spiliotis, D. *Chem. Ber.* **125**, 1589 (1992).
- ³⁰ Johnson, A. R.; Davis, W. M.; Cummins, C. C.; Serron, S.; Nolan, S. P.; Musaev, D. G.; Morokuma, K. *J. Am. Chem. Soc.* **120**, 2071 (1998).
- ³¹ March, J.; Smith, J. E. *Advanced Organic Chemistry, 5th Ed.*; John Wiley & Sons: New York, 2001.
- ³² Joergensen, F. S.; Snyder, J. P. *J. Org. Chem.* **45**, 1015 (1980).
- ³³ For a detailed study of the reaction of disulfides with Co-centered radicals, see: Aubart, M. A.; Bergman, R. G. *J. Am. Chem. Soc.* **120**, 8755 (1998).
- ³⁴ Pangborn, A.B.; Giardello, M.A.; Grubbs, R.H.; Rosen, R.K.; Timmers, F.J. *Organometallics* **1996**, *15*, 1518.
- ³⁵ Laplaza, C. E.; Johnson, M. J. A.; Peters, J. A.; Odom, A. L.; Kim, E.; Cummins, C. C.; George, G. N.; Pickering, I. J. *J. Am. Chem. Soc.* **1996**, *118*, 8623.
- ³⁶ Rakowski DuBois, M.; DuBois, D. L.; Vanerveer, M. L.; Haltiwanger, R.C. *J. Inorg. Chem.* **20**, 3064 (1981).

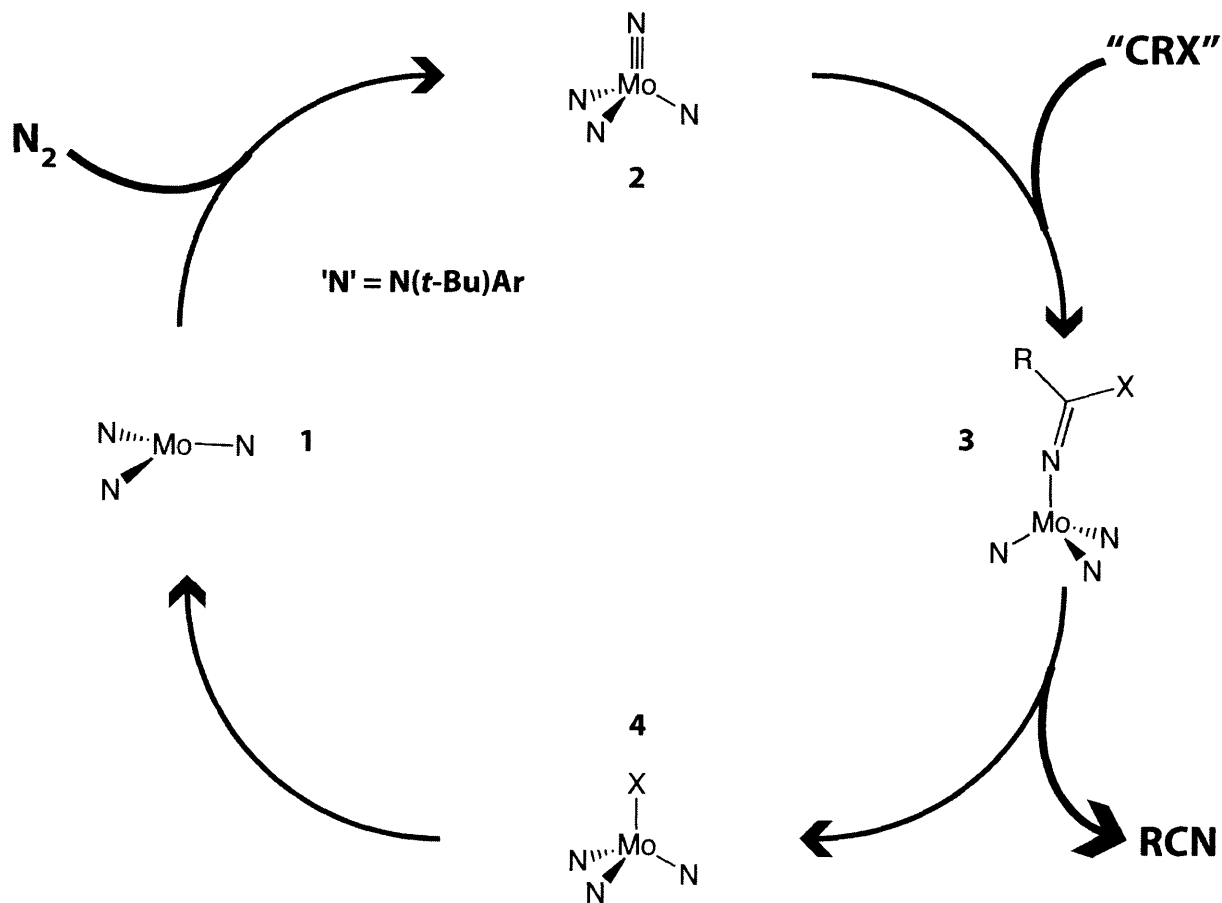
2

Beta-elimination from Mo(IV) ketiminates: A new strategy for Mo–N cleavage

Portions of the following have appeared in *Inorganic Chemistry* **42**, 8621 (2003). Reproduced with permission

2.1 Introduction

Since the isolation of the first transition metal complex of N_2 ,¹ research into the coordination chemistry of N_2 has grown into an exceedingly active field.² The simplicity and ubiquity of N_2 endows its chemistry with inherent interest; this interest is compounded by the immense practical importance of the biological³ and industrial⁴ conversions of N_2 to ammonia, neither of which are—as yet—fully understood. The 1995



Scheme 1 Proposed N_2 functionalization cycle.

report from these labs describing the room temperature cleavage of N_2 by $Mo(N[t-Bu]Ar)_3$ (**1**) was a watershed event in dinitrogen chemistry, expanding significantly on our understanding of N_2 reactivity and pointing to new prospects for the metal-mediated incorporation of N_2 into organic molecules.⁵ The realization of a such a process, however, has been hindered by the high thermodynamic stability of the Mo-N triple bond in $NMo(N[t-Bu]Ar)_3$ (**2**, BDE = 155 kcal/mol).⁶ As such, the development of new methods for the *cleavage* of Mo-N bonds is of critical importance.

In this chapter we demonstrate that appropriately-substituted Mo(IV) benzimidates are subject to β -X elimination, resulting in cleavage of the Mo–N bond with release of benzonitrile. The potential of such a reaction is illustrated by its inclusion in the proposed N₂ functionalization cycle shown in Scheme 1. In such a cycle, Mo(IV) ketimidates are synthesized from terminal nitride **2** and an appropriate carbene; β -X elimination then provides an N₂-derived nitrile along with a Mo–X species which can be reduced back to **1**. The nitrile functionality is an attractive synthetic target due to its ready conversion to a variety of nitrogen-containing molecules, including imines, carboxamides, amines, and heterocycles.⁷ The development of a concise route to such molecules starting from N₂ would have the additional benefit of allowing for the economical synthesis of ¹⁵N-labelled variants.

Beta-X elimination from metal benzimidates is conceptually related to β -X elimination from metal alkyls, which has been most heavily studied in group ten systems.⁸ Prominent among early metal examples is Buchwald's observation that Cp₂Zr(H)Cl (Schwartz's reagent) reacts with ethyl vinyl ether to form Cp₂Zr(Cl)OEt and ethylene, presumably via 1,2 insertion of the olefinic unit followed by β -OEt elimination.⁹ While no intermediates could be observed in this system, Wolczanski has succeeded in measuring β -OR elimination kinetics in the more hindered (silox)₃Ta(H)CH₂CH₂OR.¹⁰ This reaction has also been the subject of a computational study in which the C–X bond strength was determined to be the dominant factor controlling the activation barrier.¹¹ Our experimental results support a similar effect in β -X eliminations from Mo(IV) benzimidates.

2.2 Attempted synthesis of haloketimides

Based on the results presented in Chapter 1, we theorized that treatment of the benzonitrile adduct **1**•PhCN with halogen atom sources should result in haloketimides of the form X(Ph)C=N–Mo(N[*t*-Bu]Ar)₃ (**3**-X, X = Cl, Br, I). As shown in Figure 1, the use of ClCH₂CH₂Cl, BrCH₂CH₂Br, and I₂ as halogen atom sources resulted instead in the isolation of the corresponding Mo(IV) halides **4**-X (X = Cl, Br, I).¹²

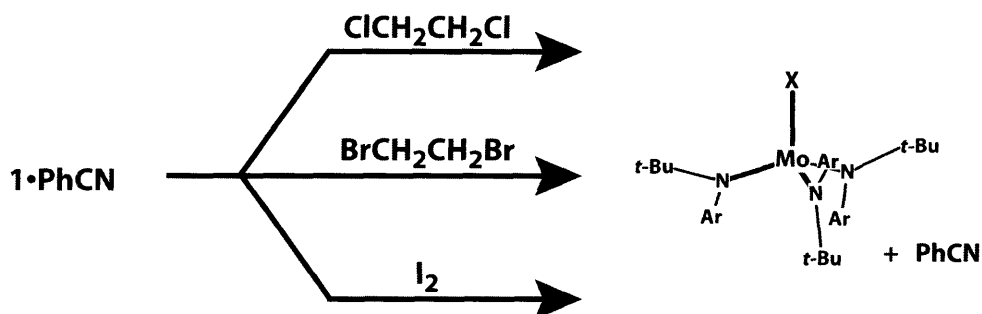


Figure 1. Treatment of $1\bullet\text{PhCN}$ with halogen atom sources.

The reaction of $1\bullet\text{PhCN}$ with $\text{ClCH}_2\text{CH}_2\text{Cl}$ was investigated in more detail, in order to ascertain whether 4-Cl was being formed via the intermediacy of 3-Cl . When the reaction is carried out in the presence of only one equivalent of PhCN , the formation of 4-Cl is complete within 2 hours. As the concentration of PhCN is increased, the rate of 4-Cl formation is attenuated, and the nitrile dimer 2 begins to form in increasing amounts. In the presence of 20 equivalents of PhCN , 2 is the major product, and the formation of 4-Cl has been almost completely suppressed. These observations suggest that 4-Cl is being formed through reaction of $\text{ClCH}_2\text{CH}_2\text{Cl}$ with free 1 present in equilibrium, similar to what was established for the reaction of $1\bullet\text{PhCN}$ with PhTeTePh .

2.3 Nitrile release from $(\text{Ar}[t\text{-Bu}]\text{N})_3\text{Mo-N}=\text{C}(\text{Ph})\text{EPh}$ ($\text{E} = \text{S}, \text{Se}, \text{Te}$)

The results of the previous section suggested the pursuit of compounds of the form 3-X featuring X groups other than halide. We thus embarked on an investigation of the susceptibility of the compounds $(\text{Ar}[t\text{-Bu}]\text{N})_3\text{Mo-N}=\text{C}(\text{Ph})\text{EPh}$ (3-EPh , $\text{E} = \text{S}, \text{Se}, \text{Te}$) synthesized in the previous chapter to $\beta\text{-EPh}$ elimination.

Heating a C_6D_6 solution of 3-SPh to $80\text{ }^\circ\text{C}$ for 2 days elicited no change in its ^1H NMR spectrum. On the other hand, 3-SePh decomposed to several products at temperatures greater than or equal to $37\text{ }^\circ\text{C}$; somewhat encouragingly, $(\text{Ar}[t\text{-Bu}]\text{N})_3\text{Mo-SePh}$ (4-SePh) could be identified in this mixture at early reaction times, despite itself eventually succumbing to decomposition under the thermolysis conditions.

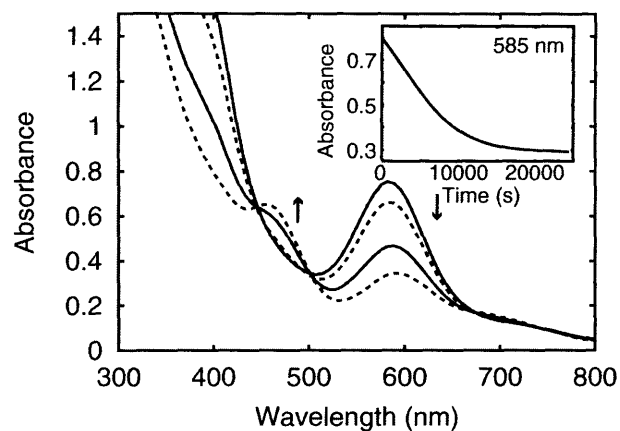
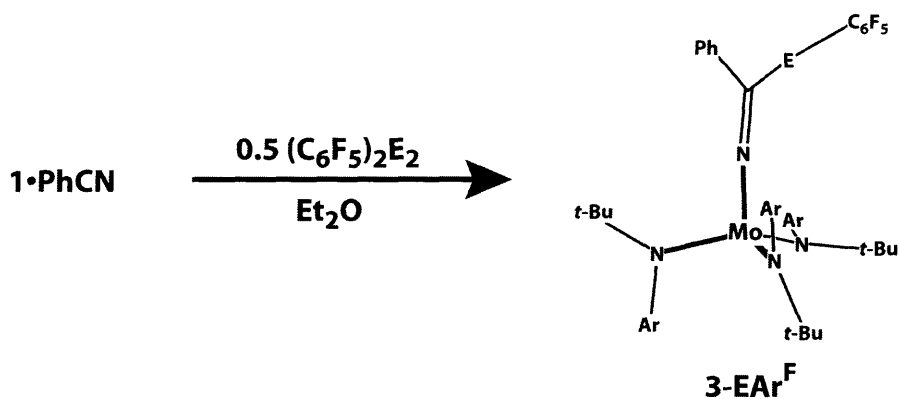


Figure 2. Thermal decomposition of **3-TePh** (35 °C, THF).

Gratifyingly, **3-TePh** was found to cleanly undergo β -elimination to form **4-TePh** and PhCN. Shown in Figure 2 is a stack plot depicting the spectral changes observed upon heating a freshly-prepared THF solution of **3-TePh** to 35 °C. The final spectrum corresponds to the spectrum of independently prepared **4-TePh**; in addition, the reaction exhibits first-order kinetics ($k_{\text{obs}} = 1.2(1) \times 10^{-4} \text{ s}^{-1}$) and isosbestic points can be observed at 448 and 495 nm.

2.4 Nitrile release from fluorinated ketimides

As shown in Equation 1, the fluorinated analogs **3-EAr^F** (E = S, Se) can be synthesized analogously to their unfluorinated counterparts through the use of the fluorinated dichalcogenides Ar^FEEAr^F (E = S, Se). Compound **3-SAr^F** was characterized by UV-vis spectroscopy, ¹H NMR, and X-ray crystallography, while the characterization of **3-SeAr^F** was limited by its thermal instability (*vide infra*) to UV-vis spectroscopy and ¹H NMR.



Equation 1

The solid-state structure of **3-SAr^F** is shown in Figure 3. For the most part, metrical parameters and gross structural features are very similar to those observed for the unfluorinated analog. The C(41)–S(4) distance is only very slightly elongated from 1.771(6) to 1.790(2) Å. Of additional note is the fact that there appear to be no inter- or intramolecular aryl–perfluoroaryl stacking interactions.¹³

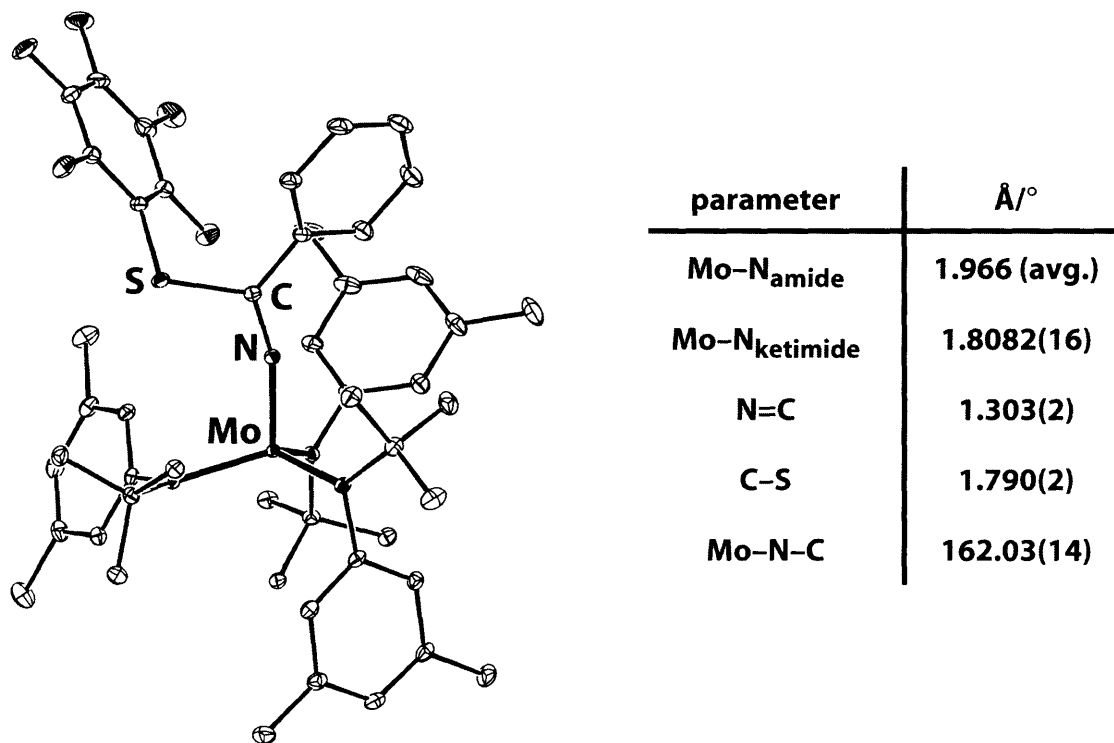


Figure 3. Solid-state structure of **3-SAr^F** (35% ellipsoids, one of two molecules in the asymmetric unit).

Compounds **3-EAr^F** (E = S, Se) undergo clean β -EAr^F elimination at rates that are significantly enhanced relative to their unfluorinated analogs; their half-lives at 25 °C are

6.5 hours ($E = S$) and *ca.* 6 minutes ($E = Se$) respectively. Spectroscopic portraits of these processes are depicted in Figure 4. The identities of the final products of both reactions were confirmed by independent syntheses of $4-EAr^F$ from **1** and Ar^FEEAr^F ($E = S, Se$). The solid-state structure of $4-SAr^F$ is shown in Figure 5. Its structural parameters are unremarkable.

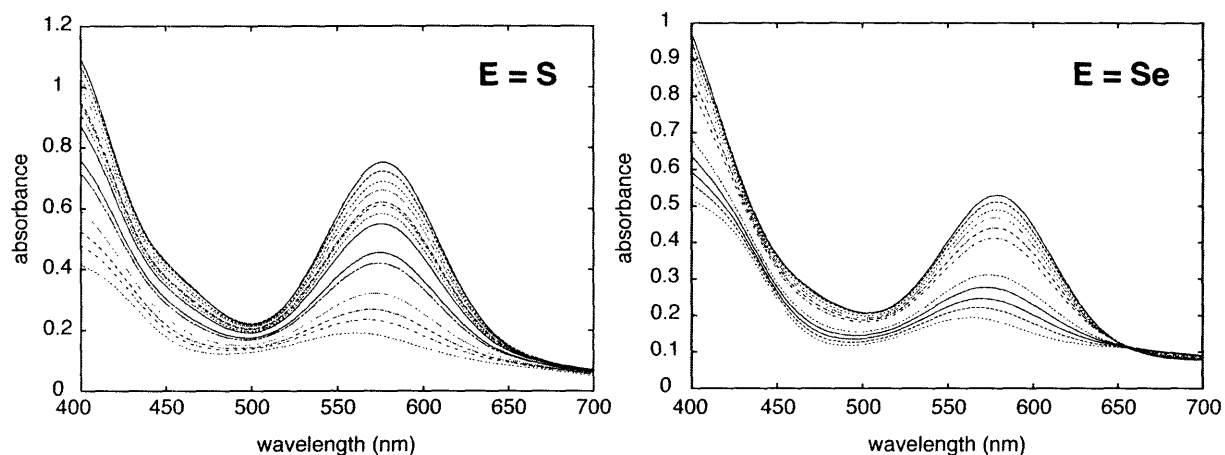


Figure 4. Spectral changes accompanying the $3-EAr^F$ to $4-EAr^F$ conversion.

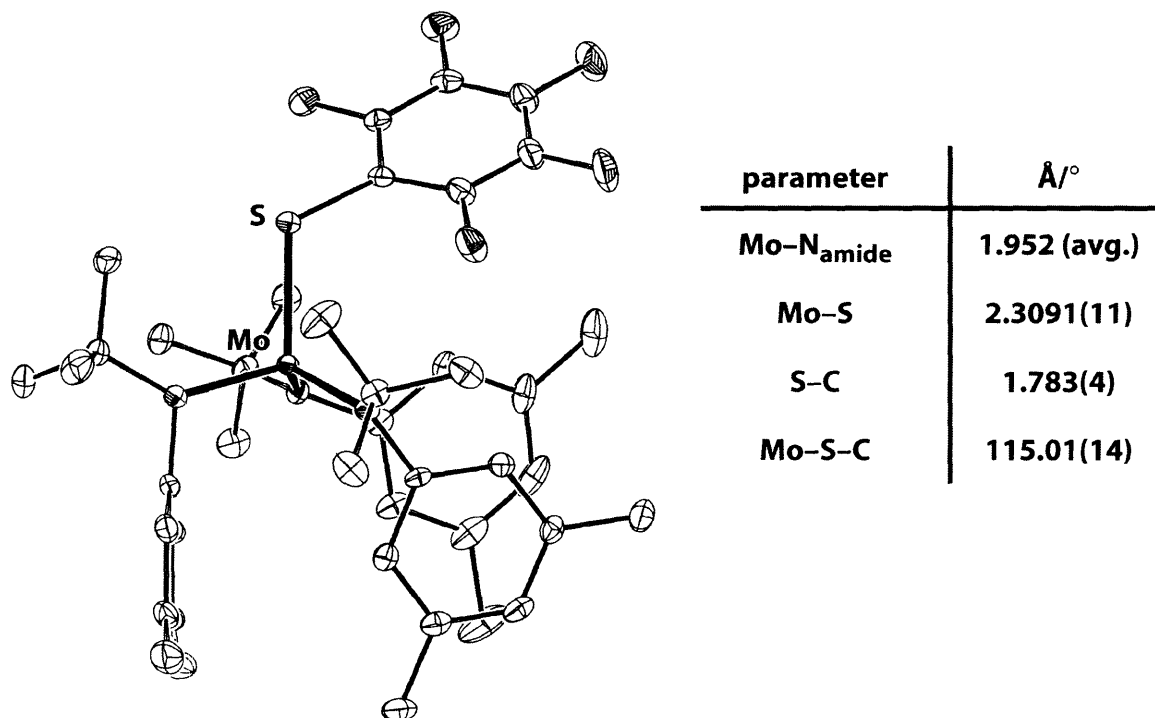
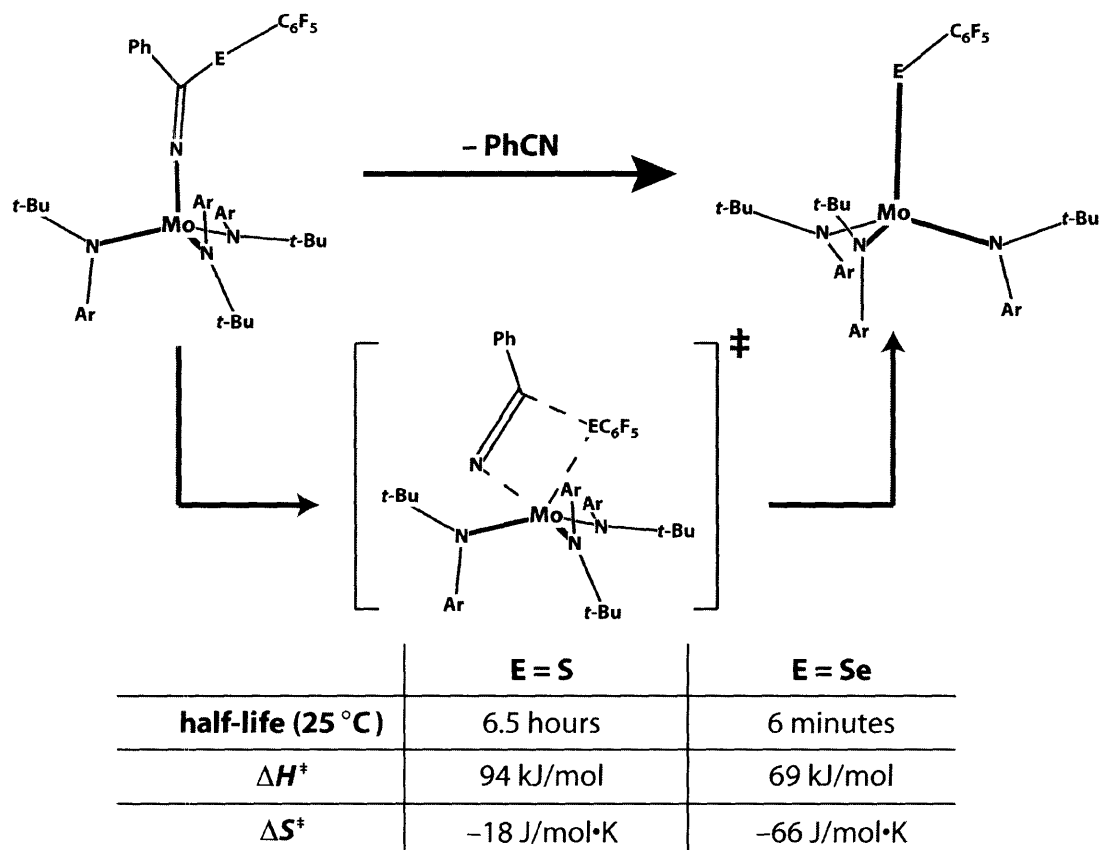


Figure 5. Solid-state structure of $4-SAr^F$ (35% ellipsoids).

Further information on β -elimination in these systems was obtained through the determination of activation parameters; for $E = S$, kinetic data were collected every $10^\circ C$

from 25–65 °C, whereas for the faster E = Se process, data were collected from 15–55 °C. The data are summarized in Scheme 2.



Scheme 2

A plausible mechanism for the conversion of **3**-EAr^F to **4**-EAr^F involves initial coordination of the E atom to the Mo center (with concomitant weakening of the E-C bond) resulting in a congested four-membered transition state, from which productive metathesis would yield PhCN and **4**-EAr^F. Such a hypothesis would predict that ΔH^\ddagger would be lower for Se than for S, due to the decrease in E-C bond strength.¹⁴ In addition, the larger Se atom would increase crowding in the transition state, resulting in a more negative ΔS^\ddagger . Further, the unimolecular nature of the mechanism predicts first-order kinetics. The observed data, then, provide no reason to discard this mechanistic proposal.

2.5 Reaction of **1**•PhCN with benzoyl peroxide

When thawing (*ca.* $-100\text{ }^{\circ}\text{C}$) Et_2O solutions of $\mathbf{1}\cdot\text{PhCN}$ and benzoyl peroxide (0.5 equivalents) are combined and allowed to warm to room temperature, a sequence of color changes from purple to blue and then back to purple is observed. ^1H NMR analysis of the final reaction mixture indicates the presence of a new, paramagnetic product and PhCN. The paramagnetic product was definitively identified as the Mo(IV) benzoate ($\text{Ar}[t\text{-Bu}]\text{N}_3\text{Mo-OC(O)Ph}$ ($\mathbf{4-OC(O)Ph}$) on the basis of X-ray crystallography. An ORTEP diagram of this compound is shown in Figure 6. The benzoate ligand adopts an η^1 conformation with a Mo-O distance of $2.0011(17)\text{ \AA}$ and a Mo-O-C angle of $124.86(17)^{\circ}$. The amide ligands are arranged in a distinctive C_s conformation, suggesting that the compound may be diamagnetic in the solid state. To the best of our knowledge, this is the first structurally verified example of an η^1 benzoate of Mo(IV).¹⁵

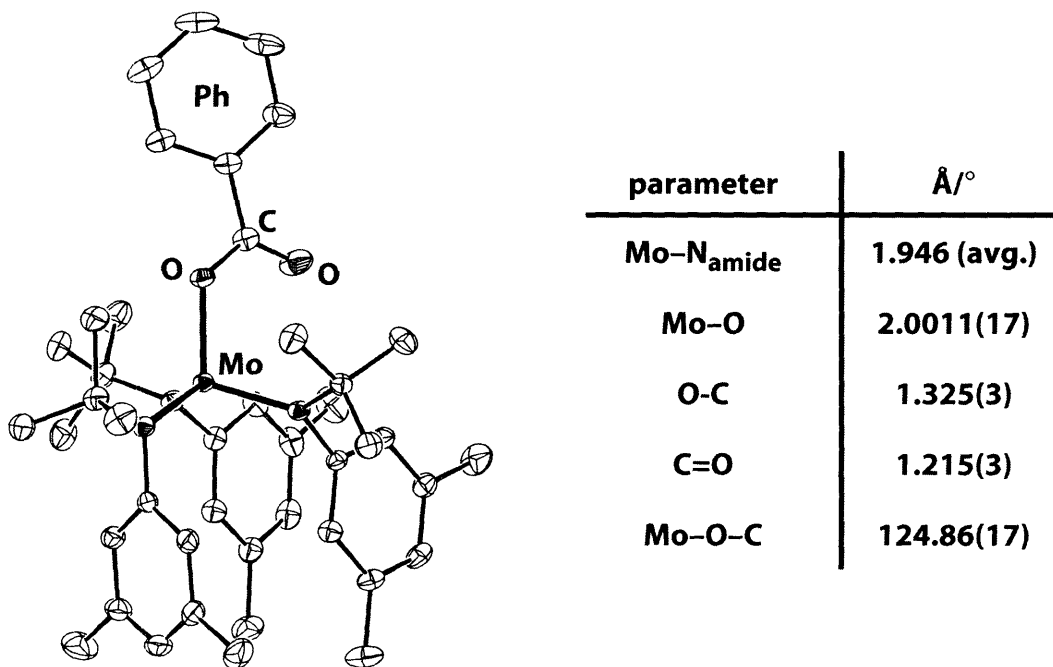


Figure 6 Solid state structure of $\mathbf{4-OC(O)Ph}$ (35% ellipsoids, one out of two molecules in the asymmetric unit).

In order to gain insight into the observed blue intermediate, the reaction was initiated at thawing toluene temperatures and then rapidly transferred to an NMR probe pre-cooled to -15°C . The spectra obtained in this fashion show a product containing three distinct anilide environments, along with two phenyl environments. As the temperature in the probe is raised, two simultaneous processes can be observed. One is the coalescence of

the resonances for the three distinct ligand environments; the other is the conversion of this product to **4-OC(O)Ph** with concomitant release of benzonitrile. As before, the final spectrum corresponds to a 1:1 mixture of **4-OC(O)Ph** and PhCN. On the basis of these data, the intermediate blue product is assigned as the benzoyl ketimide ($\text{Ar}[t\text{-Bu}]\text{N}_3\text{Mo-N}=\text{C}(\text{Ph})\text{OC}(\text{O})\text{Ph}$, **3-OC(O)Ph**).

Further information on this system comes from low-temperature kinetic measurements carried out in collaboration with the groups of Rybak-Akimova and Hoff. The initial reaction between **1**•PhCN and benzoyl peroxide can be followed by stopped-flow visible spectroscopy.¹⁶ Between -80 and -40 °C, the reaction follows clean second-order kinetics (first-order in each reagent), and activation parameters of $\Delta H^\ddagger = 8.4 \pm 1.7$ kJ/mol, $\Delta S^\ddagger = -130 \pm 17$ J/mol K can be calculated (see Figure 7). Recall from Chapter 1 that the activation parameters for the formation of the telluroketimide were 11.6 kJ/mol and -141 J/mol K respectively. In addition, the final product displays an absorption at 585 nm, as is typical of Mo(IV) ketimide complexes.

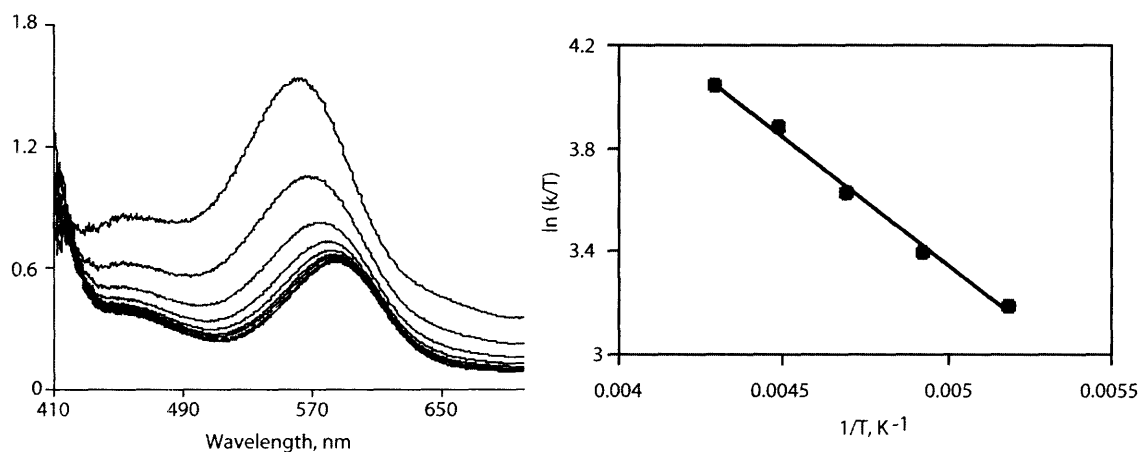


Figure 7 Left: reaction of **1**•PhCN with $(\text{PhCOO})_2$ at -80 °C; right: Eyring plot.

The elimination step has been followed using low-temperature FTIR spectroscopy. The ketimide intermediate is observed to exhibit a strong absorption at 1730 cm^{-1} , assigned as the C=O stretching band. This band decays concomitant with the appearance of a new band at 1660 cm^{-1} , assigned to the C=O stretching vibration in the benzoate **4-OC(O)Ph**. Analysis of the intensity of these bands versus time indicates that the elimination reaction obeys clean, first-order kinetics. In addition, activation parameters were determined to be $\Delta H^\ddagger = 77.8$ kJ/mol and $\Delta S^\ddagger \approx 0$ J/mol K. The vanishing entropy of

activation contrasts sharply with the behavior of the fluorinated chalcogenide-containing systems (see above). One explanation for this is that the $-\text{OC}(\text{O})\text{Ph}$ substituent is more readily accommodated by the bulky *tris*-anilide ligand set than is EC_6F_5 ($\text{E} = \text{S}, \text{Se}$), thus resulting in a less rigid transition state. An alternative hypothesis is that, due to the presence of an additional heteroatom, $\mathbf{3}\text{-OC}(\text{O})\text{Ph}$ eliminates PhCN through a *six-membered* (rather than 4-membered) cyclic intermediate. At present we are unable to distinguish between these two possibilities.

2.6 Conclusions

A series of heteroatom-substituted $\text{Mo}(\text{IV})$ benzimidates have been synthesized by the radical addition method outlined in Chapter 1, and their ability to undergo $\beta\text{-X}$ elimination has been studied. In the case in which the X group is an arylchalcogen, it is found that the rate of β -elimination increases with the molecular weight of the chalcogen. In addition, fluorination of the aryl ring facilitates the reaction. Activation parameters have been determined and support a concerted mechanism involving a unimolecular, four-membered transition state. The benzoyl-substituted ketimide, prepared from benzoyl peroxide, is also observed to undergo clean $\beta\text{-X}$ elimination.

2.7 Experimental

General Considerations: Unless stated otherwise, all operations were performed in a Vacuum Atmospheres drybox under an atmosphere of purified nitrogen. Anhydrous diethyl ether was purchased from Mallinckrodt; pentane, n-hexane, and tetrahydrofuran (THF) were purchased from EM Science. Diethyl ether, toluene, benzene, pentane, and n-hexane were dried and deoxygenated by the method of Grubbs.¹⁷ THF was distilled under nitrogen from purple sodium benzophenone ketyl. Distilled solvents were transferred under vacuum into vacuum-tight glass vessels before being pumped into a Vacuum Atmospheres drybox. C_6D_6 was purchased from Cambridge Isotopes and were degassed and dried over 4 Å sieves. THF- d_8 was passed through a column of activated alumina and stored over 4 Å sieves. The 4 Å sieves, alumina, and Celite were dried in vacuo overnight at a temperature just above 200 °C. Compounds

1,¹⁸ **6-Se**,³⁰ CpMo(CO)₃H,¹⁹ were prepared by literature methods. PhCN was distilled under vacuum before use and stored in a nitrogen-filled drybox. CpMo(CO)₃H was sublimed before use. All other compounds were used as received. ¹H and ¹³C NMR spectra were recorded on Unity 300, Mercury 300 or Varian INOVA-501 spectrometers at room temperature, unless indicated otherwise. ¹³C NMR spectra are proton decoupled. Chemical shifts are reported with respect to internal solvent: 7.16 ppm and 128.38 (t) ppm (C₆D₆). ⁷⁷Se NMR spectra were recorded on a Varian INOVA-501 spectrometer and are referenced to Me₂Se (0 ppm) by comparison to external Se₂Ph₂ (CDCl₃ 460 ppm). UV-vis absorption spectra were collected on a HP 8452A diode array spectrometer fitted with an HP 89090A Peltier temperature controller. CHN analyses were performed by H. Kolbe Mikroanalytisches Laboratorium (Mülheim, Germany).

Reaction of 1•PhCN with ClCH₂CH₂Cl: In a scintillation vial was prepared a solution of **1** (145 mg, 0.23 mmol) in 5 mL Et₂O to which was added PhCN (24.0 mg, 0.23 mmol) followed by ClCH₂CH₂Cl (13 mg, 0.13 mmol). The mixture was allowed to stir for 1 hour, during which point it turned brown. ¹H NMR indicated that **4-Cl** was the exclusive product.

Reaction of 1•PhCN with BrCH₂CH₂Br: Carried out analogously to the above experiment. ¹H NMR indicated that **4-Br** was the exclusive product. ¹H NMR (300 MHz, C₆D₆): d -7.61 (s, 3H, Ar *para*); -1.66 (s, 6H, Ar *ortho*); -0.49 (s, 18H, C₆H₃Me₂); 17.30 (br s, 27H, CMe₃) ppm.

Reaction of 1•PhCN with I₂: A solution of **1** (104 mg, 0.17 mmol) and PhCN (18 mg, 0.17 mmol) in 5 mL Et₂O was cooled to near freezing. Solid I₂ (21 mg, 0.08 mmol) was added to the thawing solution which turned green within a few seconds. ¹H NMR indicated that **4-I** was the exclusive product.

Thermolysis of 3-S: A J. Young NMR tube was charged with 19 mg (0.023 mmol) of **3-S** in 0.7 mL C₆D₆. The tube was sealed and placed in an oil bath preheated to 80 °C. Periodic monitoring by ¹H NMR revealed no observable decomposition over 2 days.

Thermolysis of 3-Se: A J. Young NMR tube was charged with 15 mg (0.017 mmol) of 3-Se in 0.7 mL C₆D₆. The tube was sealed and placed in an oil bath at 37 °C and periodically removed for monitoring by ¹H NMR. The degree of conversion to 4-Se was most readily assessed by the relative integrations of the *ortho* Se-Ph doublets of the starting material and product, at 7.437 ppm and 8.378 ppm respectively. Over the course of one day, 3-Se was observed to convert to 4-Se which itself decomposed to several unidentified products.

Thermolysis of 3-Te: A solution of 3-Te in THF was prepared as described previously. Two drops of this solution was added to a quartz UV cuvette fitted with teflon stopcock filled with THF. The cuvette was sealed, shaken to ensure homogeneity, and removed from the glovebox. The cuvette was heated to 35 °C and spectra were taken every 400 s for a total of 25000 s. The data traces at various wavelengths could were satisfactorily fitted to an exponential decay, and the resulting rate constants were within ±10% of each other.

Thermal Decomposition of 3-Se: A J. Young NMR tube was charged with 22 mg of 3-Se (26 mmol), 11 mg of dioxane (as an internal standard), and 0.7 mL of C₆D₆. The tube was sealed and placed in an oilbath at 37 °C and periodically removed for monitoring by ¹H NMR. The extent of decomposition was assessed by the relative integrations of the Se-Ph *ortho* protons (d 8.378 ppm) and dioxane.

Synthesis of 3-SAr^F: In a 50 mL roundbottom flask was prepared a solution of 1•PhCN (600 mg 1, 100 mg PhCN, 0.96 mmol) in 20 mL of Et₂O. To the purple solution was added solid Ar^FSSAr^F (192 mg, 0.48 mmol) resulting in a rapid darkening to deep blue. The reaction mixture was allowed to stir for 5 minutes, whereupon it was filtered and concentrated to dryness. Recrystallization from Et₂O furnished the product as a dark, microcrystalline solid. Yield: 503 mg, 3 crops (56%). ¹H NMR (300 MHz, C₆D₆): δ 1.32 (br s, 27H, CMe₃); 2.25 (s, 18H, C₆H₃Me₂); 6.57 (s, 2H, phenyl *ortho*); 6.63 (t, 1H, phenyl *para*); 6.69 (s, 3H, Ar *para*); 6.91 (s, 6H, Ar *ortho*); 7.01 (t, 2H, phenyl *meta*) ppm. ¹⁹F

NMR (282 MHz, C_6D_6): δ -135.43 (dd); -156.71 (t); -163.02 (m) ppm. UV-vis (Et_2O , 25 °C): λ_{max} 318 (sh, $\epsilon = 19000 M^{-1}$); 577 ($\epsilon = 7800 M^{-1}$) nm. (The thermal instability of this compound hindered acquisition of ^{13}C NMR spectra and elemental analysis.)

Spectroscopic Observation of 3-SeAr^F: A solution of **1** (17 mg, 0.027 mmol) and PhCN (*ca.* 5 mg, 0.49 mmol) was prepared in 0.5 mL C_6D_6 . To this was added a solution of $Ar^FSeSeAr^F$ (7 mg, 0.014 mmol) in 0.5 mL C_6D_6 resulting in an immediate color change to deep blue. The mixture was rapidly transferred to a J. Young NMR tube which was then removed from the box and frozen in an ice bath while being transported to the NMR spectrometer. The very first 1H NMR spectrum that is obtained shows a 10:1 mixture of **3-SeAr^F** and **4-SeAr^F**. Over the course of 30 minutes, the signals corresponding to **3-SeAr^F** can be observed to decay and those corresponding to **4-SeAr^F** grow in. 1H NMR (300 MHz, C_6D_6): 1.29 (br s, 27H, CMe_3); 2.27 (s, 18H, $C_6H_3Me_2$); 6.73 (3H, Ar *para*); 6.85 (6H, Ar *ortho*); 7.03 (t, 2H, phenyl *meta*) ppm (other resonances obscured). UV-vis (Et_2O , 25 °C): λ_{max} 579 ($\epsilon = 5500 M^{-1}$) nm.

Synthesis of 4-SAr^F: To an Et_2O solution of **1** (200 mg, 0.32 mmol) was added an Et_2O solution of Ar^FSSAr^F (64 mg, 0.16 mmol) resulting in a color change to purple-brown upon mixing. The solution was filtered through Celite and the filtrate concentrated to dryness. Recrystallization from Et_2O (-35 °C) furnished 150 mg (57%) of dark crystalline material. 1H NMR (300 MHz, C_6D_6): 1.39 (s, 27H, CMe_3); 2.05 (s, 18H, $C_6H_3Me_2$); 6.25 (br s, 6H, Ar *ortho*); 6.39 (s, 3H, Ar *para*) ppm. ^{19}F NMR (282 MHz, C_6D_6): -131.33 (dd); -159.66 (t); -163.78 (m) ppm. ^{13}C NMR: δ 21.61 ($C_6H_3Me_2$); 31.73 (CMe_3); 63.31 (N- CMe_3); 127.09; 129.03; 132.41 (m, C-F); 136.15; 136.68 (m, C-F); 140.19 (m, C-F); 143.63 (m, C-F); 146.81 (m, C-F); 151.58 ppm. UV-vis (Et_2O , 25 °C): λ_{max} 389 (sh, $\epsilon = 4500 M^{-1}$); 563 ($\epsilon = 1900$) nm. Anal Calcd. for $C_{42}H_{54}N_3MoSF_5$: C, 61.23; H, 6.61; N, 5.10. Found: C, 60.95; H, 6.68; N, 5.04.

Synthesis of 4-SeAr^F: Synthesized analogously to **4-SAr^F**. Yield: 150 mg, 54%. 1H NMR (300 MHz, C_6D_6): 1.40 (s, 27H, CMe_3); 2.04 (s, 18H, $C_6H_3Me_2$); 6.21 (br s, 6H, Ar *ortho*); 6.38 (s, 3H, Ar *para*) ppm. UV-vis (Et_2O , 25 °C): λ_{max} 387 (sh, $\epsilon = 5500 M^{-1}$); 555 ($\epsilon =$

1900) nm. Anal Calcd. for C₄₂H₅₄N₃MoSeF₅: C, 57.93; H, 6.25; N, 4.83. Found: C, 57.79; H, 6.08; N, 4.78.

Kinetics: Kinetics of β -EC₆F₅ elimination from **3**-EAr^F were measured using UV-Vis spectroscopy over a 40 °C range (E=S: 25-65 °C; E=Se: 15-55 °C). For the S-containing system, *ca.* 0.1 mM solutions were prepared from purified ketiminate and then transferred to a quartz UV cell containing a micro stirbar. For the Se-containing system, an identical protocol was followed, except that the more rapid kinetics in this system required that the starting ketiminate be generated *in situ*. In all cases, very good fits to first-order kinetics were observed. In addition, rate constants obtained from traces at three different wavelengths (400, 475, 585 nm) were within 10% of each other. The kinetic data are summarized in Tables 1 and 2.

T (K)	k_{400} (s ⁻¹)	k_{475} (s ⁻¹)	k_{580} (s ⁻¹)
298	2.91 x 10 ⁻⁵	3.00 x 10 ⁻⁵	2.85 x 10 ⁻⁵
308	9.14 x 10 ⁻⁵	1.07 x 10 ⁻⁴	1.04 x 10 ⁻⁴
318	3.38 x 10 ⁻⁴	3.22 x 10 ⁻⁴	3.31 x 10 ⁻³
328	9.49 x 10 ⁻⁴	9.47 x 10 ⁻⁴	1.01 x 10 ⁻³
338	2.71 x 10 ⁻³	2.77 x 10 ⁻³	2.85 x 10 ⁻³

Table 1 Kinetics of β -elimination from **3**-SAr^F.

T (K)	k_{400} (s ⁻¹)	k_{475} (s ⁻¹)	k_{580} (s ⁻¹)
288	7.36 x 10 ⁻⁴	7.04 x 10 ⁻⁴	7.56 x 10 ⁻⁴
298	2.04 x 10 ⁻³	1.88 x 10 ⁻³	2.15 x 10 ⁻³
308	5.33 x 10 ⁻³	5.42 x 10 ⁻³	5.56 x 10 ⁻³
318	1.21 x 10 ⁻²	1.24 x 10 ⁻²	1.23 x 10 ⁻²
328	2.50 x 10 ⁻¹	2.80 x 10 ⁻²	2.90 x 10 ⁻²

Table 2 Kinetics of β -elimination from **3**-SeAr^F.

Crystallographic structure determinations: The X-ray crystallographic data collections were carried out on a Siemens Platform three circle diffractometer mounted with a CCD or APEX-CCD detector and outfitted with a low temperature, nitrogen-stream aperture.

The structures were solved using direct methods, in conjunction with standard difference Fourier techniques and refined by full-matrix least-squares procedures. A summary of the crystallographic data for complexes **3-SAr^F**, **4-SAr^F**, and **4-OC(O)Ph** is given in Table 3. An empirical absorption correction (either psi-scans or SADABS) was applied to the diffraction data for all structures. All non-hydrogen atoms were refined anisotropically. Unless otherwise specified, all hydrogen atoms were treated as idealized contributions and refined isotropically. All software used for diffraction data processing and crystal-structure solution and refinement are contained in the SAINT+ (v6.45) and SHELXTL (v6.14) program suites, respectively (G. Sheldrick, Bruker AXS, Madison, WI).

	3-SAr^F	4-SAr^F	4-OC(O)Ph
formula	C ₄₉ H ₅₉ F ₅ MoN ₄ S	C ₄₂ H ₅₄ F ₅ MoN ₃ S	C ₄₃ H ₅₀ MoN ₃ O ₂
fw	927.00	823.88	736.80
space group	<i>P</i> $\bar{1}$	<i>P</i> 2 ₁ / <i>c</i>	<i>P</i> $\bar{1}$
<i>a</i> , Å	10.6395(10)	11.0092(6)	10.8341(11)
<i>b</i> , Å	12.8842(14)	18.7121(11)	19.982(2)
<i>c</i> , Å	18.843(2)	20.1675(11)	20.568(2)
α , deg	70.329(4)		89.669(2)
β , deg	74.155(3)	110.5280(10)	81.701(2)
γ , deg	76.599(3)		75.221(2)
<i>V</i> , Å ³	2311.8(4)	4003.0(4)	4258.2(7)
<i>Z</i>	4	4	4
<i>D</i> , g/cm ³	1.332	1.367	1.149
μ (Mo K α), mm ⁻¹	0.387	0.436	0.343
temp, K	100	173	193
F(000)	968	1720	1548
GoF(<i>F</i> ²)	1.057	1.204	1.051
R(<i>F</i>), %	0.0371	0.0827	0.0322
wR(<i>F</i>), %	0.0865	0.1386	0.0864

Table 3 Crystallographic parameters for **3-SAr^F**, **4-SAr^F**, and **4-OC(O)Ph**.

¹ Allen, A. D.; Senoff, C. V. *Chem. Comm.*, 621 (1965).

² Recent reviews: (a) MacKay, B. A.; Fryzuk, M. D. *Chem. Rev.* **104**, 385 (2004). (b) Fryzuk, M. D.; Johnson, S. A. *Coord. Chem. Rev.* **200-202**, 379 (2000). (c) Hidai, M. M.

-
- Y. Chem. Rev.* **95**, 1115 (1995). (d) Gambarotta, S. *J. Organomet. Chem.* **500**, 117 (1995).
- ³ (a) Rees, D. C. *Annu. Rev. Biochem.* **71**, 221 (2002). (b) Rees, D. C.; Howard, J. B. *Curr. Opin. Chem. Biol.* **4**, 559 (2000).
- ⁴ Appl, M. *Ammonia*; Wiley-WCH: Weinheim, 1999.
- ⁵ (a) Laplaza, C. E.; Cummins, C. C. *Science* **268**, 861 (1995). (b) Laplaza, C. E.; Johnson, M. J. A.; Peters, J.; Odom, A. L.; Kim, E.; Cummins, C. C.; George, G. N.; Pickering, I. J. *J. Am. Chem. Soc.* **118**, 8623 (1996).
- ⁶ Cherry, J. P. F.; Johnson, A. R.; Baraldo, L. M.; Tsai, Y.-C.; Cummins, C. C.; Kryatova, S. V.; Rybak-Akimova, E. V.; Capps, K. B.; Hoff, C. D.; Haar, C. M.; Nolan, S. P. *J. Am. Chem. Soc.* **123**, 7271 (2001).
- ⁷ Larock, R. C. *Comprehensive Organic Transformations, 2nd Ed.*; Wiley-VCH: New York, 1999.
- ⁸ (a) Albeniz, A. C.; Espinet, P.; Lin, Y.-S. *Organometallics* **16**, 5964 (1997). (b) Wiger, G.; Albelo, G.; Rettig, M. F.; *J. Chem. Soc., Dalton Trans.* 2242 (1974). (c) Zhu, G.; Lu, X. *Organometallics* **14**, 4899 (1995). (d) Kaneda, K.; Uchiyama, T.; Fujiwara, Y.; Imanaka, T.; Teranishi, S. *J. Org. Chem.* **44**, 55 (1979). (e) Nguetack, J.-F.; Bolitt, V.; Sinou, D. *J. Chem. Soc., Chem. Commun.* 1893 (1995). (f) Duan J.-P.; Cheng, C.-H. *Tetrahedron Lett.* **34**, 4019 (1993).
- ⁹ Buchwald, S. L.; Nielsen, R. B.; Dewan, J. C. *Organometallics* **7**, 2324 (1988).
- ¹⁰ Strazisar, S. A.; Wolczanski, P. T. *J. Am. Chem. Soc.* **123**, 4728 (2001).
- ¹¹ Cundari, T. R.; Taylor, C. D. *Organometallics* **22**, 4047 (2003).
- ¹² (a) Fürstner, A.; Mathes, C.; Lehmann, C. W. *J. Am. Chem. Soc.* **121**, 9453 (1999). (b) Peters, J. C.; Baraldo, L. M.; Baker, T. A.; Johnson, A. R.; Cummins, C. C. *J. Organomet. Chem.* **591**, 24 (1999).
- ¹³ Coates, G.W.; Dunn, A. R.; Henling, L. M.; Dougherty, D. A.; Grubbs, R. H. *Angew. Chem. Int. Ed. Eng.* **36**, 248 (1997).
- ¹⁴ (a) Pauling, L. *The Nature of the Chemical Bond*, 3rd ed.; Cornell University Press: Ithaca, New York, 1960. (b) McMillen, D. F.; Golden, D. M. *Annu. Rev. Phys. Chem.* **33**, 493 (1982). (c) Leeck, D. T.; Li, R.; Chyall, L. J.; Kenttämää, H. I. *J. Phys. Chem.* **100**, 6608 (1996).
- ¹⁵ For other Mo benzoates and acetates: Wlodarczyk, A.; Edwards, A. J.; McCleverty, J. A. *Polyhedron* **7**, 103 (1988).
- ¹⁶ Due to the known UV-induced decomposition of benzoyl peroxide, the use of a UV lamp was avoided during spectroscopic measurements.
- ¹⁷ Pangborn, A.B.; Giardello, M.A.; Grubbs, R.H.; Rosen, R.K.; Timmers, F.J. *Organometallics* **1996**, *15*, 1518.
- ¹⁸ Laplaza, C. E.; Johnson, M. J. A.; Peters, J. A.; Odom, A. L.; Kim, E.; Cummins, C. C.; George, G. N.; Pickering, I. J. *J. Am. Chem. Soc.* **1996**, *118*, 8623.
- ¹⁹ Rakowski DuBois, M.; DuBois, D. L.; Vanerveer, M. L.; Haltiwanger, R.C. *J. Inorg. Chem.* **20**, 3064 (1981).

3

Synthesis of an oxotitanium(IV) anion

3.1 Introduction

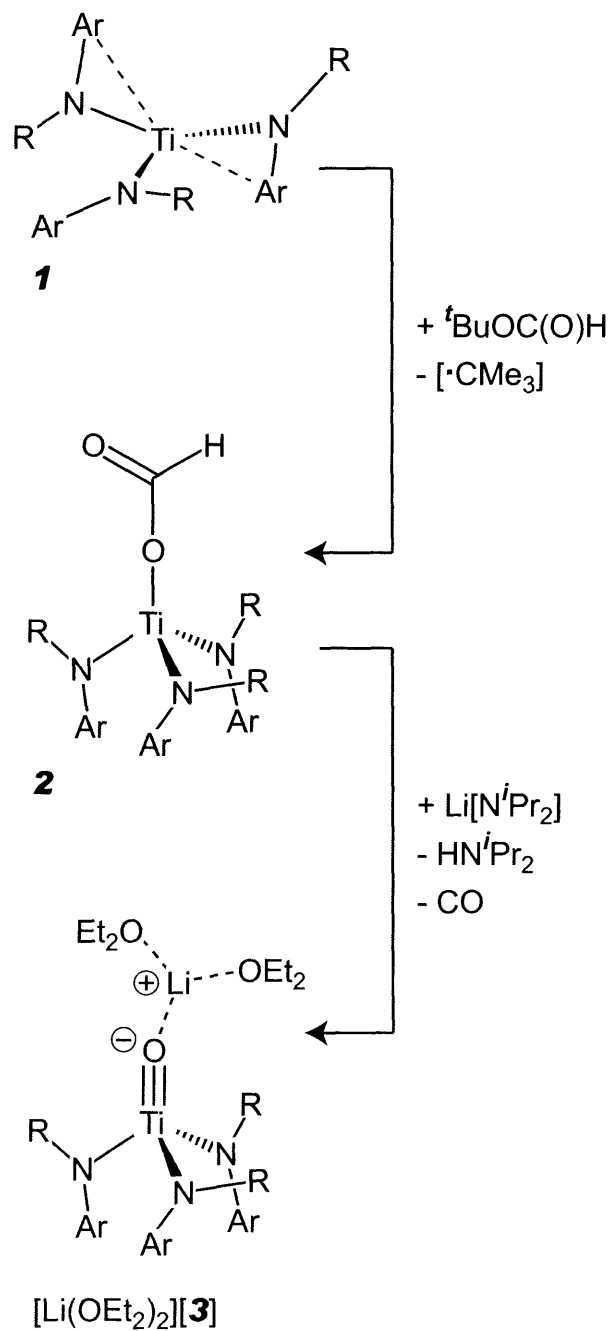
In recent years, both transition metal formates and oxos have been studied intensively; the former as model compounds in the rich and varied chemistry of syngas on metal surfaces,^{1,2} and the latter due to their importance in biological³ and industrial oxidations.⁴ Historically, the oxo ligand has been encountered primarily in conjunction with the middle metals of the transition series;⁵ this observation has motivated a number of recent syntheses of both early-⁶⁻⁸ and late-metal^{9,10} oxos. We report here on an unprecedented, base-triggered formate decarbonylation, resulting in the synthesis of the first anionic oxo of titanium(IV). DFT calculations have been carried out in order to elucidate the electronic structure of the new compounds.

3.2 Synthesis of a titanium formate

Treatment of an emerald green ethereal solution of $\text{Ti}[\text{N}(t\text{-Bu})\text{Ar}]_3$ ($\text{Ar} = 3,5\text{-Me}_2\text{C}_6\text{H}_3$, **1**)¹¹ with 1 equiv. of *t*-butyl formate at 25° C results in an immediate color change to red-brown, followed by precipitation of a yellow solid over the course of a few minutes. On the basis of ¹H and ¹³C NMR spectroscopy, X-ray crystallography, and elemental analysis, this solid is identified as $[\text{Ar}(t\text{-Bu})\text{N}]_3\text{TiOC}(\text{O})\text{H}$, **2**. The key formate resonance is observed at 8.36 ppm.

The formation of formate **2** can be accounted for via initial generation of a titanium-stabilized ketyl radical, followed by *t*-Bu radical ejection to generate the observed product (see Scheme 1). As shown in Figure X, a similar sequence of events has been observed upon treatment of **1** with $\text{O}_2\text{Mo}(\text{O}-t\text{-Bu})_2$.¹² In both cases, the final product is the result of formal displacement of CMe_3 radical by **1**.

The solid-state structure of formate **2** is shown in Figure 1. The molecule crystallizes on a crystallographic 3-fold axis, with the result that the formate moiety is disordered over three positions. The geometry at titanium is approximately tetrahedral with an O(1)-Ti(1)-N(1) angle of 110.8°. The observed Ti-O distance of 1.868(4) Å is similar to that observed in other compounds containing the *tris-t*-butylanilide ligand set.^{12,13} The three-fold disorder, which we have not been able satisfactorily resolve, prevents discussion of additional metrical parameters.



Scheme 1 Synthesis of **2** and **3**.

3.3 Deprotonation of **2**

The successful deprotonation of **2** would provide a compound in which the CO₂ anion is stabilized by coordination to a Ti center. Such a compound would be of considerable interest in that the reduction potential of free CO₂ is -1.90 V vs. NHE.^{14,15} In the event, treatment of **2** with a slight excess of LiN(*i*-Pr)₂ in Et₂O resulted in the formation of a

new crystalline product whose ^1H NMR spectrum displayed a single $\text{N}(t\text{-Bu})\text{Ar}$ environment. An X-ray diffraction study revealed the product to be titanium(IV) oxoanion **3**, likely formed by facile CO ejection subsequent to deprotonation. We have previously observed decarbonylation of isoelectronic $[(\text{Ar}[t\text{-Bu}]\text{N})_3\text{Nb}=\text{N}=\text{C}=\text{O}]^-$ to form an anionic nitridoniobium complex.¹⁶ Detection of liberated CO in the present system was carried out by vacuum transfer of the volatiles onto $(\text{Ph}_3\text{P})_3\text{RhCl}$ (Wilkinson's catalyst), resulting in formation of $(\text{Ph}_3\text{P})_2\text{Rh}(\text{CO})\text{Cl}$ as documented in the literature.¹⁷ The generation of $\text{HN}(i\text{-Pr})_2$ was confirmed in a separate experiment.

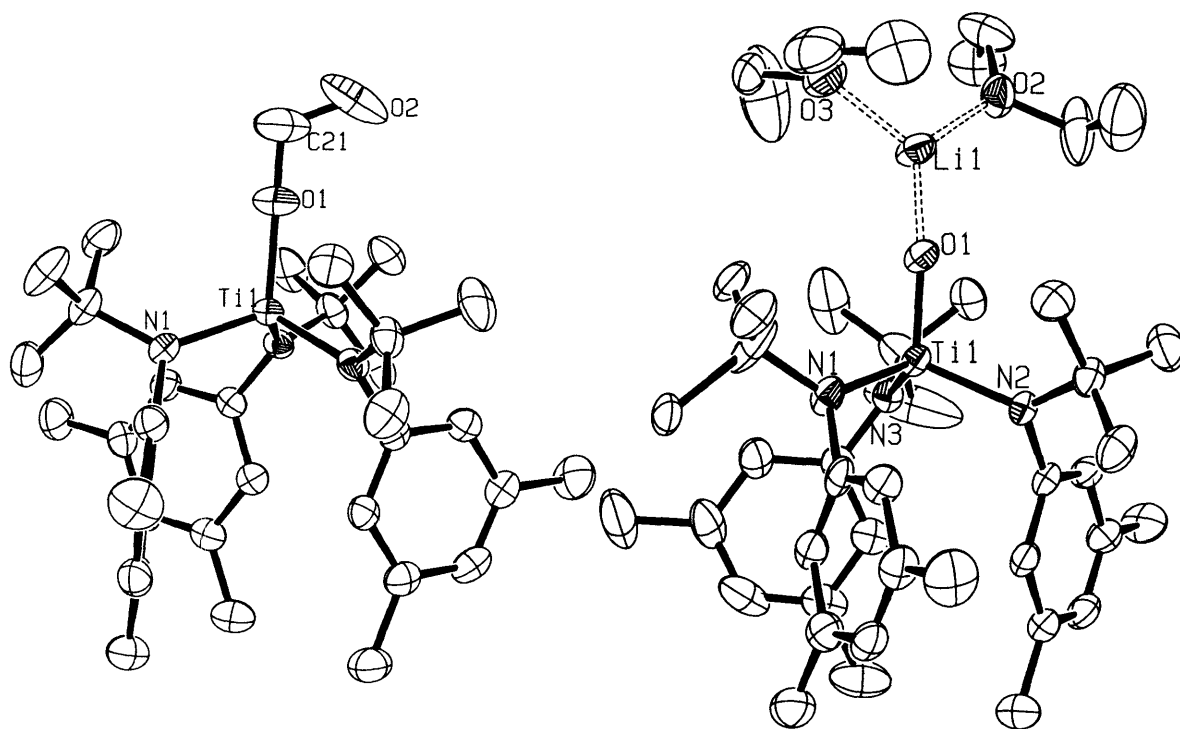


Figure 1 Solid-state structures of **2** and **3** (35% ellipsoids). Selected bond distances (Å) and bond angles (°) for **2**: Ti(1)-O(1) 1.868(4), Ti(1)-N(1) 1.929(3), O(1)-C(21) 1.299(10), C(21)-O(2) 1.291(15), O(1)-Ti(1)-N(1) 110.70(8), C(21)-O(1)-O(2) 113.7(8). **3**: Ti(1)-O(1) 1.717(2), Ti(1)-N(1) 1.986(3), Ti(1)-N(2) 1.989(2), Ti(1)-N(3) 1.990(3), O(1)-Li(1) 1.801(6), Ti(1)-O(1)-Li(1) 167.8(2).

The solid-state structure of **3** (see Figure 1), reveals the expected coordination of the titanoxide anion to the Li cation, with a Li-O distance of 1.801(6) Å. The Li atom is coordinated additionally by two molecules of Et_2O , adopting an overall trigonal planar geometry. The Ti-O distance, at 1.717(2) Å, is significantly contracted relative to **2**. While anionic titanium(IV) oxos have not been previously structurally characterized, typical Ti-O distances in neutral titanyles range from 1.61 to 1.68 Å.⁵ Andersen has prepared the anionic oxotitanium(III) compound $[\text{Cp}^*_2\text{TiOLi}(\text{THF})]_2$, which features an

average Ti-O distance of 1.787 Å,¹⁸ while Stephan's oxozirconium(IV) anion, [Cp*₂Zr(H)OLi(THF)]₂, exhibits a Zr-O distance of 1.847 Å.¹⁹ These comparisons suggest that the Ti-O interaction in **3** is best viewed as a multiple bond.



Figure 2 Ti-O π -bonding orbitals in **3-m**.

To further address this issue, we have carried out DFT calculations on the model compounds (NH₂)₃TiOC(O)H (**2-m**) and [Li(OMe₂)₂][(NH₂)₃TiO] (**3-m**). The key features of the experimental structures are satisfactorily reproduced at the BP86 level of density functional theory.²⁰ Inspection of the Laplacian of the electron density²¹ indicates that, in both cases, the Ti-O bond is characterized by considerable ionic character, as anticipated based on the large difference in electronegativities between Ti and O. On moving from **2-m** to **3-m**, however, the value of the electron density at the bond critical point increases from 0.1134 to 0.1815 a.u., consistent with a substantial increase in bond order and, thus, covalency. Additionally, a pair of degenerate orbitals corresponding to orthogonal Ti-O π bonds is observed in the DFT analysis (see Figure 2). Since the electron localization function (ELF) has been particularly valuable for illuminating complex issues of chemical bond multiplicity,²² we have also examined the ELF isosurface plot for **3-m**.²³ In the ELF, triple bonds give rise to a toroidal basin surrounding the bond axis. For **3-m**, it is seen that such a toroidal basin is present and is shifted close to the O atom, nearly merging with the oxygen lone pair basin. By all accounts, the titanoxide anion of interest herein manifests a quite polar triple bond.

The chemistry presented herein provides precedent for bound formate decarbonylation as triggered by deprotonation. The existence of such a transformation may be significant with regard to the reactions of CO and CO₂ on metal surfaces.^{1,2} Furthermore, oxoanion **3** is likely to be a potent nucleophile as well as useful metallo-ligand, prospects currently under investigation. Finally, the valence-isoelectronic

relationship of $[\text{OTi}(\text{N}[t\text{-Bu}]\text{Ar})_3]^{1-}$ to the previously described neutral $[\text{OV}(\text{N}[t\text{-Bu}]\text{Ar})_3]$ and cationic $[\text{OMo}(\text{N}[t\text{-Bu}]\text{Ar})_3]^{1+}$ complexes reveals **3** to be the newest member of an intriguing series of four-coordinate oxometal entities.^{24,25}

3.4 Experimental

General Considerations: Unless stated otherwise, all operations were performed in a Vacuum Atmospheres drybox under an atmosphere of purified nitrogen. Anhydrous diethyl ether was purchased from Mallinckrodt; pentane, n-hexane, and tetrahydrofuran (THF) were purchased from EM Science. Diethyl ether, toluene, benzene, pentane, and n-hexane were dried and deoxygenated by the method of Grubbs.²⁶ THF was distilled under nitrogen from purple sodium benzophenone ketyl. Distilled solvents were transferred under vacuum into vacuum-tight glass vessels before being pumped into a Vacuum Atmospheres drybox. C_6D_6 was purchased from Cambridge Isotopes and were degassed and dried over 4 Å sieves. The 4 Å sieves, alumina, and Celite were dried in vacuo overnight at a temperature just above 200° C. Compound **1** was prepared as reported in reference 12 in the main text. *t*-Butyl formate was passed through alumina and stored over molecular sieves. All other compounds were used as received. ^1H and ^{13}C NMR spectra were recorded on Unity 300, Mercury 300 or Varian INOVA501 spectrometers at room temperature, unless indicated otherwise. Chemical shifts are reported with respect to internal solvent: 7.15 ppm and 128.38 (t) ppm (C_6D_6). CHN analyses were performed by H. Kolbe Mikroanalytisches Laboratorium (Mülheim, Germany).

Synthesis of $(\text{Ar}[t\text{-Bu}]\text{N})_3\text{TiOC}(\text{O})\text{H}$ (2**):** $\text{Ti}(\text{N}[t\text{-Bu}]\text{Ar})_3$ (700 mg, 1.21 mmol) was dissolved in 50 mL of pentane. To the green solution was added *t*-butyl formate (124 mg, 1.21 mmol) in 5 mL of pentane resulting in an immediate darkening. The solution was allowed to stir for 30 m, and then volatiles were removed in vacuo. The resulting bright yellow solid was transferred to a fine frit and washed with pentane until the washings were clear. Yield: 614 mg, 81%. ^1H NMR, 500 MHz (C_6D_6): 1.26 (s, 27H, *t*-Bu); 2.16 (s, 18H, Ar- CH_3); 6.22 (br s, 6H, *o*-ArH); 6.69 (s, 3H, *p*-ArH); 8.36 (br s, 1H, OC(O)-H) ppm. ^{13}C NMR, 125 MHz (C_6D_6): 21.95 ($\text{C}(\text{CH}_3)_3$); 30.94 (Ar- CH_3); 62.69 ($\text{C}(\text{CH}_3)_3$);

127.36; 128.10; 137.14; 151.75; 162.05 (OC(O)H) ppm. Anal Calcd. for $C_{37}H_{55}N_3O_2Ti$: C, 71.48; H, 8.92; N, 6.76. Found: C, 71.28; H, 8.96; N, 6.68.

Synthesis of (Ar[*t*-Bu]N)₃TiOLi(Et₂O)₂ (3): Titanium formate **2** (420 mg, 0.68 mmol) was slurried in 20 mL of Et₂O in a 100 mL round-bottom flask and frozen in the glovebox coldwell. In a 20 mL scintillation vial, LiN(*i*-Pr)₂ was dissolved in 5 mL Et₂O and similarly frozen. The thawing solutions were combined and allowed to warm to room temperature. After 1 h, the reaction mixture was orange and nearly homogenous. The solution was filtered through Celite, concentrated to a volume of 10 mL, and stored at -35 °C. Large block-shaped crystals grew within hours and could be isolated simply by decanting off the mother liquor. Yield: 302 mg, 60% (three crops). ¹H NMR, 300 MHz (C₆D₆): 1.39 (s, 27H, *t*-Bu); 2.32 (s, 18H, Ar-CH₃); 6.70 (s, 6H, *o*-ArH); 6.76 (s, 3H, *p*-ArH) ppm. ¹³C NMR, 125 MHz (C₆D₆): 22.19 (C(CH₃)₃); 32.78 (Ar-CH₃); 58.28 (C(CH₃)₃); 126.01; 129.28; 137.41; 153.68 ppm. Anal Calcd. for $C_{44}H_{74}N_3O_3TiLi$: C, 70.66; H, 9.97; N, 5.62. Found: C, 70.23; H, 9.89; N, 5.72.

Quantification of CO evolution in the synthesis of 3: In the glovebox, a 25 mL Schlenk tube (**A**) fitted with Teflon stopcock was charged with **2** and LiN(*i*-Pr)₂ and sealed. A 50 mL round-bottom flask (**B**) was charged with (PPh₃)₃RhCl and 10 mL of toluene, fitted with a 180° degree adapter, and sealed. Both flasks were removed from the glovebox, attached to a high vacuum manifold, and thoroughly evacuated. The Et₂O from flask **B** was condensed into flask **A** at -196° C. Flask **A** was sealed and allowed to warm to room temperature. After 1h, flask **B** was cooled to -196° C and the volatiles from flask **A** were allowed to condense into flask **B**. Flask **B** was sealed and allowed to warm to room temperature, whereupon it turned purple. ³¹P NMR analysis of the contents of flask **B** revealed the formation of (PPh₃)₂Rh(CO)Cl.

Crystallographic structure determinations: The X-ray crystallographic data collections were carried out on a Siemens Platform three circle diffractometer mounted with a CCD or APEX-CCD detector and outfitted with a low temperature, nitrogen-stream aperture. The structures were solved using direct methods, in conjunction with standard difference

Fourier techniques and refined by full-matrix least-squares procedures. A summary of the crystallographic data for complexes **2** and **3** is shown in Table 1. An empirical absorption correction (either psi-scans or SADABS) was applied to the diffraction data for all structures. All non-hydrogen atoms were refined anisotropically. Unless otherwise specified, all hydrogen atoms were treated as idealized contributions and refined isotropically. All software used for diffraction data processing and crystal-structure solution and refinement are contained in the SAINT+ (v6.45) and SHELXTL (v6.14) program suites, respectively (G. Sheldrick, Bruker AXS, Madison, WI).

	2	3
formula	C ₃₇ H ₅₄ TiN ₃ O ₂	C ₄₄ H ₆₈ LiN ₃ O ₃ Ti
fw	620.73	741.85
space group	<i>R</i> $\bar{3}$	<i>P</i> 2 ₁ 2 ₁ 2 ₁
<i>a</i> , Å	15.7365(7)	13.3353(10)
<i>b</i> , Å	15.7365(7)	13.3843(9)
<i>c</i> , Å	24.686(2)	25.8835(18)
α , deg		
β , deg		
γ , deg		
<i>V</i> , Å ³	5294.1(6)	4626.7
<i>Z</i>	6	4
<i>D</i> , g/cm ³	1.168	1.065
μ (Mo K α), mm ⁻¹	0.277	0.222
temp, K	193	193
<i>F</i> (000)	2010	1608
GoF(<i>F</i> ²)	1.091	1.036
<i>R</i> (<i>F</i>), %	0.0542	0.0587
w <i>R</i> (<i>F</i>), %	0.1316	0.1493

Table 1 Crystallographic parameters for **2** and **3**.

Computations: Calculations were carried out using the ADF2004.01²⁷ software package. Visualization of the Laplacian and determination of bond critical points were performed using the Xaim software package.²⁸ The ELF isosurface was generated using the DGRID software package.²⁹

-
- ¹ D. H. Gibson, *Coord. Chem. Rev.* **186**, 335 (1999).
- ² I. Wender, *Fuel. Processing Tech.* **48**, 189 (1996).
- ³ *Cytochrome P-450: Structure, Mechanism and Biochemistry*; Plenum: New York, **1995**.
- ⁴ G. Centi, E. Trefiro, J. R. Ebner, and V. Franchetti, *Chem. Rev.* **88**, 55 (1999).
- ⁵ W. A. Nugent and J. M. Mayer. *Metal-Ligand Multiple Bonds*; Wiley: New York, **1988**.
- ⁶ M. J. Carney, P. J. Walsh, F. J. Hollander, and R. G. Bergman, *J. Am. Chem. Soc.* **111**, 8751 (1989).
- ⁷ M. R. Smith III, P. T. Matsunaga, and R. A. Andersen, *J. Am. Chem. Soc.* **115**, 7049 (1993).
- ⁸ J. E. Hill, P. E. Fanwick, and I. P. Rothwell, *Inorg. Chem.* **28**, 3602 (1989).
- ⁹ R. S. Haymotherwell, G. Wilkinson, B. Hussainbates, and M. B. Hursthouse, *Polyhedron* **12**, 2009 (1993).
- ¹⁰ P. Barthazy, M. Worle, and A. Mezzeti, *J. Am. Chem. Soc.* **121**, 480 (1999).
- ¹¹ P.W. Wanandi, W. M. Davis, C. C. Cummins, M. A. Russell, and D. E. Wilcox, *J. Am. Chem. Soc.* **117**, 2110 (1995).
- ¹² J. C. Peters, A. R. Johnson, A. L. Odom, P. W. Wanandi, W. M. Davis, and C. C. Cummins, *J. Am. Chem. Soc.* **118**, 10175 (1996).
- ¹³ T. Agapie, P. L. Diaconescu, D. J. Mindiola, and C. C. Cummins, *Organometallics* **21**, 1329 (2002).
- ¹⁴ H. A. Schwarz and R. W. Dodson, *J. Phys. Chem.* **93**, 409 (1989).
- ¹⁵ P. S. Surdhar, S. P. Mezyk, and D. A. Armstrong, *J. Phys. Chem.* **93**, 336 (1989).
- ¹⁶ M. G. Fickes, A. L. Odom, and C. C. Cummins, *Chem. Comm.* 1993 (1997).
- ¹⁷ J. A. Osborn, F. H. Jardine, J. F. Young, and G. Wilkinson, *J. Chem. Soc., Sect. A*, 1711 (1996).
- ¹⁸ W. W. Lukens, P. T. Matsunaga, and R. A. Andersen, *Organometallics* **17**, 5240 (1998).
- ¹⁹ A. J. Hoskin and D. W. Stephan, *Organometallics* **18**, 2479 (1999).
- ²⁰ (a) A. D. Becke, *Phys. Rev. A* **38**, 3098 (1988). (b) J. P. Perdew, *Phys. Rev. B* **33**, 8822 (1986).
- ²¹ R. F. W. Bader, *Chem. Rev.* **91**, 893 (1991).
- ²² H. Grutzmacher, T. F. Fassler, *Chem. Eur. J.* **6**, 2317 (2000).
- ²³ (a) A. D. Becke, K. E. Edgecombe, *J. Chem. Phys.* **92**, 5397 (1990). (b) B. Silvi, A. Savin, *Nature* **371**, 683 (1994). (c) A. Savin, R. Nesper, S. Wengert, T. F. Fassler, *Angew. Chem. Int. Ed. Eng.* **36**, 1809 (1997).
- ²⁴ J. K. Brask, V. Dura-Vila, P. L. Diaconescu, and C. C. Cummins, *Chem. Comm.*, 902 (2002).
- ²⁵ A. R. Johnson, W. M. Davis, C. C. Cummins, S. Serron, S. P. Nolan, D. G. Musaev, and K. Morokuma, *J. Am. Chem. Soc.* **120**, 2071 (1998).
- ²⁶ Pangborn, A.B.; Giardello, M.A.; Grubbs, R.H.; Rosen, R.K.; Timmers, F.J. *Organometallics* **15**, 1518 (1996).
- ²⁷ (a) G. te Velde, F.M. Bickelhaupt, S.J.A. van Gisbergen, C. Fonseca Guerra, E.J. Baerends, J.G. Snijders, T. Ziegler, *J. Comput. Chem.*, 2001, **22**, 931. (b) C. Fonseca Guerra, J. G. Snijders, G. te Velde, and E. J. Baerends, *Theor. Chem. Acc.*, 1998, **99**. (c) ADF2004.01, SCM, Theoretical Chemistry, Vrije Universiteit, Amsterdam, The Netherlands, <http://www.scm.com>

²⁸ <http://www.quimica.urv.es/XAIM/> (accessed January 2005)

²⁹ M. Kohout, program Dgrid, 2.4 ed., Max Planck Institute for Chemical Physics of Solids, Dresden, **2004**.

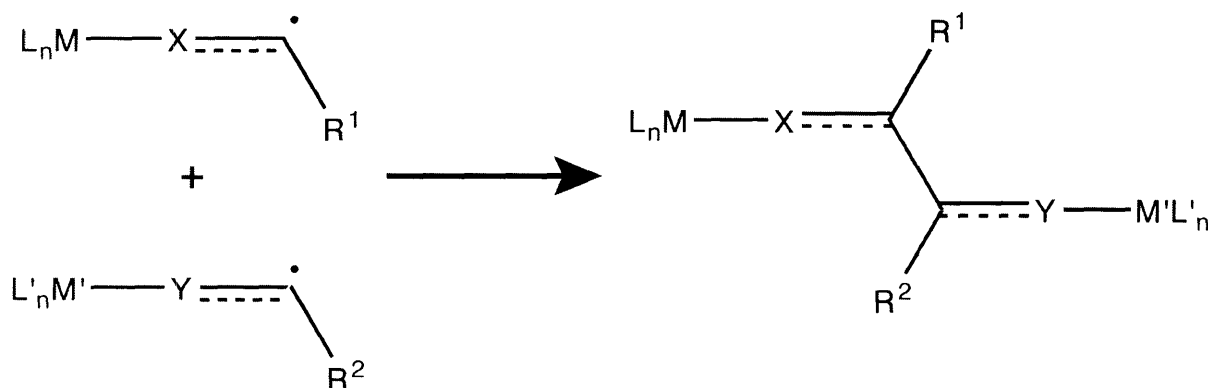
4

Four-component couplings with Mo and Ti:
the one-electron activation of CO₂

4.1 Introduction

As discussed in the introduction to this work, a recurring motif in reductive coupling chemistry has been the expansion of the reaction scope to include a wide variety of “carbonyl-like” substrates (e.g. imines, nitriles, and cumulenes). A parallel theme has been the development of methods for reductive *cross*-couplings, i.e. reactions in which two dissimilar carbonyl (or equivalent) compounds are coupled. Provided that the formation of homocoupling products can be suppressed, reductive cross-coupling can provide efficient access to highly desirable organic products such as unsymmetrical 1,2-diols and amino alcohols.

The first approach to this problem came in 1976, when Corey and coworkers reported that the Mg(Hg)/TiCl₄ system was capable of the reductive cross-coupling of a variety of cyclic ketones with acetone when acetone was present in excess.¹ Some years later came several reports in which the use of better-defined reductants allowed for the preparation of preformed, η^2 metal-substrate adducts. Treatment of these adducts with one equivalent of second substrate resulted in clean formation of heterocoupled products.^{2,3} Representative is Buchwald’s synthesis of the η^2 -imine complex Cp₂Zr(THF)(η^2 -Me₃SiN=C(H)Ph), which undergoes C–C reductive coupling not only with other imines, but also with nitriles, acetylenes, ketones, and terminal olefins.⁴ In such an approach, an overall two-electron transformation is carried out at a single metal center; as a consequence, these reactions typically employ d² metal centers or synthons thereof.

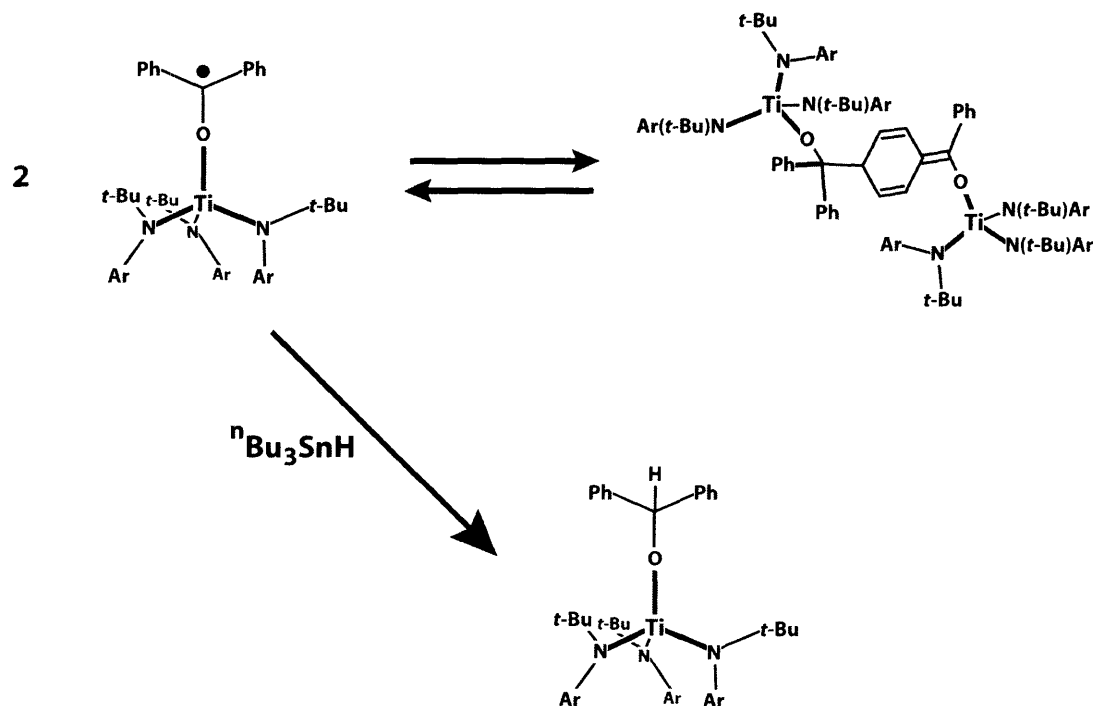


Scheme 1 Bimetallic reductive cross-coupling.

One can also envision a bimetallic version of the strategy described above. As shown in Scheme 1, each coupling partner can be activated by a different (likely one-electron) metal center. Appropriate tuning of the steric and electronic properties of each metal/substrate pair can result in a situation in which homocoupling is slow relative to heterocoupling. In this chapter we report on the realization of this strategy using the compounds $(\text{Ar}[t\text{-Bu}]\text{N})_3\text{M}$ ($\text{M} = \text{Mo}$, **1**; $\text{M} = \text{Ti}$, **2**). Specifically, we describe the reductive cross-coupling of PhCN with benzophenone, pyridine, and—most notably— CO_2 , a substrate typically reluctant to undergo one-electron chemistry.⁵ The former two couplings are of added interest as they involve concomitant dearomatization, thereby forming products of high molecular complexity from simple starting materials. While dearomatization is not typically a feature of reductive couplings, it is well-established in reductive alkylations employing alkali metals.⁶

4.2 Reductive coupling of PhCN and benzophenone

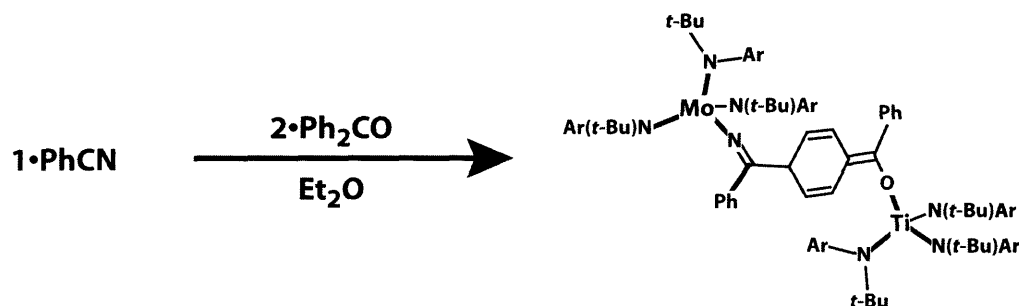
Previous work from these labs has shown that treatment of **2** with Ph_2CO results in the establishment of the monomer/dimer equilibrium shown in Scheme 2.⁷ Similar



Scheme 2. (Adapted from ref. 7)

equilibria exist for other systems in which a ketyl radical is bound to a metal center stabilized by sterically bulky ligands.⁸ As in the case of trityl radical, the formation of a head-to-head (Pinacolic) dimer is obviated on steric grounds.⁹ Nonetheless, $2\cdot\text{Ph}_2\text{CO}$ can serve as a source of ketyl radical, as shown by its reaction with ${}^n\text{Bu}_3\text{SnH}$ to form the corresponding diphenylmethoxide complex.

In contrast, treatment of $2\cdot\text{Ph}_2\text{CO}$ with $1\cdot\text{PhCN}$ results in bond formation at the *para* carbon of $2\cdot\text{Ph}_2\text{CO}$ (see Equation 1). Green, diamagnetic **3a** displays distinctive vinyl resonances between 5 and 6 ppm in its ${}^1\text{H}$ NMR spectrum, similar to those observed for $(2\cdot\text{Ph}_2\text{CO})_2$.⁷ Although **3a** gave clean ${}^1\text{H}$ and ${}^{13}\text{C}$ NMR spectra, its high lipophilicity hindered the preparation of analytically pure samples. Fortunately, the use of 2,6- $\text{Me}_2\text{C}_6\text{H}_3\text{CN}$ in place of PhCN allowed for the synthesis of compound **3b**, which proved significantly easier to isolate in analytically pure form. In addition, we obtained a crystal structure of **3b**, albeit of low quality, which confirmed the connectivity of this molecule, and—by extension—of **3a**.



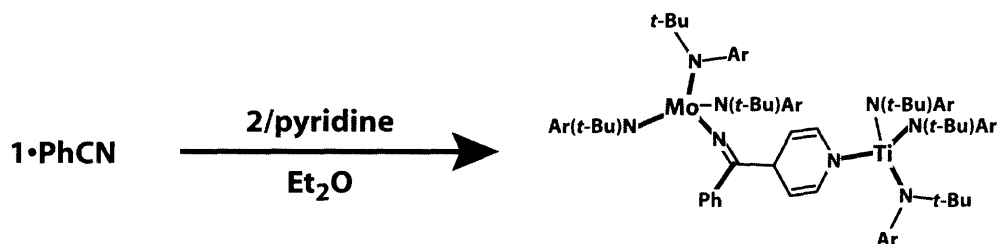
Equation 1

Itoh and coworkers have reported that Cp_2TiPh mediates the reductive cyclization of γ - and δ -cyanoketones to furnish, upon hydrolysis, 5- and 6-membered α -hydroxycycloalkanones.¹⁰ The reaction requires >2 equivalents of Cp_2TiPh , supporting the author's contention that activation of both carbonyl and cyano moieties is necessary. In addition, it was shown that alkenyl ketones are inert to the reaction conditions. Contrary to what is observed in the present case, Cp_2TiPh displayed no detectable reaction with monofunctional ketone or nitrile substrates. Similar transformations have also been effected using SmI_2 under conditions involving photolysis and excess *t*-BuOH; the authors propose that only the ketone functionality interacts with SmI_2 .¹¹ Finally, electrochemical protocols have also been reported.^{12,13}

4.3 Reductive coupling of PhCN and pyridine

Addition of *ca.* 1 equivalent of pyridine to solutions of **2** triggers a subtle, but noticeable, change in hue. This color change can be magnified through cooling or increasing the concentration of pyridine. Removal of all solvent under vacuum followed by redissolution results in the regeneration of the original color of **2**. These results suggest that pyridine binds to **2** in an equilibrium fashion.

In accord with these observations, when a solution containing **2** and one equivalent of pyridine is treated with **1**•PhCN, a new diamagnetic compound results (see Equation 2). Recrystallization from Et₂O furnishes **4** in good yield (63%) as green microcrystals. The ¹H NMR spectrum exhibits, in addition to signals corresponding to two anilide environments in a 1:1 ratio, two peaks in the vinyl region of the spectrum which integrate to two protons each. In addition, downshifted aryl peaks attributable to a pyridyl moiety are noticeably absent. These data indicate that **2**•py, present in equilibrium, has been trapped by **1**•PhCN with bond formation occurring at the *para* (4) position of the ring, so as to result in a dihydropyridine moiety. The preference for 1,4—rather than 1,2—coupling is reminiscent of the system presented in the previous section; in both cases, it is presumed that steric factors are responsible.

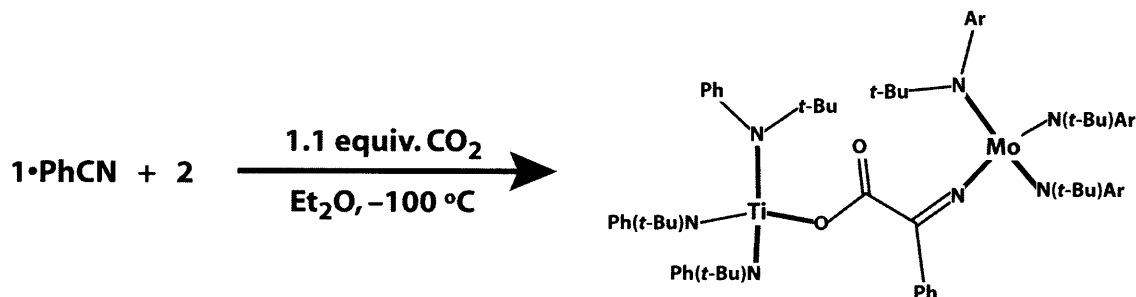


Equation 2

Dihydropyridines are typically synthesized by a two-step protocol involving alkylation at nitrogen followed by reaction of the resulting cation with a nucleophile.¹⁴ Depending on the nucleophile, this procedure can produce significant amounts of the 1,2-substituted compound, thus limiting its general utility. The above process thus constitutes a useful, complementary process for the tandem dearomatization and 1,4-bifunctionalization of pyridine.

4.4 Reductive Coupling of PhCN and CO₂

Treatment of a purple, ethereal solution of **1**•PhCN at -100 °C with **2**, followed rapidly by CO₂ (1.1 equiv, introduced via syringe), was found to elicit upon mixing a color change to cherry red. After workup, the new, diamagnetic compound (Ar[*t*-Bu]N)₃Mo-N=C(Ph)C(O)O-Ti(N[*t*-Bu]Ar)₃ (**5**) was isolated as dark red crystals in 59%



Equation 3

yield (see Equation 3). The ¹³C labeled variant, **5**-¹³C, is conveniently prepared from ¹³CO₂ and exhibits a signature ¹³C NMR signal at 170.7 ppm for the labeled carbon. Also, a weak absorption in the IR at 1635 cm⁻¹ is assigned to ν_{CO}. In **5**-¹³C, this absorption shifts to 1564 cm⁻¹ (the harmonic oscillator approximation predicts 1563 cm⁻¹). While an X-ray diffraction study of **5** confirmed the proposed connectivity, extensive disorder prevented the determination of reliable metrical parameters. Fortunately, substitution of Ti(N[*t*-Bu]Ph)₃ (**6**) for **2** permitted the synthesis of (Ar[*t*-Bu]N)₃Mo-N=C(Ph)C(O)O-Ti(N[*t*-Bu]Ph)₃ (**7**), a single-crystal X-ray diffraction study of which was consummated with ease.

The molecular structure of **7**, shown in Figure 1, clearly displays the freshly created, CO₂-derived, carboxyiminato unit that spans the Mo/Ti centers. The carboxyiminato moiety is both orthogonal to its phenyl substituent and essentially planar. Accordingly, the newly-formed C41-C42 bond distance is 1.487(5) Å, while the N4-C41 distance is 1.350(5) Å. Both the latter value and the short Mo1-N4 distance of 1.759(3) Å are similar to corresponding parameters observed previously for Mo(IV) ketiminato complexes. Multiple Mo1-N4 bonding is facilitated by the nearly linear (169.9(3)°) Mo1-N4-C41 linkage. The Ti1-O1 distance (1.855(3) Å) is quite similar to that reported for titanium trisanilide enolate **2**-OC(=CH₂)NPhMe (1.847(3) Å),⁷ and while the carboxylate

residue interacts with Ti in a monodentate fashion, still the Ti1-O1-C42 angle is an acute $136.8(3)^\circ$. Both Ti and Mo experience a pseudotetrahedral coordination environment.

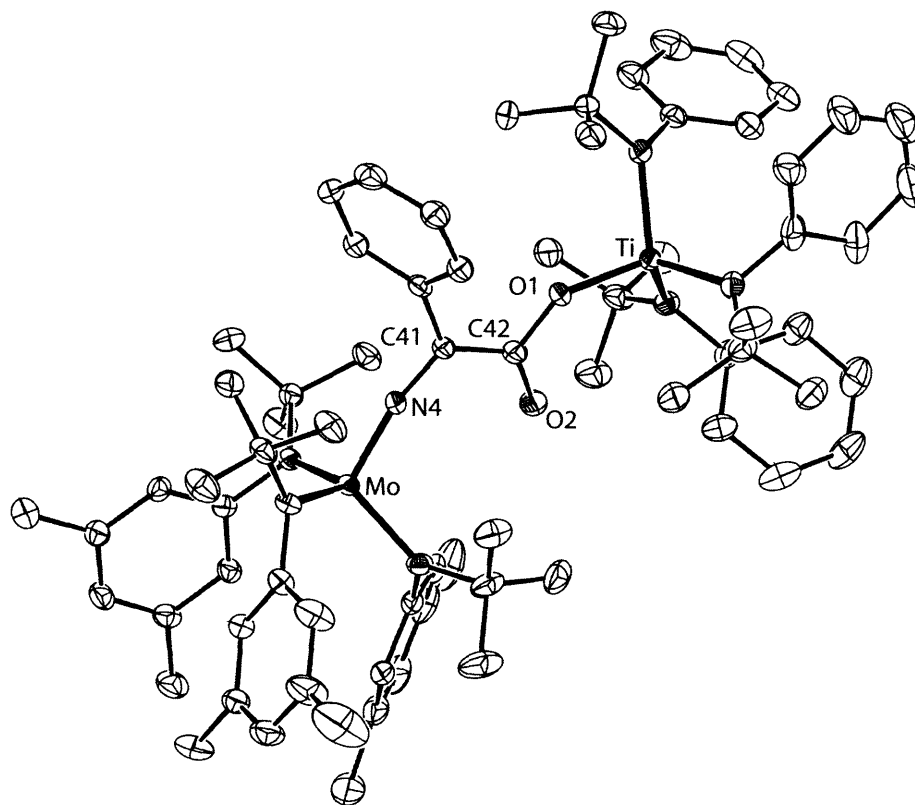


Figure 1 Solid-state structure of **7** (35% ellipsoids, see text for structural parameters).

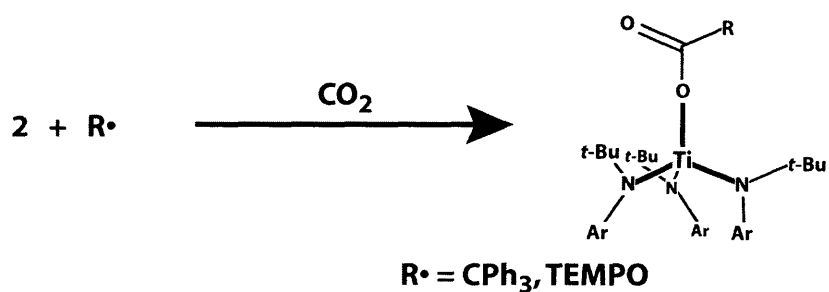
While the reductive, head-to-head coupling of CO_2 (to oxalate) has been a goal of the chemical community for some time,¹⁵ the one-electron *cross*-coupling of CO_2 is without precedent. Success in the former endeavor has been most notably obtained with $(\text{Cp}^*)_2\text{Sm}$, which cleanly reacts with CO_2 (1 atm.) to form oxalate-bridged $(\text{Cp}^*)_2\text{Sm}(\mu, \eta^2: \eta^2\text{-C}_2\text{O}_4)\text{Sm}(\text{Cp}^*)_2$ in greater than 90% yield.⁵ In a related reaction, a Ti(III) alkyl species has been reported to react with CO_2 to yield predominantly (80%) the product of CO_2 insertion into the Ti-alkyl bond; the de-alkylated oxalate-bridged compound was observed as a byproduct, with the fate of the alkyl moiety unknown.¹⁶ Intriguingly, the formation of oxalate from CO_2 has also been reported for a Cu(I) system; the yield could be increased from 21% to 53% through the use of CsHCO_3 in place of CO_2 .¹⁷ Finally, it should be mentioned that the conversion of CO_2 to oxalate is readily accomplished electrochemically.¹⁸

4.5 Attempted trapping of $2\bullet\text{CO}_2$

The formation of **5** is presumed to occur through radical combination of the known $1\bullet\text{PhCN}$ and putative $2\bullet\text{CO}_2$. The observed reactivity along with electronegativity considerations suggest that $2\bullet\text{CO}_2$ should have an O-bound structure. Such an intermediate was also invoked in the $(\text{Cp}^*)_2\text{Sm}$ -mediated coupling of CO_2 ,⁵ and has recently been observed and structurally characterized for U(III).¹⁹ DFT calculations on $2\bullet\text{CO}_2$ indicate that both η^1 and η^2 structures are energy minima, and that the CO_2 carbon is endowed with considerable radical character.²⁰

In order to shed further light on this issue, we desired to trap $2\bullet\text{CO}_2$ with compounds other than $1\bullet\text{PhCN}$. To our surprise, treatment of **2** with the potent H atom donor ${}^n\text{Bu}_2\text{SnH}_2$ in the presence of CO_2 did not result in formation of the known titanium formate.²¹ We thus turned our attention to traps that, like $1\bullet\text{PhCN}$, possessed significant radical character.

In control experiments, the stable free radicals trityl and 2,2,6,6-tetramethylpiperidine-1-oxyl (TEMPO) were found to undergo no reaction with **2** over a period of 1 hour at 25 °C. Accordingly **2** was treated with CO_2 in the presence of either trityl or TEMPO in the hopes of observing the reactions depicted in equation 4. However, no reaction was detected in either case. The lack of reaction with trityl is likely due in part to the fact that at low temperature—when the concentration of $2\bullet\text{CO}_2$ is likely to be highest—trityl is present in solution primarily as its head-to-tail dimer.⁹



Equation 4

Theorizing that more reactive radicals were necessary for the trapping of $2\bullet\text{CO}_2$, we turned our attention to radicals that could be generated *in situ*. To our surprise, the $2\bullet\text{Ph}_2\text{CO}$ and $2\bullet\text{pyridine}$ adducts described above proved incapable of trapping $2\bullet\text{CO}_2$ under a variety of experimental conditions.

We next carried out the experiment depicted in Figure 2. We envisioned that **2** would be capable of halogen abstraction from ClPPh₂ to generate transient Ph₂P radical.²² It was hoped that this radical would be reactive enough to react with **2**•CO₂ to form the indicated product. In a control experiment, **2** was treated 0.5 equivalents of ClPPh₂ at -100° C and the mixture allowed to warm to room temperature. The only diamagnetic products observed were Cl-Ti(N[*t*-Bu]Ar)₃ and Ph₂P-PPh₂.²³ This experiment suggested that **2** is not only capable of halogen atom abstraction from ClPPh₂, but it attacks PPh₂ radical at a rate that is slow relative to its dimerization.

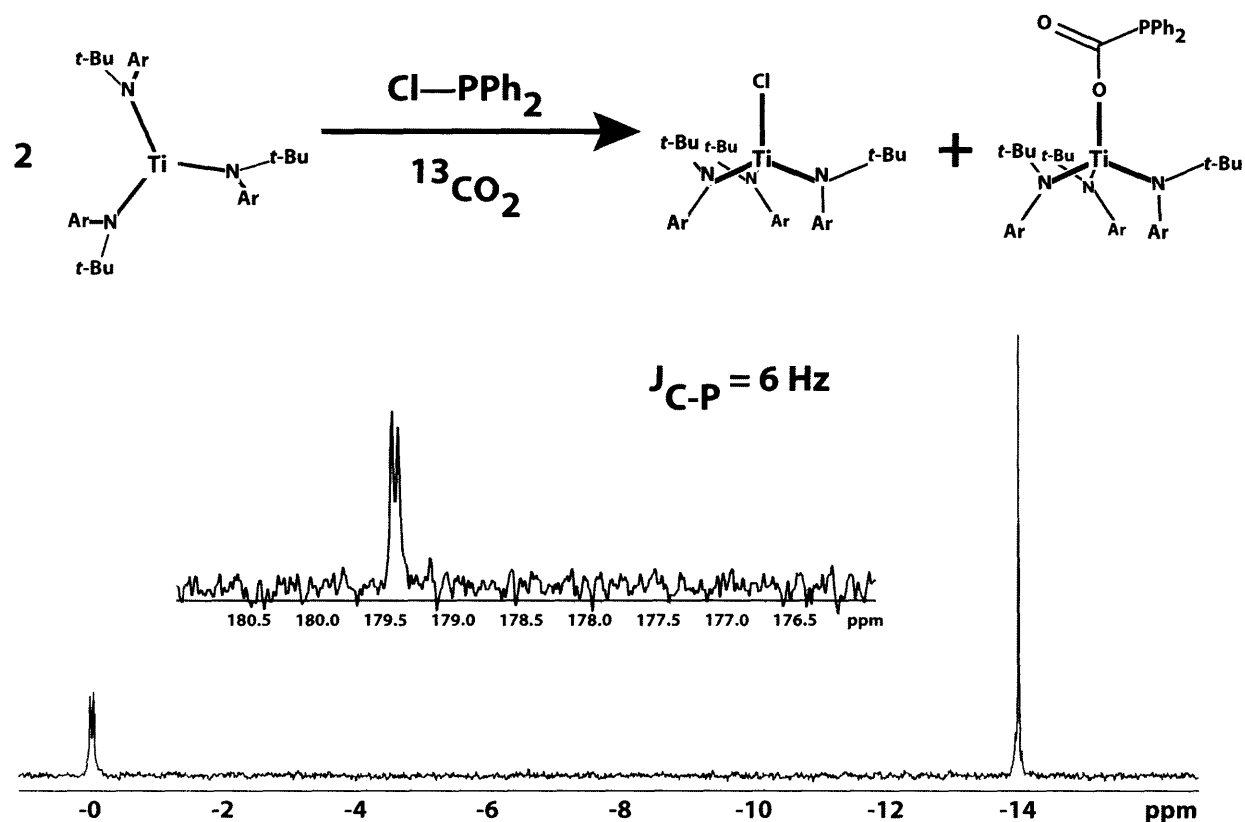


Figure 2

Encouraged by this result, we cooled an Et₂O solution containing two equivalents of **2** to -100 °C and treated it with one equivalent each of ClPPh₂ and CO₂. The reaction mixture was then allowed to stir for 1 hour at -40 °C during which time it turned yellow-brown. ¹H NMR Analysis of the reaction mixture indicated that the predominant products were Cl-Ti(N[*t*-Bu]Ar)₃ and Ph₂P-PPh₂. In addition, however, a new product containing one anilide environment was observed. A corresponding peak in the ³¹P NMR was

observed at *ca.* 0 ppm. When the reaction was carried out using $^{13}\text{CO}_2$, this peak split into a doublet with $J_{\text{CP}} = 6$ Hz. The ^{13}C NMR for this compound exhibited a doublet at 179.4 ppm with the same coupling constant. On the basis of this spectroscopic data, we conclude that the desired product has indeed formed, albeit in low yield. Unfortunately, we were unable to separate this product from its byproducts.

In Chapter 3, we described the transformation of formate $(\text{Ar}[t\text{-Bu]N})_3\text{Ti-OC(O)H}$ to titanoxide $(\text{Ar}[t\text{-Bu]N})_3\text{Ti-OLi(OEt)}_2$ upon treatment with $\text{LiN}(i\text{-Pr})_2$. The simplest mechanism for such a transformation involves the initial formation of anionic $(\text{Ar}[t\text{-Bu]N})_3\text{Ti-OCO}^-$ (**8**). Theorizing that such an intermediate might also be synthesized by the one-electron reduction of $2\cdot\text{CO}_2$, we explored treating **2** with CO_2 in the presence of various reductants. The use of Cp_2Co and Na/Hg amalgam resulted in no reaction. The stronger reductant sodium naphthalenide reacted rapidly with **2** to form a mixture of unknown products, precluding its use in experiments involving CO_2 .

4.5 Conclusions

The three reactions presented here constitute rather unusual extensions of the classical Pinacol coupling and testify to the unique electronic and steric properties of the metal *tris*-anilides **1** and **2**. In addition, these reactions contribute to our understanding of the reactivity of CO_2 , a subject of considerable practical importance. Finally, these reactions constitute relatively rare examples of four-component couplings that proceed selectively to one product.²⁴⁻²⁶ Efforts at elucidating the nature of the reactive $2/\text{CO}_2$ system have been only partially successful. Nonetheless, the principles outlined here bode well for the development of new methods for the incorporation of CO_2 into organic molecules.

4.6 Experimental

General Considerations: Unless stated otherwise, all operations were performed in a Vacuum Atmospheres drybox under an atmosphere of purified nitrogen. Anhydrous diethyl ether was purchased from Mallinckrodt; pentane, n-hexane, and tetrahydrofuran (THF) were purchased from EM Science. Diethyl ether, toluene, benzene, pentane, and n-hexane were dried and deoxygenated by the method of Grubbs.²⁷ THF was distilled under nitrogen from purple sodium benzophenone ketyl. Distilled

solvents were transferred under vacuum into vacuum-tight glass vessels before being pumped into a Vacuum Atmospheres drybox. C₆D₆ was purchased from Cambridge Isotopes and were degassed and dried over 4 Å sieves. THF-d₈ was passed through a column of activated alumina and stored over 4 Å sieves. The 4 Å sieves, alumina, and Celite were dried in vacuo overnight at a temperature just above 200 °C. Compounds **1**,²⁸ **2**,²³ and **6**²⁶ were prepared by literature methods. PhCN was distilled under vacuum before use and stored in a nitrogen-filled drybox. Ph₂CO was recrystallized from dry THF. Pyridine was distilled, stored over 4 Å sieves, and passed through activated alumina immediately before use. All other compounds were used as received. ¹H and ¹³C NMR spectra were recorded on Unity 300, Mercury 300 or Varian INOVA-501 spectrometers at room temperature, unless indicated otherwise. ¹³C NMR spectra are proton decoupled. Chemical shifts are reported with respect to internal solvent: 7.16 ppm and 128.38 (t) ppm (C₆D₆). CHN analyses were performed by H. Kolbe Mikroanalytisches Laboratorium (Mülheim, Germany). A summary of the compound numbering scheme is given in Table 1.

Compound	
1	Mo(N[<i>t</i> -Bu]Ar) ₃
2	Ti(N[<i>t</i> -Bu]Ar) ₃
3a	Coupling product of 1 •PhCN and 2 •Ph ₂ CO
3b	Coupling product of 1 •2,6-Me ₂ C ₆ H ₃ CN and 2 •Ph ₂ CO
4	Coupling product of 1 •PhCN and 2 •pyridine
5	Coupling product of 1 •PhCN and 2 •CO ₂
6	Ti(N[<i>t</i> -Bu]Ph) ₃
7	Coupling product of 1 •PhCN and 6 •CO ₂

Table 1

Synthesis of 3a: In a scintillation vial was prepared a solution of **1** (140 mg, 0.22 mmol) and PhCN (23 mg, 0.22 mmol) in 4 mL of Et₂O. This vial was cooled to -35 °C in the glovebox freezer during which time a solution of **2** (130 mg, 0.23 mmol) and Ph₂CO (41 mg, 0.23 mmol) in 5 mL of Et₂O was prepared in a separate vial. The two solutions were combined and allowed to warm to room temperature, at which point the reaction mixture was a bright green. Filtration and solvent removal yielded a crude product which was

revealed by ^1H NMR to be 95% pure, with $\text{HN}(t\text{-Bu})\text{Ar}$ as the primary impurity. If necessary, further purification can be accomplished through washing with small quantities of cold hexamethyldisiloxane. Due to its exceedingly high lipophilicity, we have been unable to obtain this compound in analytically pure form. ^1H NMR (300 MHz, C_6D_6): δ 1.21 (s, 27H, Ti CMe_3); 1.27 (br s, 27H, Mo CMe_3); 1.32 (sh, 1H, allyl C–H); 2.23 (br s, 18H, Mo $\text{C}_6\text{H}_3\text{Me}_2$); 2.32 (s, 18H, Ti $\text{C}_6\text{H}_3\text{Me}_2$); 5.29 (2 overlapping peaks, 2H, vinyl C–H); 6.01 (s, 1H, vinyl C–H); 6.04 (s, 1H, vinyl C–H); 6.35 (d, 2H, phenyl *ortho*); 6.66 (s, 3H, Ar *para*); 6.70 (s, 6H, Ar *ortho*); 6.77 (partially obscured t, 1H, phenyl *para*); 6.81 (s, 3H, Ar *para*); 7.00 (s, 6H Ar, *ortho*); 7.28 (t, 2H, phenyl *meta*); 7.59 (d, 2H, phenyl *ortho*) ppm; two additional aryl resonances obscured. ^{13}C NMR (125 MHz, C_6D_6): 22.00 ($\text{C}_6\text{H}_3\text{Me}_2$); 22.11 ($\text{C}_6\text{H}_3\text{Me}_2$); 30.85 (Ti CMe_3); 31.75 (Mo CMe_3); 62.15 (Ti N– CMe_3); 47.38 (allyl); 63.2 (br, Mo N– CMe_3); 115.76; 124.91; 125.53; 126.36; 126.77; 126.98; 127.41; 128.65, 128.23; 130.35; 130.49; 131.24; 135.94; 136.87; 137.89; 139.79; 152.23; 161.45; 168.2 (br, Mo–N=C) ppm.

Synthesis of 3b: In a scintillation vial was prepared a solution of **1** (162 mg, 0.26 mmol) and 2,6– $\text{Me}_2\text{C}_6\text{H}_3\text{CN}$ (34 mg, 0.26 mmol) in 5 mL of Et_2O . This vial was cooled to -35 °C in the glovebox freezer. In a separate vial was prepared a solution of **2** (150 mg, 0.26 mmol) and Ph_2CO (48 mg, 0.26 mmol) in 5 mL of Et_2O , which was also cooled to -35 °C. The chilled solutions were combined and allowed to warm to room temperature. Stirring for an additional 90 minutes was necessary for completion of the reaction as judged by the development of a green hue. The reaction mixture was then gently concentrated to incipient crystallization, at which point the vial was transferred to the glove box freezer. Crystals grew overnight and were collected by decanting off of the mother liquor. Yield: 250 mg (2 crops, 63%). ^1H NMR (500 MHz, C_6D_6): δ 1.15 (s, 27H, Ti CMe_3); 1.21 (br s, 27H, Mo CMe_3); 2.26 (s, 36H, overlapping Ti and Mo $\text{C}_6\text{H}_3\text{Me}_2$); 2.62 (s, 3H, nitrile $\text{C}_6\text{H}_3\text{Me}_2$); 2.73 (s, 3H, nitrile $\text{C}_6\text{H}_3\text{Me}_2$); 4.4 (br s, 1H, vinyl C–H); 4.5 (br s, 1H, vinyl C–H); 5.29 (s, 1H, vinyl C–H); 5.78 (s, 1H, vinyl C–H); 6.44 (br s, 6H, Ar *ortho*); 6.70 (s, 3H, Ar *para*); 6.73 (s, 3H, Ar *para*); 6.79 (br s, 6H, Ar *ortho*); 6.99 (t, 1H, nitrile $\text{C}_6\text{H}_3\text{Me}_2$ *para*); 7.07 (d, 1H, nitrile $\text{C}_6\text{H}_3\text{Me}_2$ *meta*); 7.10 (d, 1H, nitrile $\text{C}_6\text{H}_3\text{Me}_2$ *meta*); 7.20 (t, 1H, phenyl *para*); 7.31 (t, 2H, phenyl *meta*); 7.51 (d, 2H, phenyl

ortho) ppm. ^{13}C NMR (125 MHz, C_6D_6): 21.89 ($\text{C}_6\text{H}_3\text{Me}_2$); 22.11 ($\text{C}_6\text{H}_3\text{Me}_2$); 30.97 (Ti CMe_3); 31.77 (Mo CMe_3); 45 (br, allyl); 62.02 (Ti N- CMe_3); 62.0 (br, Mo N- CMe_3); 115.58; 116.28; 123.5; 124.46; 126.73; 126.89; 127.63; 127.96; 128.03; 129.00; 130.72; 136.70; 137.21; 139.00; 139.27; 139.71; 139.93, 152.67; 160.17; 168.7 (br, Mo-N=C) ppm. Anal Calcd. for $\text{C}_{94}\text{H}_{127}\text{N}_7\text{OMoTi}$: C, 74.53; H, 8.45; N, 6.47. Found: C, 74.40; H, 8.38; N, 6.41.

Synthesis of 4: **1** (300 mg, 0.48 mmol) and PhCN (50 mg, 0.48 mmol) were combined in 6 mL of Et_2O . The resulting purple solution was frozen in the glovebox coldwell. In a separate vial, **2** (277 mg, 0.48 mmol) and pyridine (74 mg, 2 equivalents) were combined in 3 mL Et_2O . This solution was also cooled to freezing in the glovebox coldwell. The solutions were removed from the coldwell and the thawing solution of **2**•py was added to thawing **1**•PhCN dropwise over 1 min. Upon warming to room temperature, the reaction mixture had acquired a dark green hue. Volatiles were removed in vacuo.

Recrystallization from Et_2O (-35°C) furnished **4** as dark green microcrystals (422 mg, 2 crops, 63%). ^1H NMR (500 MHz, C_6D_6): 1.30 (br s, 27H, Mo CMe_3); 1.34 (s, 27H, Ti CMe_3); 2.26 (s, 18H, $\text{C}_6\text{H}_3\text{Me}_2$); 2.32 (s, 18H, $\text{C}_6\text{H}_3\text{Me}_2$); 4.55 (d, 2H, vinyl C-H); 5.14 (br s, 2H, vinyl C-H); 6.72 (s, 3H, Ar *para*); 6.76 (s, 3H, Ar *para*); 6.81 (t, 1H, phenyl *para*); 6.95 (br s, 6H Ar *ortho*); 6.99 (s, 6H, Ar *ortho*); 7.25 (t, 2H, phenyl *meta*) ppm. ^{13}C NMR (125 MHz, C_6D_6): 21.84 ($\text{C}_6\text{H}_3\text{Me}_2$); 21.98 ($\text{C}_6\text{H}_3\text{Me}_2$); 31.08 (CMe_3); 31.83 (br, CMe_3); 41.80 (allyl); 63.21 (N CMe_3); 66.24 (N CMe_3); 103.29; 124.58; 126.58; 126.73; 127.23; 127.58; 128.17; 129.65; 136.13; 137.39; 137.78; 137.92; 150.06, 170.68 (Mo-N=C) ppm (one aryl peak missing). Anal Calcd. for $\text{C}_{84}\text{H}_{118}\text{N}_8\text{MoTi}$: C, 75.53; H, 8.90; N, 8.39. Found: C, 75.17; H, 8.98; N, 8.05.

Synthesis of 5: In a typical preparation, a 100 mL round bottom flask with sidearm was charged with **1** (400 mg, 0.64 mmol), PhCN (66 mg, 0.64 mmol) and 10 mL of Et_2O . The flask was loosely stoppered with a rubber septum and frozen in the coldwell.

Concurrently, a scintillation vial was charged with **2** (370 mg, 0.64 mmol) in 10 mL of Et_2O and cooled to -35°C . When the **1**•PhCN was completely frozen, it was removed from the coldwell and the chilled solution was added rapidly. Working quickly, the flask

was resealed with a rubber septum (the original septum will be brittle at this point, so it is useful to have a fresh septum around) and removed from the glovebox, whereupon CO₂ (16 mL, *ca.* 1.1 equiv.) was added at once via syringe. A subtle change in hue from dark purple to wine red takes place at this point, although it is often obscured by the frost that collects on the flask. The reaction mixture is allowed to warm to room temperature at which point all volatiles are removed *in vacuo*. The resulting residue was recrystallized from Et₂O (−35 °C). Yield: 257 mg, 5 crops (60%). ¹H NMR (300 MHz, C₆D₆): 1.40 (s, 27H, Ti CMe₃); 1.47 (s, 27H, Mo CMe₃); 2.13 (18H, Mo C₆H₃Me₂); 2.26 (18H, Ti C₆H₃Me₂); 6.30 (br s, 6H, Ar *ortho*); 6.43 (br s, 6H, Ar *ortho*); 6.68 (s, 3H, Ar *para*); 6.73 (s, 3H, Ar *para*); 7.16 (t, 1H, phenyl *para*); 7.43 (t, 2H, phenyl *meta*); 7.77 (br s, 2H phenyl *ortho*) ppm. ¹³C NMR (75 MHz, C₆D₆): 21.39 (C₆H₃Me₂); 21.64 (C₆H₃Me₂); 30.80 (CMe₃); 31.72 (br, CMe₃); 61.85 (NCMe₃); 64.43 (NCMe₃); 125.54; 125.96; 126.55; 128.41; 129.01; 129.17; 133.25; 136.09; 137.03; 137.73; 138.30; 150.0 (v br); 152.90; 170.21 ppm. IR (C₆D₆): 1635 (C=O) cm^{−1}. Anal Calcd. for C₈₀H₁₁₃N₇O₂MoTi: C, 71.25; H, 8.45; N, 7.27. Found: C, 71.36; H, 8.55; N, 7.25.

Synthesis of 5-¹³C: Synthesized as in the previous substituting ¹³CO₂ for CO₂. ¹³C NMR (125 MHz, C₆D₆): 170.1 ppm. IR (C₆D₆): 1564 (C=O) cm^{−1}.

Synthesis of 7: Synthesized analogously to **5**, employing 252 mg (0.40 mmol) of **1**, 200 mg (0.40 mmol) of **6** (in place of **2**), 41 mg (0.40 mmol) of PhCN, and *ca.* 9 mL (0.40 mmol) of CO₂. Recrystallized from pentane (−35 °C). Yield: 202 mg, 2 crops (40%). ¹H NMR (300 MHz, C₆D₆): 1.35 (s, 27H, Ti CMe₃); 1.47 (s, 27H, Mo CMe₃); 2.14 (18H, Mo C₆H₃Me₂); 6.26 (br s, 6H, Ar *ortho*); 6.43; 6.68 (s, 3H, Ar *para*); 6.72 (s, 6H, Ti phenyl *ortho*); 7.00 (t, 3H, Ti phenyl *para*); 7.15 (t, 6H, Ti phenyl *meta*); 7.17 (partially obscured t, 1H, phenyl *para*); 7.42 (t, 2H, phenyl *meta*); 7.74 (br s, 2H phenyl *ortho*) ppm. ¹³C NMR (75 MHz, C₆D₆): 21.39 (C₆H₃Me₂); 30.77 (CMe₃); 31.69 (CMe₃); 62.10 (NCMe₃); 64.47 (NCMe₃); 124.49; 126.63; 127.36; 128.49; 129.08; 129.77; 133.27; 137.06; 138.35; 149.91; 152.83; 170.07 ppm (two aryl peaks missing).

Attempted trapping of 2•CO₂ with ⁿBu₂SnH₂: A 100 mL round bottom flask with sidearm was charged with **2** (200 mg, 0.35 mmol), ⁿBu₂SnH₂ (70 mg, 0.30 mmol), and 17 mL of Et₂O. The flask was sealed, removed from the glovebox, and cooled to –78 °C in a dry ice/acetone bath, at which point CO₂ (8 mL, 0.36 mmol) was added *via* syringe. No immediate color change was observed. The mixture was allowed to stir at –78 °C for 15 minutes, at which point the dry ice/acetone bath was removed. After an additional 15 minutes, the reaction mixture maintained the characteristic green color of **2**. Thus, it was decided to re-cool the flask to –78 °C and add additional CO₂ (10 mL, 0.45 mmol). The mixture was then allowed to warm to room temperature over 25 minutes, at which point volatiles were removed *in vacuo*. ¹H NMR analysis showed the presence of both starting materials, along with HN(*t*-Bu)Ar and small amounts of other anilide-containing products. Titanium formate H(O)CO–Ti(N[*t*-Bu]Ar)₃ was not observed.

Attempted trapping of 2•CO₂ with trityl radical: A 100 mL round bottom flask with sidearm was charged with **2** (100 mg, 0.17 mmol), trityl radical (50 mg, 1.2 equiv.), and 15 mL of Et₂O. The resulting green solution was cooled to freezing in the glovebox coldwell. The flask was then rapidly removed from the box and CO₂ was added (4 mL, 0.18 mmol). The mixture was allowed to warm to room temperature with stirring. The green color of **2** persisted. ¹H NMR analysis showed HN(*t*-Bu)Ar as the only diamagnetic product.

Attempted trapping of 2•CO₂ with TEMPO: A 100 mL round bottom flask with sidearm was charged with **2** (100 mg, 0.17 mmol), TEMPO (50 mg, 1.2 equiv.), and 15 mL of Et₂O. The resulting green solution was cooled to freezing in the glovebox coldwell. The flask was then rapidly removed from the box and CO₂ was added (4 mL, 0.18 mmol). The mixture was allowed to warm to room temperature with stirring. The green color of **2** persisted. ¹H NMR analysis indicated that no reaction had occurred.

Attempted trapping of 2•CO₂ with 2•py: A solution of **2** (200 mg, 0.35 mmol) in 15 mL THF was transferred to a 100 mL round bottom flask with sidearm. To this solution was added pyridine (*ca.* 25 mg, 0.33 mmol) resulting in a subtle color change to bluish-

green. The flask was then sealed, removed from the box, and cooled to liquid nitrogen temperatures. Carbon dioxide (10 mL, 0.45 mmol) was added *via* syringe and the mixture was allowed to warm to room temperature. After 45 minutes, the solution had taken on a green-brown color. Volatiles were removed *in vacuo*. ^1H NMR analysis of the resulting residue showed several diamagnetic products including $\text{HN}(t\text{-Bu})\text{Ar}$ along with unreacted **2**.

Attempted trapping of $2\cdot\text{CO}_2$ with $2\cdot\text{Ph}_2\text{CO}$: A solution of **2** (200 mg, 0.35 mmol) in 10 mL Et_2O was prepared in a 100 mL round bottom flask with sidearm. This solution was cooled to freezing in the glovebox cold well. Concurrently, a scintillation vial was charged with Ph_2CO (32 mg, 0.18 mmol) in 8 mL Et_2O and cooled to $-35\text{ }^\circ\text{C}$. The contents of this vial were rapidly added to the frozen solution of **2**. The flask was removed from the box and treated with CO_2 (4 mL, 0.18 mmol) *via* syringe. No immediate color change was observed. The solution was allowed to warm to room temperature at which point all volatiles were removed *in vacuo*. ^1H NMR analysis of the green residue indicated that no reaction had occurred.

Reaction of **2 with ClPPh_2 :** A scintillation vial was charged with **2** (100 mg, 0.17 mmol) in 3 mL of Et_2O . A second vial was charged with ClPPh_2 (100 mg, 0.09 mmol) in 2 mL of Et_2O . Both solutions were cooled to near freezing and then combined. The reaction mixture was allowed to warm to room temperature. After approximately 40 seconds, the mixture began to turn brown. Upon reaching room temperature, the reaction mixture was orange. Volatiles were removed *in vacuo*. ^1H NMR and ^{31}P NMR analysis indicated $\text{Cl-Ti}(\text{N}[t\text{-Bu}]\text{Ar})_3$ and $\text{Ph}_2\text{P-PPh}_2$ were the only products.

Attempted trapping of $2\cdot\text{CO}_2$ with $\cdot\text{PPh}_2$: A 100 mL round bottom flask with sidearm was charged with **2** (200 mg, 0.35 mmol) and 15 mL of Et_2O . A scintillation vial was charged with ClPPh_2 (38 mg, 0.17 mmol) and 4 mL Et_2O . Both solutions were cooled to freezing in the glovebox coldwell. The ClPPh_2 was briefly thawed and added to still-solid **2**. The flask was sealed, removed from the glovebox, and transferred to a $-40\text{ }^\circ\text{C}$ bath (MeCN/N_2). Carbon dioxide (^{13}C labeled, 4 mL, 0.17 mmol) was added *via* syringe. The

mixture was allowed to stir for 30 minutes, whereupon it turned orange. The cooling bath was removed, and volatiles were removed *in vacuo*. ^1H , ^{13}C , and ^{31}P NMR spectra indicated $\text{Cl-Ti}(\text{N}[t\text{-Bu}]\text{Ar})_3$ and $\text{Ph}_2\text{P-PPh}_2$ as major products along with a new product whose spectral data is given here. ^1H NMR (500 MHz, C_6D_6): δ 1.28 (s, 27H, CMe_3); 2.22 (s, 18H, $\text{C}_6\text{H}_3\text{Me}_2$); 7.13 (d, 2H, phenyl *ortho*); 7.23 (t, 1H, phenyl *para*), 7.83 (t, 2H, phenyl *meta*) ppm. ^{13}C NMR (125 MHz, C_6D_6): δ 179.41 (d, $J_{\text{CP}} = 6$ Hz). ^{31}P NMR (121 MHz): δ -0.1 (d, $J_{\text{CP}} = 6$ Hz) ppm.

Attempted trapping of $2\cdot\text{CO}_2$ with Na/Hg: A 100 mL round bottom flask with sidearm was charged with **2** (100 mg, 0.17 mmol), Na/Hg amalgam (8.5 mg Na, 0.38 mmol), and 15 mL of Et_2O . The resulting green solution was cooled to freezing in the glovebox coldwell. The flask was then rapidly removed from the box and CO_2 was added (4 mL, 0.18 mmol). The mixture was allowed to warm to room temperature with stirring. The green color of **2** persisted. ^1H NMR analysis indicated that no reaction had occurred.

Attempted trapping of $2\cdot\text{CO}_2$ with Cp_2Co : A 100 mL round bottom flask with sidearm was charged with **2** (100 mg, 0.17 mmol), Cp_2Co (33 mg, 0.17 mmol), and 15 mL of THF. The resulting greenish-brown solution was cooled to freezing in the glovebox coldwell. The flask was then rapidly removed from the box and CO_2 was added (4 mL, 0.18 mmol). The mixture was allowed to warm to room temperature with stirring. The green color of **2** persisted. ^1H NMR analysis indicated that no reaction had occurred.

X-ray structure determination of **7:** The X-ray crystallographic data collection was carried out on a Siemens Platform three circle diffractometer mounted with a CCD detector and outfitted with a low temperature, nitrogen-stream aperture. The structure was solved using direct methods, in conjunction with standard difference Fourier techniques and refined by full-matrix least-squares procedures. A summary of the crystallographic data is shown in Table 1. An empirical absorption correction (SADABS) was applied to the diffraction data. All non-hydrogen atoms were refined anisotropically. Unless otherwise specified, all hydrogen atoms were treated as idealized contributions and refined isotropically. All software used for diffraction data processing and crystal-

structure solution and refinement are contained in the SAINT+ (v6.45) and SHELXTL (v6.14) program suites, respectively (G. Sheldrick, Bruker AXS, Madison, WI).

	7
formula	C ₇₉ H ₁₀₁ MoN ₇ O ₂ Ti
fw	1324.51
space group	<i>P</i> $\bar{1}$
<i>a</i> , Å	11.4158(5)
<i>b</i> , Å	18.4340(8)
<i>c</i> , Å	20.0106(9)
α , deg	112.2270(10)
β , deg	94.7310(10)
γ , deg	100.7660(10)
<i>V</i> , Å ³	3774.8(3)
<i>Z</i>	2
<i>D</i> , g/cm ³	1.165
μ (Mo K α), mm ⁻¹	0.320
temp, K	193
F(000)	1408
GoF(<i>F</i> ²)	1.040
R(<i>F</i>), %	0.0492
wR(<i>F</i>), %	0.1258

Table 2 Crystallographic parameters for **7**.

¹ Corey, E. J.; Danheiser, R. L.; Chandrasekaran, S. *J. Org. Chem.* **41**, 260 (1976).

² (a) Steinhuebel, D. P.; Lippard, S. J. *J. Am. Chem. Soc.* **121**, 11762 (1999). (b) Hou, Z.; Yamazaki, H.; Kobayashi, K.; Fujiwara, Y.; Taniguchi, J. *J. Chem. Soc., Chem. Comm.* 722 (1992). (c) Freudenberger, J. H.; Konradi, A. W.; Pedersen, S. F. *J. Am. Chem. Soc.* **111**, 8014 (1999). (d) Waymouth, R. M.; Clauser, K. R.; Grubbs, R. H. *J. Am. Chem. Soc.* **108**, 6385 (1986). (e) Askham, F. R.; Carroll, K. M. *J. Org. Chem.* **58**, 7328 (1993).

³ (a) Roskamp, E. J.; Pedersen, S. F. *J. Am. Chem. Soc.* **109**, 6551 (1987). (b) Ito, H.; Taguchi, T.; Hanzawa, Y. *Tetrahedron Lett.* **33**, 4469 (1992).

⁴ Buchwald, S. L.; Watson, B. T.; Wannamaker, M. W.; Dewan, J. C. *J. Am. Chem. Soc.* **111**, 4486 (1989).

⁵ For a rare example of CO₂ reductive coupling, see: Evans, W. J.; Seibel, C. A.; Ziller, J. W. *Inorg. Chem.* **1998**, 37, 770.

⁶ (a) Birch, A. J. *Pure. Appl. Chem.* **68**, 553 (1996). (b) Holy, N. L. *Chem. Rev.* **74**, 243 (1973). (c) Garst, J. F.; Smith, C. D. *J. Am. Chem. Soc.* **98**, 1976 (1976).

-
- ⁷ Agapie, T.; Diaconescu, P. L.; Mindiola, D. J.; Cummins, C.C. *Organometallics* **21**, 1329 (2002).
- ⁸ (a) Covert, K. J.; Wolczanski, P. T.; Hill, S. A.; Krusic, P. J. *Inorg. Chem.* **31**, 66 (1992). (b) Hou, Z.; Fujita, A.; Zhang, Y.; Miyano, T.; Yamazaki, H.; Watasuki, Y. *J. Am. Chem. Soc.* **120**, 754 (1998).
- ⁹ (a) Gomberg, M. *J. Am. Chem. Soc.* **22**, 757 (1900). (b) Neumann, W. P.; Uzick, W.; Zarkadis, A. K. *J. Am. Chem. Soc.* **108**, 1986.
- ¹⁰ Yamamoto, D.; Matsumi, D.; Itoh, K. *Chem. Comm.* 875 (1998).
- ¹¹ Molander, G. A.; Wolfe, C. N. *J. Org. Chem.* **63**, 9031 (1998).
- ¹² (a) Shono, T.; Kise, N.; Fujimoto, T.; Tominaga, N.; Morita, H. *J. Org. Chem.* **57**, 7175 (1992). (b) Shono, T.; Kise, N.; *Tetrahedron Lett.* **31**, 1303 (1990).
- ¹³ Other examples: (a) Corey, E. J.; Pyne, S. G. *Tetrahedron Lett.* **24**, 2821 (1983). (b) Zhou, L.; Zhang, Y.; Shi, D. *Tetrahedron Lett.* **39**, 8491 (1998). (c) Zhou, L.; Zhang, Y. *Tetrahedron* **56**, 2953 (2000).
- ¹⁴ Bennasar, M.-L.; Juan, Cecilia; Bosch, J. *Chem. Comm.*, 2459 (2000).
- ¹⁵ For an interesting discussion of the head-to-head vs. head-to-tail dimerization of CO₂, see the following papers and references cited therein: (a) Arena, F.; Floriani, C.; Chiesi-Villa, A.; Guastini, C. *Inorg. Chem.* **25**, 4589 (1986). (b) Gambarotta, S.; Arena, F.; Floriani, C.; Zanazzi, P. F. *J. Am. Chem. Soc.* **104**, 5082.
- ¹⁶ Frohlich, H. J.; Heike, S. *Z. Chem.* **23**, 348 (1983).
- ¹⁷ Farrugia, L. J.; Lopinski, S.; Lovatt, P. A.; Peacock, R. D. *Inorg. Chem.* **40**, 558 (2001).
- ¹⁸ (a) Becker, J. Y.; Vainas, B.; Eger, R.; Kaufman, L. J. *J. Chem. Soc., Chem. Commun.*, 1471 (1985). (b) Kushi, Y.; Nagao, T.; Nishioka, K.; Isobe, K.; Tanaka, K. *Chem. Lett.*, 2175 (1994). (c) Kushi, Y.; Nagao, T.; Nishioka, K.; Isobe, K.; Tanaka, K. *J. Chem. Soc., Chem. Commun.*, 1223 (1995).
- ¹⁹ Castro-Rodriguez, I.; Nakai, H.; Zakharov, L. N.; Rheingold, A. L.; Meyer, K. *Science* **305**, 1757.
- ²⁰ Cummins, C., unpublished results.
- ²¹ Kuivila, H. G.; *Synthesis*, 499 (1970).
- ²² (a) Adeleke, B. B.; Wan, J. K. F. *J. Chem. Soc., Perkin Trans. 2*, 225 (1980). (b) Geoffroy, M.; Lucken, E. A. C.; Mazeline, C. *Mol. Phys.* **28**, 839 (1974). (c) Cook, W. T.; Vincent, J. S.; Bernal, I.; Ramirez, F. *J. Chem. Phys.* **61**, 3479 (1974). (d) Wong, S. K. M.; Wan, J. K. S. *Spec. Lett.* **3**, 135 (1970). (e) Schmidt, U.; Kabitzke, K.; Markau, K.; Mueller, A. *Chem. Ber.* **99**, 1497 (1966). (f) Schmidt, U.; Geiger, F.; Mueller, A.; Markau, K. *Angew. Chem.* **75**, 640 (1963).
- ²³ Peters, J. C.; Johnson, A. R.; Odom, A. L.; Wanandi, P. W.; Davis, W. M.; Cummins, C. C. *J. Am. Chem. Soc.* **1996**, 118, 10175.
- ²⁴ Weber L.; Illgen, K.; Almstetter, M. *Synlett* 1999, 366.
- ²⁵ Orru, R. V. A.; de Greef, M. *Synthesis* 2003, 1471.
- ²⁶ Balme, G.; Bossharth, E.; Monteiro, N. *Eur. J. Org. Chem.* 2003, 4101.
- ²⁷ Pangborn, A.B.; Giardello, M.A.; Grubbs, R.H.; Rosen, R.K.; Timmers, F.J. *Organometallics* **1996**, 15, 1518.
- ²⁸ Laplaza, C. E.; Johnson, M. J. A.; Peters, J. A.; Odom, A. L.; Kim, E.; Cummins, C. C.; George, G. N.; Pickering, I. J. *J. Am. Chem. Soc.* **1996**, 118, 8623.

Appendix

Synthesis of a Ti(III) paddlewheel

A.1 Insertion of CO₂ into the Ti–N(*t*-Bu)Ar bond

Chapter 4 describes our efforts to coax one-electron reactivity from CO₂ using Ti(N[*t*-Bu]Ar)₃ (**1**). In the course of conducting those experiments, we observed the following example of Ti(N[*t*-Bu]Ar)₃-promoted *two-electron* reactivity. While this reaction pathway is considerably more common, it provided a product of some interest.

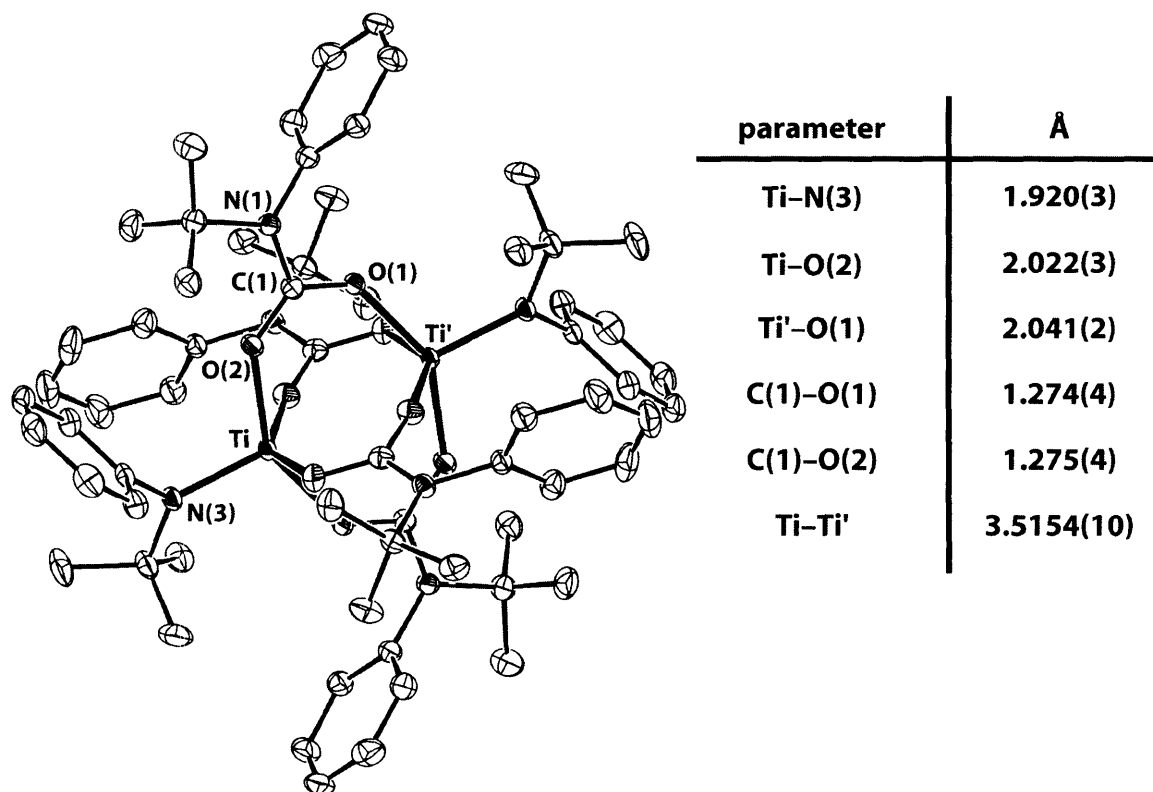


Figure 1 Solid-state structure of **4** (30% ellipsoids).

When a solution of **1** in Et₂O is cooled to –40 °C (MeCN/N₂), treated with 4 eq. of CO₂, and allowed to stir for 2.5 hours, a lime green precipitate (**2**) develops. This material, **2**, can be collected by filtration in *ca.* 80% yield. The ¹H NMR spectrum of this material suggests that it is diamagnetic and contains two different anilide environments. Unfortunately, we were unable to grow crystals of this compound of suitable quality for an X-ray diffraction study. Substitution of Ti(N[*t*-Bu]Ph)₃ (**3**) for **1** allowed for the synthesis of the analogous compound (**4**), however, which proved to be more amenable to crystallization.

The structure of **4** is shown in Figure 1. As can be clearly seen, **4** is formed through CO₂ insertion into two out of the three Ti amide bonds followed by dimerization,

resulting in a paddlewheel structure. While CO₂ insertion into early metal–amide bonds is a relatively common process,¹ it has not been thus far encountered with the sterically encumbering *t*-butyl anilide ligands.² The long Ti–Ti distance of 3.5154(10) Å appears to preclude a metal–metal bond,³ rendering the observed diamagnetism somewhat puzzling.

A.2 Experimental

General Considerations: Unless stated otherwise, all operations were performed in a Vacuum Atmospheres drybox under an atmosphere of purified nitrogen. Anhydrous diethyl ether was purchased from Mallinckrodt; pentane and tetrahydrofuran (THF) were purchased from EM Science. Diethyl ether and pentane were dried and deoxygenated by the method of Grubbs.⁴ THF was distilled under nitrogen from purple sodium benzophenone ketyl. Distilled solvents were transferred under vacuum into vacuum-tight glass vessels before being pumped into a Vacuum Atmospheres drybox. C₆D₆ was purchased from Cambridge Isotopes and were degassed and dried over 4 Å sieves. The 4 Å sieves, alumina, and Celite were dried in vacuo overnight at a temperature just above 200 °C. Compounds **1** and **3** were synthesized by the literature method.⁵ All other compounds were used as received. ¹H NMR spectra were recorded on a Varian INOVA-501 spectrometer at room temperature, unless indicated otherwise. Chemical shifts are reported with respect to internal solvent: 7.16 ppm. CHN analyses were performed by H. Kolbe Mikroanalytisches Laboratorium (Mülheim, Germany).

Synthesis of 2: In the glovebox, a 250 mL round-bottom flask with sidearm was charged with **1** (696 mg, 1.21 mmol) and 30 mL Et₂O. The flask was briefly evacuated through the sidearm, and then sealed and removed from the glovebox. Upon cooling to –40 °C (N₂/MeCN), CO₂ (100 mL, 4.46 mmol, 3.7 eq) was added via syringe. The emerald green solution was allowed to stir for 2.5 h, during which time the temperature of the cooling bath had risen to 0 °C, and a lime green precipitate had formed. The flask was warmed to ambient temperature and the volatiles removed in vacuo. The resulting lime green powder was slurried in 10 mL of pentane and filtered, and the solid was further washed with 5 mL pentane and 5 mL Et₂O. The solid was dried to yield 640 mg (80%) of the desired product. ¹H NMR (500 MHz, C₆D₆): δ 1.48 (s, 9H, amide CMe₃); *ca.* 1.6 (br sh,

18H, carboxamide CMe_3); *ca.* 2.3 (br s, 12H, carboxamide $C_6H_3Me_2$); 2.46 (s, 6H, amide $C_6H_3Me_2$); *ca.* 6.4 (v br, 4H, carboxamide *ortho*); 6.75 (s, 2H, amide *ortho*); 6.79 (s, 1H, amide *para*); *ca.* 7.6 (v br, 2H, carboxamide *para*) ppm (assignments are tentative). Anal. Calcd. for $C_{76}H_{108}N_6O_8Ti_2$: C, 68.66; H, 8.19; N, 6.32. Found: C, 68.19; H, 7.93; N, 6.29.

Synthesis of 4: Compound **4** was synthesized analogously to **2**, using **3** in place of **1**. Crystals were grown from a THF/Et₂O mixture.

X-ray structure determination of 4: The X-ray crystallographic data collection was carried out on a Siemens Platform three circle diffractometer mounted with a CCD detector and outfitted with a low temperature, nitrogen-stream aperture. The structure was solved using direct methods, in conjunction with standard difference Fourier techniques and refined by full-matrix least-squares procedures. A summary of the crystallographic data is shown in Table 1. An empirical absorption correction (SADABS) was applied to the diffraction data. All non-hydrogen atoms were refined anisotropically. Unless otherwise specified, all hydrogen atoms were treated as idealized contributions and refined isotropically. All software used for diffraction data processing and crystal-structure solution and refinement are contained in the SAINT+ (v6.45) and SHELXTL (v6.14) program suites, respectively (G. Sheldrick, Bruker AXS, Madison, WI).

	4
formula	C ₆₈ H ₉₃ N ₆ O ₉ Ti ₂
fw	1234.43
space group	<i>P</i> $\bar{1}$
<i>a</i> , Å	11.6091(16)
<i>b</i> , Å	12.8853(18)
<i>c</i> , Å	24.358(3)
α , deg	104.5094
β , deg	92.288(4)
γ , deg	101.522(5)
<i>V</i> , Å ³	3432.8(8)
<i>Z</i>	2
<i>D</i> , g/cm ³	1.194
μ (Mo K α), mm ⁻¹	0.290
temp, K	193
F(000)	1318
GoF(<i>F</i> ²)	1.002
R(<i>F</i>), %	0.0574
wR(<i>F</i>), %	0.1306

Table 1 Crystallographic parameters for **4**.

¹ Chisholm, M. H.; Extine, M. W. *J. Am. Chem. Soc.* **99**, 792 (1977).

² For an example of CO₂ insertion into a less hindered amide in the presence of *t*-butyl anilide, see: Cherry, J. P. F., Ph. D. Thesis; Massachusetts Institute of Technology: Cambridge, Massachusetts, 26 (1997).

³ Cotton, F. A.; Walton, R.A. *Multiple bonds between metal atoms*; Oxford University Press: New York, 1993.

⁴ Pangborn, A.B.; Giardello, M.A.; Grubbs, R.H.; Rosen, R.K.; Timmers, F.J. *Organometallics* **1996**, *15*, 1518.

⁵ Peters, J. C.; Johnson, A. R.; Odom, A. L.; Wanandi, P. W.; Davis, W. M.; Cummins, C. C. *J. Am. Chem. Soc.* **1996**, *118*, 10175.

Acknowledgements

This thesis could not have been written without the help and support of several people. At MIT, I have to thank Kit Cummins first and foremost for having the courage to take me on and for being a seemingly inexhaustible source of chemical creativity. I would also like to thank Steve Lippard and Alan Davison, both for serving on my committee and for their guidance and support over the years.

During my time in the Cummins group, I had the privilege to interact with several talented chemists who turned out to be wonderful people as well. When I first arrived in the group, I shared a lab with Paul Chirik, John-Paul Cherry, and Theo Agapie, all of whom taught me a great deal about the practice of chemistry in the Cummins group. My early years in the group were also significantly enhanced by my interactions with Fran Stephens, Paula Diaconescu, James Tsai, Justin Brask, and James Blackwell. Josh Figueroa entered the group at the same time as I and, as such, we have been through a lot together; I am grateful to be able to call him a friend. Christopher Clough arrived in the lab just in time to save Josh and me from drowning in our own seriousness, and he continues to be a wonderful source of levity in the group, even if I may not always appreciate it. I also owe Josh and Chris a round of thanks for their crystallographic assistance. Finally, it's been a pleasure to get to know the next generation of Cummins group scientists—Glen Alliger, John Curley, Alex Fox, and Nick Piro—and I wish them well in their chemical endeavors.

I have also been the beneficiary of the skill and hard work of several Chemistry Department support staff: group secretary Allison Kelsey; graduate administrator and miracle worker Susan Brighton; NMR lab support staff David Bray, Mark Wall, and Jeff Simpson; and department crystallographers Bill Davis and Peter Mueller.

Outside of MIT, I would like to thank Pika and the many good friends I made there, including Alexxx Andersen, Luke Phelan, Jamie and Manda Riehl, Vanessa Speed, Leila Hasan, Michael Nagle, Clay Ward, Amelia Virostko, Rikky Muller, Matt Hancher, Teri Yamana, and Kate Ricke; Patty, Lamine, Sasha, Susan, Mike and everybody else at Rambax MIT; current and former JP roommates Rebecca, Jason, Josh, and Nzovu; Cozette Carroll; the MIT activist community; and a very special thank you to Ananda Leininger.

Finally, I would like to thank my parents for their love and continued support, without which I would not have had even the courage to begin.

ARJUN MENDIRATTA

Department of Chemistry
Massachusetts Institute of Technology
77 Massachusetts Avenue, Room 6-328
Cambridge, Massachusetts 02139

Phone: (617) 452-2528
Fax: (617) 258-5700
E-mail: arjunm@mit.edu

Education

Ph.D., Chemistry, Massachusetts Institute of Technology, June 2005
Thesis: "Reductive Coupling and Related Reactions with Mo and Ti *tris*-Anilides" Advisor:
Christopher C. Cummins

B.S., Chemistry, California Institute of Technology, 2000

Research Experience

2005 — 2001: Massachusetts Institute of Technology, Prof. C. C. Cummins
inorganic synthesis, manipulation of highly air-sensitive compounds, multinuclear NMR spectroscopy (^{11}B , ^{51}V , ^{77}Se , ^{125}Te), DFT calculations, kinetics

2000: California Institute of Technology, Prof. J. E. Bercaw
organometallic synthesis, vacuum line techniques, NMR lineshape analysis

1999 — 1998: California Institute of Technology, Prof. W. A. Goddard
computational chemistry, calculation of nonlinear optical properties

1997: California Institute of Technology, Prof. S. R. Marder
organic synthesis, nonlinear optics

Awards and Honors

NSF Predoctoral Fellow, Massachusetts Institute of Technology, 2002-2005.

Angela and Tony Fish Bequest, travel grant, Royal Society of Chemistry, 2004.

Dupont-MIT Alliance Fellow, Massachusetts Institute of Technology, 2000-2001.

Publications

- "Heterodinuclear (Mo/Ti) Radical Cross-Couplings of Benzonitrile with Pyridine, Benzophenone, and CO₂." **Mendiratta A**, Cummins CC, *J. Am. Chem. Soc.*, submitted for publication.
- "Synthesis of a four-coordinate titanium(IV) oxoanion via deprotonation and decarbonylation of complexed formate." **Mendiratta A**, Figueroa, JS, Cummins CC *Chem. Comm.*, accepted for publication.

- “Molybdenum Chalcogenobenzimidato Complexes: Radical Synthesis and Nitrile Extrusion via β -EPh (E = S, Se, and Te) Elimination.” **Mendiratta A**, Cummins CC, Kryatova OP, Rybak-Akimova, EV, McDonough JE, Hoff, CD *Inorg. Chem.* **2003**, *42*, 8621.
- “Reactions of Organic Nitriles with a Three-Coordinate Molybdenum(III) Complex and with a Related Molybdaziridine-Hydride.” Tsai Y-C, Stephens FH, Meyer K, **Mendiratta A**, Gheorghiu MD, Cummins CC *Organometallics* **2003**, *22*, 2902.
- “Ancillary Ligand and Olefin Substituent Effects on Olefin Dissociation for Cationic Zirconocene Complexes Bearing a Coordinated Pendant Olefin.” Brandow C, **Mendiratta A**, Bercaw JE *Organometallics* **2001**, *20*, 4253.
- “Synthesis and Properties of a Diarylaminoferrocene and its Radical Cation.” **Mendiratta A**, Barlow S, Day MW, Marder SR *Organometallics* 1999, *18*, 454.